Dear Editor,

Thank you for giving us the opportunity to revise our manuscript “Tracking the global flows of atmospheric moisture”. We greatly appreciate the helpful and detailed comments by both reviewers, which have contributed to an extension of our analyses and an improved manuscript. Please find below all review comments with our responses given in blue. Where we refer to line numbers, they apply to the document version with tracked changes. Apart from implementing the reviewers’ comments, we altered the structure of the methods section and performed some further minor edits. We hope that you and the reviewers will find our revised manuscript suitable for publication in *Hydrology and Earth System Sciences*.

Note that we have appended the track-changes versions of the manuscript and the supplement to this document, as per the *Hydrology and Earth System Sciences*-intstructions.

Please let us know if you have further questions or requests.

Best regards,

Obbe Tuinenburg and Arie Staal

Reviewer 1
Munir Ahmad Nayak

Dear Dr. Louise

Thank you for sending the manuscript to me for a review. Below you will see a short summary of the manuscript, followed by my specific (major) comments, and then technical corrections (minor comments) at the end.

Summary
Tracking moisture in the atmosphere over time has many applications in the fields of hydrology and meteorology, such as finding the major moisture sources of particular extreme precipitation event at a given location. Moisture tracking models can be represented with a variety of schemes, which include Eulerian and Lagrangian (in two and three dimensions) frameworks, different integration time steps, different sets of vertical forcings, representations of vertical wind velocities, locations of moisture releases to the atmosphere, etc. The results of moisture tracking, for example evaporation recycling rate, the distance travelled by moisture, etc., will depend on the scheme chosen. The authors experiment a set of evaporation tracking schemes to asses the sensitivity of tracking results to different schemes. In summary, the steps used in the manuscript can be written as: a.) Select seven point-sources of evaporation across the globe, b.) track the evaporation (during first five days of July 2012) from these locations using a tracking scheme, c.) keep track of precipitation locations, i. e., latitude and longitude points

where precipitation happened, d.) repeat the above three steps with different model settings, and e) compare the tracking results. Based on the comparisons among different schemes, the authors propose an "optimal" tracking scheme for general hydrological applications: 3D Lagrangian, 500 particles released per mm evaporation, moisture releases at surface, linear interpolation in time and space, adding as many vertical forcings as possible, etc.
The manuscript is very clearly written, and overall, I think it can be of interest to many readers of HESS and other similar journals. There, however, are some places in the manuscript where authors should provide more justifications and clarifications; I added these in the "specific comments" section below. I hope the authors can address these comments, after which the manuscript may be suitable for publication in HESS. I will be looking forward to reading a revised draft.

Thank you for the encouragements and we are happy to see that the manuscript was clear.

Specific comments
1. When an air parcel moves, it gains and losses moisture along its track, the gain and loss can be attributed directly to the location where the change happens if the parcel is within the boundary layer. When the parcel is out of the boundary layer, the change locations are not clearly evident, since they can come from remote sources (Sodemann et al., 2008), which are difficult to evaluate. It is not clear how the "original" evaporation (Lines 95-96) is maintained throughout the parcel's track. More clarity on this will help in interpreting many results presented in section 3, for example evaporation footprint.

In the current model, no distinction is made between moisture within the boundary layer and that above it. We are treating the allocation in the same way regardless of the current vertical position of the parcel. That means that we are allocating the surface fluxes (and the moisture gains and losses) to all moisture in the atmospheric column, and thus to all parcels present at that location. The "original evaporation" in this case reflects the evaporation at the location and moment the parcel was released, which is probably a different location than the parcel along the track. We then allocate moisture along the parcel's path according to the ratio of P/PW at the current location of the parcel. As stated, this is done independent of vertical position of the parcel, meaning we assume perfect vertical mixing throughout the atmospheric column. We changed the lines around the former lines 95-96 to state that it is about the amount of original evaporation transported with the parcel (lines 104-108 in the document with tracked changes): "However, once there is precipitation at the location of the parcel, a fraction of the moisture (precipitation over precipitable water of the entire atmospheric column, $\frac{P}{PW}$) that is still present in the parcel is allocated to rain out in that location. This assumes that all moisture in the atmospheric column has the same probability of raining out. Thus, the amount of original evaporation remaining decreases with downwind moisture transport.".

Regarding whether the moisture can be attributed to remote or local sources, we actually think that moisture above the boundary layer can be attributed more easily. If the only difference between the boundary layer (BL) and free troposphere (FT) is the mixing (strong in the BL, not so strong in the FT), the source regions of parcels in the free troposphere can be more easily determined because the parcels will move with the large-scale winds. In the boundary layer,

there is more mixing and therefore more vertical displacement of parcels. Given that this study shows that atmospheric moisture transport can be quite sensitive to vertical displacement assumptions, we could assume that it is more difficult to pinpoint the original moisture source of boundary layer moisture compared to free tropospheric moisture. Nevertheless, we did not look at the difference between boundary layer and non-boundary layer moisture here, but consider it worthwhile for future research to test explicitly what the sensitivities of moisture recycling to boundary layer and non-boundary layer vertical mixing are.

2. Section 2.1.4: During convective up- and down drafts, horizontal winds also show significant changes in magnitude and direction; the particles can then be displaced vertical depending on the changes in the vertical winds, instead of assigning random vertical displacements to them, which seems arbitrary. If feasible, another scheme based on this large horizontal wind gradients may be added in the present framework.

Thank you for this suggestion. We agree that the unconditional mixing scheme currently employed is a simplification of reality. As suggested, large-scale conditions may influence the vertical mixing rate. Furthermore, it is possible to use the convective mass fluxes to determine local vertical mixing rates, as we did in Staal et al. (2018, *Nature Climate Change* 8:539-543). As the goal of the current work is to test the sensitivity of different kinds of assumption on moisture tracking, we have chosen to limit the analyses to the current mixing assumptions of four mixing strengths that all happen regardless of atmospheric conditions. For future work, a sensitivity analysis of more physical vertical displacements would be relevant.

3. The basic structure of the model is not presented anywhere. I suggest adding a stepwise procedure on how the tracking is performed. Actually, response to this might answer my first comment 1 also.

We have rewritten the model description section (2.1) and presented the moisture tracking procedure in a more stepwise way (lines 98-112). Furthermore, we restructured the Methods section with a more logical order of presentation of model structure and assumptions, and experiments.

4. This baseline model is 3D Lagrangian with 10,000 parcels released per mm; the 3D model in L243, table 1, and other results almost identical to the baseline model. This does not seem a reasonable way to compare models and present results, since baseline itself is not “True Tracking” and cannot be a perfect reference. It might be a good idea to use other models’ output as reference, such as HYSPLIT (Draxler and Hess, 1998), LAGRANTO (Wernli, H., and H. C. Davies, 1997).

“True tracking” is, of course, impossible. However, a three-dimensional Lagrangian scheme with an extremely large amount of parcels (10,000 for each mm evaporation) uses the available information in the most elaborate way. That is, no information is lost. For this reason, we considered that the best possible baseline. We chose not to compare our results with those form other models in the literature, which were generally developed for ERA-Interim data. Rather, our aim is to test how the ERA5 data can be used best for moisture tracking purposes. Revisiting

existing models would address different questions. We prefer to remain within our original scope and not use other models as reference.

5. In Section 3.2, it is argued that number of parcels released does not affect tracking results greatly. We should note, however, that number of parcels may matter to capture convective/converging and diverging events, as stated by the authors in section 2.2.4. Here, the simulations are run only for one case (July 2012), which may not have large convergence or divergence at any time. We should be careful in generalizing these results to all events, unless simulations results of some specific convective events show similar results.

We agree that we must be careful in generalizing our results. Because of possible biases resulting from using only one case, we did our experiments for seven locations spread around the globe. Indeed, some locations were more sensitive to certain changes in model settings than others. However, in general the results were robust. Apart from these seven cases we published our code including options to change the settings according to our methods. Thus, users of the model can perform their own sensitivity analysis if they want to, or change the settings to suit specific research questions. We added in lines 533-534 that we tracked only for one month the moisture released during five days is an additional reason for caution in generalizing our results.

Technical corrections
Define “footprints” at the beginning, somewhere in the introduction.

Thank you for spotting this. We now define “footprint” as “the distribution of precipitation resulting from evaporation from a point or area” in line 50.

One of the aims of the manuscript was to evaluate model structure; however, it is not clear where model structures have changed. Perhaps, Eulerian and Lagranian can be taken as different model structures, but this needs to be written explicitly.

Thank you for spotting this. We now define model structure as “Eulerian or Lagrangian and the number of spatial dimensions” in lines 76-77.

L25-26: Fig. 1 does not specifically show moisture recycling as indicated here.

We removed the reference to Figure 1 in this sentence.

L46-48: Rather than “assumptions”, I feel they are more like user “choices”.

We agree and rephrased to “choices” in these lines.

L44: Here, I suggest writing “parcels” instead of “particles”.

We replaced “particle” with “parcel” throughout the manuscript.

L51-54: It is not clear how the results will be incorrect; also, clearly explain why the Eulerian

model simulations will not be as fast as Lagrangian when moisture is released from small areas.

We moved the explanation of why the results will be incorrect from the methods to the introduction in lines 54-56: “If the time step is chosen too large, real moisture transport may occur faster than the simulation grid and time step allow for (i.e., if the Courant number $C=\frac{v\Delta t}{\Delta x}>1$). If the time step is taken too small, numerical diffusion will occur, meaning that moisture transport in the model will be faster than in the forcing data.”

To explain why Eulerian models will not be as fast as Lagrangian for small areas we added “The reason is that they are insensitive to an increase in scale, as all grid cells are updated with the same speed regardless of the amount of moisture present.” in lines 58-59.

L60: Do you mean “which resulted in Courant numbers exceeding one …”?

We removed this part of the sentence, because it was unnecessarily complicating.

L125: I am not sure if I understand why vertical mixing is to be carried out every time interval and how is it performed; more details on this can help readers.

The vertical mixing is carried out every time step in the sense that every time step, a random number [0-1] is determined. If this number is smaller than dt/mixing_rate_hour (dt is the internal time step, mixing_rate_hour is the mixing strength in terms of how many times vertical mixing happens on average, in our case 1 hour, 6 hours, 24 hours and 120 hours), the random vertical displacement occurs. By carrying out the mixing procedure (including random number assessment) every time step, two things are achieved:
1. Mixing happens on average once per mixing_rate_hour hours (so once every 1, 6, 24 or 120 hours);
2. The mixing happens at random moments throughout the trajectory, so there is no bias regarding to mixing at specific moments.

We have added some additional description in section 2.1.8 (lines 255-259): “During every time step, there is a small probability (dt/mix-strength) of running the vertical displacement. We summarize these stochastic vertical displacement versions of the model by the mix-strength (unit: hours), or average time for one repositioning of one parcel, which is once per hour, once per six hours, once per 24 hours and once per 120 hours. This procedure ensures that for each parcel, mixing happens on average once in the time period described by the mixing strength and that the mixing happens at random moments during the trajectory. Thus, no biases occur due to mixing at specific prescribed moments.”.

L130-L133: Rephrase for more clarity.

We have added units to the data used and remove the “division by the grid cell length” part, which may have been confusing. Now, the section states that the 2D flow speed is driven by the vertically integrated flow speed. Of course the grid cell length is still relevant for the calculation, but as it is not relevant for the 3D vs 2D discussion, we removed it here.

L150: Do you mean “particle” instead of “parcel”? Try to be consistent.

We now consistently refer to parcels.

L153: No, this does not seem realistic; you might not be able to capture convergence or divergence with this scheme, just because it is random.

We agree that it was too strongly phrased. We removed this sentence.

L178: Here, 10,000 particles are released per mm of evaporation over first 5 days of July 2012? Evaporation from a point source at any instant will be transported during each time step; are we releasing parcels at one instant, say t=0, or over multiple time steps (t =0, t=1, and so on.). Add a few lines to clearly explain how parcels are released, and how evaporation over 5 days will be captured by parcels released.

Yes, 10,000 parcels are released for every mm of evaporation during those five days. We added “All evaporation within this period is accounted for” in lines 164-165.

L189: In table 1: I would also add a simple metric “mean distance travelled”.

Thank you for this suggestion. When we ran our simulations, unfortunately, we did not record the distance that the parcels travelled through the atmosphere. We did, however, record the distances between the source locations and those of the sink locations. This is already present in Table 1 (mean latitudinal distance and mean longitudinal distance).

L225-234: The entire section can be as a separate row in Table 1.

Thank you for this suggestion. We added new rows to Table 1 with the results presented in section 3.1, which are averages of the data that were already provided.

L250: Low value of CRR is observed in 2D Lagrangian case, not Eulerian; see Figure 3c also

Thank you for spotting this. We meant the high value of CRR in the 2D Eulerian case and corrected the sentence accordingly.

L254: Fig. S5, not S4.

Thank you for spotting this. We corrected it.

L259-262: Give clear reasons of so much computational time difference between 3D Lagrangian and 3D Eulerian schemes. In other words, why do we think 3-D Eulerian takes so much time?

The reason is that Eulerian models update the moisture content of all grid cells, even when the actual tracked moisture is in just a part of it. This information is added in lines 58-59.

Figures 6, 7 and other similar figures: Since these figures do not shown clear differences, perhaps it is better to show differences directly, i.e., map of baseline footprint minus footprint from the given set up.

We appreciate this suggestion, but showing differences would serve another purpose than ours. Lack of difference among simulations is—in our case—a relevant result. If we chose to display the differences (only) in the cases where they are very small, the collection of figures would highlight the model settings to which the model is insensitive to rather than the ones that it is sensitive to.

Figure S25B: There is an unusual straight color line in this panel; can that be removed?

Thank you for spotting this. This straight line was due to an error in the plotting. The ERA5 data (and our model) runs on longitudes from 0-360, while Matplotlib expects longitudes from -180-180. We made an error shifting grids, which we now corrected.

Section 3.5: Were the models run with interpolation or with nearest neighbor method. Also, the results here can be concisely presented in a tabular form, rather than text.

As explained in section 2.2.4, all Lagrangian runs were forced by interpolated data, unless stated otherwise, in which case the nearest neighbor was used. Thus, mentioned section uses interpolation.

Section 3.6: Will it be feasible to test sensitivity to timestep dt = 3 hours?

Yes, it is. We expanded our sensitivity analysis to time steps, now including dt = 3h and dt = 6h. The respective figures in the main text and the supplement were updated with two new panels. Also the Methods (section 2.2.7) and the Results (section 3.7) were updated accordingly. Note that time steps >1h imply a degraded temporal resolution compared to the forcing data. We added this information in lines 233-234: "… 3 h, and 6 h. Note that the latter two imply a degradation of the temporal resolution. For these cases we averaged hourly data on wind speed and direction." The additional tests did not change the settings of our optimal model.

Section 3.7: I am not sure if I clearly understand the purpose of mixing and its usefulness in practice. Perhaps provide more details.

The purpose of the vertical mixing is to approximate the role of turbulence in atmospheric moisture transport. Turbulence may be a very important driver of mixing, but this is not covered by reanalysis data. Accounting for vertical mixing as we do may compensate for that. We clarified this in lines 388-389: "Turbulence may cause considerable vertical mixing in the atmosphere, but because the rate of this mixing is unknown, …".

References

1. Sodemann, H., C. Schwierz, and H. Wernli, 2008: Interannual variability of Greenland winter precipitation sources: Lagrangian moisture diagnostic and North Atlantic

Oscillation influence. *J. Geophys. Res.*, **113**, D03107.
2. R. Draxler, R., and G. Hess, 1998: An overview of the HYSPLIT_4 modelling system for trajectories. *Aust. Meteorol. Mag.*, **47**.
3. Wernli, H., and H. C. Davies, 1997: A lagrangian-based analysis of extratropical cyclones. I: The method and some applications. Quart. J. Roy. Meteor. Soc., 123, 467–
Reviewer 2

In this study, a Lagrangian moisture tracking model driven by ERA5 reanalysis data is presented, and recommendations concerning both input data resolution and model set-up in light of accuracy and efficiency are given based on sensitivity experiments. This method is designed for tracking the fate, or as the authors phrase it, the 'footprint' of evaporative moisture released at point locations around the globe. Such a sensitivity analysis comes at the right time, as ERA5 drastically improved both the temporal and spatial resolution as compared to the widely used ERA-Interim in moisture tracking studies, yet this wealth of data is also accompanied with data storage limitations, and considerable simulation time increases. This well-written, nicely presented study may therefore boost scientific progress by providing guidelines on how to use ERA5 data most efficiently, and additionally, demonstrates the power of Lagrangian modelling for tracing moisture. Although generally easy to understand, some descriptions lack clarity, and I believe the manuscript could be ameliorated if the authors considered the following points listed below (not sorted), and thus become suitable for publication in HESS.

Thank you for these encouraging words.

- **Number of particles:** If I understand it correctly, then even the setting with the lowest number, 100 particles per mm of evaporation, is still high compared to some previous studies; in case of e.g. Manaus, for a range of say 3 to 6 mm of daily evaporation, this would correspond to 300 to 600 particles being released per day.
Studies such as Gimeno et al. (2012) and many, many others follow the method introduced in Stohl & James (2004) and are based on air parcels (that, altogether, represent the entire atmosphere), and not a 'collection of water particles', as is the case here, but I believe the number of particles may still be compared. Even though some studies based on the Stohl & James (2004) approach do not even mention the number of parcels (or 'particles'), a lot of publications are based on simulations with 6-hourly timesteps for which 2 million air parcels for the entire globe are used (e.g. Sorí et al., 2017; García-Herrera et al., 2019, …). Läderach & Sodemann (2016) used 5 million parcels globally, which corresponds to an average of about 70 parcels per column residing over each grid cell at any given timestep, so that about 280 parcels are available per grid cell and day, compared to about 120 in many other papers (2 million parcels globally). Therefore, the setting used in this study with 'only' 100 particles per mm of evaporation, at least in the case of high evaporation rates as in Manaus, still results in far more particles than were employed in many peer-reviewed moisture tracking studies. Indeed, as the authors point out in the discussion, larger study areas and longer analysis periods likely decrease the number of particles needed. Still, it would be interesting to see an extended Fig. 4 for e.g. 50, 25 or even 10 particles per mm of evaporation, and this might also reveal a lower limit, since even 'only' 100

particles perform nearly as well as 10’000. Considering the near-linear runtime dependency on the number of particles, this information might be valuable.

Thank you for this suggestion and we agree. Therefore, we extended our sensitivity analysis for the number of parcels with 50 and 10 parcels per mm evaporation. We added two new panels to the respective figures in the main text (Fig. 4) and the supplement (Figs. S8-S13), and updated the respective sections in the Methods (2.2.2) and Results (3.2). Lowering the amount of parcels in this way had a small effect on the statistics and made the footprints less smooth. Therefore, we decided to keep the setting of our optimal model at 500 parcels mm^{-1} evaporation. Moreover, we mentioned in the methods section that the number of parcels used here is high compared to other moisture tracking studies (lines 194-196 in the version with tracked changes).

- **Particle vs parcel:** Related to the comment above, I am not sure if the usage of ‘particle’ throughout most of the manuscript is ideal. Particle by definition implies a small size, but depending on the number of particles (per unit of evaporation) used, each particle represents a considerable amount of water, and obviously not a tiny droplet or even a single water molecule, as one might first think. As of now, both ‘particle’ and ‘parcel’ are used in the manuscript, so I suggest to remove one of these to ensure consistency, preferably the former.

We now consistently refer to parcels throughout the manuscript.

- **Omega:** It is unclear to me why the authors decided to omit omega in their default configuration. In this context, it is important to point out that the statement on l. 423 is incorrect: the approach of Stohl et al. (2005) does use omega, yet it is complimented by random vertical displacements of air parcels to represent convective (vertical) redistribution.

Thanks, we changed the statement to reflect that the study by Stohl et al. (2005) does include omega and uses a scheme based on turbulent mixing to create additional vertical displacements (lines 487-489): “Therefore, moisture tracking models may complement the omega-based vertical displacement by using a mixing scheme based on turbulent mixing (Stohl et al., 2005), or …”.

Also, the argument starting on l. 436, “We assume that this speed of mixing is rapid enough to supersede larger-scale vertical flows so as to simplify the model and exclude omega“, seems to contradict a previous statement, in which the large effect of omega (vs no omega) is highlighted; moreover, evaporation footprints with and without omega are only similar for (probably unrealistically) fast mixing times of 1 hour, which strongly indicates that this aforementioned ‘superseding’ does not really take place for mixing at timescales of 24 hours. The lack of a proper reference, since the baseline model is essentially identical to the 3D Lagrangian model (a major limitation that is not really emphasized in the manuscript), clearly makes it difficult to justify any choice here; however, I am not convinced by the explanations provided so far, other than omitting omega ‘for simplicity’ and to achieve faster simulation times.

Thanks for raising this issue. We agree that we may have been too quick to disregard inclusion of omega for the weaker mixing assumptions. It is true that the baseline model is 'just' the 3D Lagrangian model, because it is quite hard to get reliable mixing, or source-sink relations of atmospheric moisture, especially in the context of the current study in which many sensitivity test are performed.

Nevertheless, we changed the manuscript in the method section to state that there are some sensitivity analyses for which we have a true value of moisture recycling (the numerical ones; time step, degraded resolutions, number of particles, etc.) and there are some for which we do not have a true estimate (vertical mixing, release height) (lines 173-176): "For some of the sensitivity tests, these criteria are evaluated against the simulation with the most detailed settings (most parcels, highest resolution, etc.), in which case there is a numerical true estimate. However, for some tests, there is no information to derive a true value. For these tests, the uncertainty remains higher and we derive the sensitivity of moisture recycling to the assumptions."

We have changed the discussion (lines 502-505) and conclusion (lines 547-548) to reflect that the vertical transport is the main uncertainty regarding moisture tracking.

As a small note, given the data volume of the ERA5 data, the reason for excluding the omega data (or reducing the forcing data in general) has more to do with computer memory (RAM) use of the simulation than with the CPU time needed. Once all data is loaded into RAM, looking up specific values is done in about constant time.

- **Horizontal resolution:** Especially because of the authors' valuable recommendation not to degrade the vertical resolution, it would be helpful for the scientific community to know whether the same is true for degrading the horizontal resolution. As stated in the manuscript, many previous Lagrangian studies are based on input data at 0.75x0.75°, or even 1.0x1.0° horizontal resolution, so that upgrading to 0.25x0.25° represents a massive improvement. However, this comes at the cost of extensive input data size, which makes studies covering multiple decades rather than a few days extremely challenging. I suggest adding this analogously to the degradation of vertical information; e.g. for increments of 0.25° from 0.25x0.25° up to 1.0x1.0°. For the same reasons, investigating the sensitivity to temporal resolution would be helpful too, but I am aware that the authors cannot include everything in their manuscript.

Thank you for this suggestion and we agree that testing for degrading horizontal resolution is a worthwhile addition to our paper. Therefore, apart from 0.25°, we performed our analyses also for 0.5°, 1.0°, and 1.5°. We added a new Fig. 8, supplementary Figs. S32-37 and new sections 2.2.6 and 3.6.

The horizontal degradation had quite considerable effects on the statistics, so we decided not to change the settings of our optimal model based on these new experiments.

- **Tracking time:** 99% of moisture allocated, or 30 days: Dirmeyer & Brubaker (2007) used 90% & 15 days, and nearly all tracking studies do not exceed 15 (or even 10!)

days either, as the trajectory accuracy is known to decrease with increasing length (Stohl & Seibert, 1998). Due to how the model is set up, at least if I understand it correctly (see also below), this choice might not really affect the results, but I still suggest to check if the conclusions hold for considerably shorter trajectory lengths, such as 15 or 10 days.

We appreciate the suggestion, but we would advise the model users against using short tracking times. It happens often that after ten days not all tracked moisture has been allocated yet, in which case continuing the tracking will be better than terminating it. This happens especially over drier areas. Although we agree that the uncertainty increases with time, the quality of the forcing data is not reduced with longer tracking, as they are observation-based and not model-based.

- **Model description:** is insufficient. According to my understanding, tracked moisture remains static until precipitation occurs ('over' the grid cell underneath), and then decreases accordingly to the ratio of precipitation over precipitable water (of the entire column, I presume?). If so, this invokes another assumption, namely that each water (vapor) molecule within a tropospheric column has the same odds of condensing and precipitating (Dirmeyer & Brubaker, 2007). Please clarify.

Yes, this is correct. The allocation happens according to the ratio of P/PW, in which PW is the precipitable water of the entire column. This indeed assumes that every unit of water in the entire column has an equal probability of precipitating out of the column. We have added this fact and assumption explicitly in the model description section (lines 104-107): "However, once there is precipitation, a fraction of the moisture (precipitation over precipitable water of the entire atmospheric column, $\frac{P}{PW}$) that is still present in the atmosphere is allocated to rain out in that location. This assumes that all moisture in the atmospheric column has the same probability of raining out."

Minor comments and suggestions
In addition to the major comments above, a few additional comments and suggestions are listed here.
- l. 25: This sentence describes *continental* moisture recycling, not the more general concept of moisture recycling as it is most commonly defined (e.g. Brubaker et al., 1993; Dirmeyer et al., 2009). I suggest to include 'Continental' at the beginning of this sentence, and replace 'continental evaporation' e.g. by 'terrestrial evaporation'. This would also be consistent with the results section, where the continental recycling ratio (CRR) is used already.

Thank you, we revised it as suggested.

- l. 113: Not all Lagrangian models are initialized with a collection of water particles, but indeed, this is true for the approach presented in the manuscript. I suggest rephrasing this.

We rephrased this sentence to “In Lagrangian models, the internal model state is not a model grid, but generally a collection of water parcels.” (line 128).

- l. 166: Is this the only instance where the (very short) study period is referred to? I think it would be justified to add a sentence in the discussion to remind the reader of this limitation.

In lines 533-534 in the Discussion, we added “… that we tracked only moisture for one month that evaporated during five days mean[s] that one should be cautious with generalizing the implications of these outcomes.”

- l. 171: Is there any reason behind the choice of both Utrecht and Stockholm, which are rather ‘close’ both geographically and climatologically compared to all other point sources, other than the authors’ affiliations? This is merely a question/comment, not a suggestion, since the conclusions drawn by the authors do not depend on this choice.

As you suspected, the choice of these two European study locations is no coincidence. Indeed, the two are relatively close, but we found it worthwhile to include a high-latitude evaporation source in addition to a more centrally located European location, as moisture recycling models have not always been performing well at higher latitudes. But apart from that, choosing both Utrecht and Stockholm helps us to communicate (the performance of) our model at our institutions.

- l. 265: Is the usage of time units (#particle mm -1 **h -1**) correct here? Besides, elsewhere in the text, the number of particles simply relates to some evaporation amount/volume (without referring to time at all), which is already a sufficient description to me.

Thank you for spotting this mistake. We deleted the reference to time in this sentence.

- l. 306: Do the authors have an explanation as to why the simulation time increases with fewer vertical levels? I do not doubt that this is correct, I simply find it counter-intuitive.

We agree that this is counter intuitive, as all simulations were run on the same computer. However, the simulations for the degraded vertical were run at a different moment than the other ones, which may explain the small difference of 1% in their CPU time.

- l. 423 contains an incorrect statement, as Stohl et al., 2005 do not disregard omega in their approach (also mentioned above)

We apologize for this incorrect reference and modified the example it was based on.

- Fig. 9: Why does B resemble Fig. 3D more than C? According to the text (l. 204), the default choice for the 3D Lagrangian model is 2’000 particles per mm of evaporation.

Figure 9B (now Figure 10B) equals Figure 3D, because both use the default settings of the model: no omega, 6h mixing, and 2000 parcels. All panels in Figure 10 use 2000 parcels per mm.

Further comments
Below are a few additional, language-related comments.
- l. 36: “Universal approach **es** and principle **s** moisture tracking models **is** that they apply…”, this reads a bit weird to me.
- l. 105: “courser” => coarser?
- l. 127: “weighed” => weighted?
3
- l. 185: “on full resolution” => at full resolution?
- l. 345: “CRR decreased much more rapidly ***with (increasing)*** mixing time than ...”, maybe a word (or two) went missing here?
- l. 442: “ ***The*** Continental recycling ratio”, not sure if this is correct without any article

Thank you very much for these detailed comments. We fixed these mistakes. In the last case we changed it to “Continental recycling ratios …”.

Concluding remarks
The paper investigates a multitude of choices and assumptions related to setting up a (Lagrangian) moisture tracking framework based on ERA5 data, and even though the main figures are only for a single location (Manaus) among a total of seven, and the analysis time is very short, I believe this choice is justified. Except for the discussion on vertical mixing and omega, as well as the interpretation on the sensitivity to the number of particles, the conclusions stated in the study make sense to me. Additional experiments (e.g. horizontal & temporal information degradation) and some more explanations might complete the package, hence I would gladly serve as a reviewer again and look forward to reading the revised paper.

Thank you very much.

References
Brubaker, K. L., Entekhabi, D. & Eagleson, P. S. Estimation of continental precipitation recycling. *J. Clim.* **6,** 1077–1089 (1993).
Dirmeyer, P. A., Schlosser, C. A. & Brubaker, K. L. Precipitation, recycling, and land memory: An integrated analysis. *J. Hydrometeorol.* **10,** 278–288 (2009).
García-Herrera, R. et al. The European 2016/17 drought. *J. Clim.* **32,** 3169–3187 (2019).
Läderach, A. & Sodemann, H. A revised picture of the atmospheric moisture residence time. *Geophys. Res. Lett.* **43,** 924–933 (2016).
Sodemann, H., Schwierz, C. & Wernli, H. Interannual variability of Greenland winter precipitation sources: Lagrangian moisture diagnostic and North Atlantic Oscillation influence. *J. Geophys. Res.* **113,** 1–17 (2008).
Sorí, R., Nieto, R., Vicente-Serrano, S. M., Drumond, A. & Gimeno, L. A Lagrangian perspective
of the hydrological cycle in the Congo River basin. *Earth Syst. Dyn.* **8,** 653–675 (2017).

Stohl, A. & Seibert, P. Accuracy of trajectories as determined from the conservation of meteorological tracers. *Q. J. R. Meteorol. Soc.* **124,** 1465–1484 (1998).
Stohl, A., Forster, C., Frank, A., Seibert, P. & Wotawa, G. Technical note: The Lagrangian particle dispersion model FLEXPART version 6.2. *Atmos. Chem. Phys.* **5,** 2461–2474 (2005).

Tracking the global flows of atmospheric moisture

Obbe A. Tuinenburg[1,2,3], Arie Staal[2,3]

[1] Copernicus Institute for Sustainable Development, Utrecht University, Utrecht, 3508 TC, the Netherlands
[2] Stockholm Resilience Centre, Stockholm University, Stockholm, SE-10691, Sweden
[3] Bolin Centre for Climate Research, Stockholm, SE-10691, Sweden

Correspondence to: Obbe A. Tuinenburg (o.a.tuinenburg@uu.nl)

Abstract. Many processes in hydrology and Earth system science relate to continental moisture recycling, the contribution of terrestrial evaporation to precipitation. For example, the effects of land-cover changes on regional rainfall regimes depend on this process. To study moisture recycling, a range of moisture tracking models are in use that are forced with output from atmospheric models, but differ in various ways. They can be Eulerian (grid-based) or Lagrangian (trajectory-based), have two or three spatial dimensions, and rely on a range of other assumptions. Which model is most suitable depends on the purpose of the study, but also on the quality and resolution of the data with which it is forced. Recently, the high-resolution ERA5 reanalysis dataset has become the state-of-the-art, paving the way for a new generation of moisture tracking models. However, it is unclear how the new data can best be used to obtain accurate estimates of atmospheric moisture flows. Here we develop a set of moisture tracking models forced with ERA5 data and systematically test their performance regarding continental evaporation recycling ratio, distances of moisture flows, and 'footprints' of evaporation from seven point sources across the globe. We report simulation times to assess possible trade-offs between accuracy and speed. Three-dimensional Lagrangian models were most accurate and ran faster than Eulerian versions for tracking water from single grid cells. The rate of vertical mixing of moisture in the atmosphere was the greatest source of uncertainty in moisture tracking. We conclude that the recently improved resolution of atmospheric reanalysis data allows for more accurate moisture tracking results in a Lagrangian setting, but that considerable uncertainty regarding turbulent mixing remains. We present an efficient Lagrangian method to track atmospheric moisture flows from any location globally using ERA5 reanalysis data and make the code for this model publicly available.

1 Introduction

~~Moisture~~ Continental moisture recycling is the process ~~in which~~whereby ~~continental~~ terrestrial evaporation re-precipitates on land ~~(Fig. 1)~~, which is increasingly well understood and recognized as an important process in the Earth system. As a mechanism linking remote areas on the planet, it affects how land-cover changes influence regional precipitation (Spracklen et al., 2018), how droughts may or may not spatially propagate (Zemp et al., 2014), and whether continental interior areas receive enough precipitation for agriculture (Keys et al., 2016). With the growing interest in the topic and with increasing data availability, moisture recycling models are being used to address a wider range of questions and on higher spatial and temporal

detail. Examples include the regional hydroclimatic effects of deforestation in the Amazon (Staal et al., 2020) and the dependency of cities' water supply on upwind land areas (Keys et al., 2018).

In moisture recycling model studies, moisture is tracked through the atmosphere. This is generally done using an 'offline' model; all such models share some features, but also differ in notable ways. Universal approaches and principles among offline moisture tracking models ~~is~~ are that they apply the atmospheric water balance (Burde and Zangvil, 2001), they run *a posteriori* using atmospheric reanalysis data or other atmospheric model output (Van der Ent et al., 2013), and at each time step, the atmospheric moisture budget is updated based on wind, evaporation, and precipitation estimates. Their output, therefore, quantifies estimates of water transfer among any combination of locations or areas on Earth (Fig. 1).

The most notable way in which moisture tracking models differ is ~~in~~ their representation of space. The models can be categorized into Eulerian models, which are grid-based, and Lagrangian models, which are trajectory-based. In Eulerian models, moisture flows between discrete grid cells at each time step; in Lagrangian models, individual ~~particles~~ parcels have a location with coordinates that are updated at each time step (Fig. 2).

Besides ~~assumptions~~ choices regarding their grid representation (Eulerian or Lagrangian), all studies that use offline moisture tracking models make ~~assumptions~~ choices regarding vertical mixing of the moisture at the start of the tracking and during its path through the atmosphere, integration time step, interpolation, and resolution of the forcing dataset. In each moisture recycling study, assumptions are chosen such that a suitable trade-off is achieved between accuracy of the representation of the downwind moisture 'footprint' of evaporation (the distribution of precipitation resulting from evaporation from a point or area), amount of data needed, and simulation time (Van der Ent et al., 2013). For example, in Eulerian models, the grid-cell size may be determined by available data, but the integration time step is not. If an explicit numerical scheme is used and the moisture flows within a single time step are much larger or smaller than the length of the grid cell, the model will give incorrect results due to numerical inaccuracies. If the time step is chosen too large, real moisture transport may occur faster than the simulation grid and time step allow for (i.e., if the Courant number $C = \frac{v\Delta t}{\Delta x} > 1$). If the time step is taken too small, numerical diffusion will occur, meaning that moisture transport in the model will be faster than in the forcing data. The advantage of using a Eulerian model, however, is that it is relatively fast for simulations in which moisture is released from a large fraction of the globe. The reason is that they are insensitive to an increase in scale, as all grid cells are updated with the same speed regardless of the amount of moisture present. In Lagrangian models, a larger number of ~~particle~~parcels released per unit of evaporation increases the computing time, making it beneficial to minimize the number of tracked ~~particle~~parcels. However, if this number is chosen too small, the simulation is unable to capture atmospheric moisture convergence and divergence. In both Lagrangian and Eulerian models, the modeller should determine the optimal values to minimize errors.

Often, assumptions and uncertainties in moisture recycling studies are not reported. However, until now, data limitations constrained certain choices such as the minimal spatial resolution~~, which prevented Courant numbers exceeding one in Eulerian models~~. Many recent moisture recycling studies have used ERA-Interim reanalysis data (Van der Ent et al., 2010; Van der Ent and Savenije, 2011; Tuinenburg et al., 2012; Zemp et al., 2014, 2017; Staal et al., 2018, 2020; Wang-Erlandsson et al., 2018), with a temporal resolution of six hours and a spatial resolution of 0.75° (Dee et al., 2011), as their forcing data. However, with the recent replacement of ERA-Interim by the ERA5 dataset, which has a temporal resolution of one hour and a spatial resolution of 0.25°, the trade-offs caused by the assumptions in the moisture recycling models may have shifted. The drawback of using higher-resolution data is that moisture tracking becomes more data-intensive and computing times may increase significantly. ~~We h~~Here we assess the trade-offs and sensitivities in various atmospheric moisture recycling models forced by ERA5 reanalysis data with the aim to identify an optimal model to track the global flows of atmospheric moisture. We ask how atmospheric moisture flows can best be represented given the quality of the presently available reanalysis data. Specifically, we test the sensitivities of downwind precipitation locations to potentially important model assumptions for tracking the evaporation from seven point locations across the globe. These assumptions relate to model structure (Eulerian or Lagrangian and the number of spatial dimensions), forcing data resolution, number of tracked ~~particle~~parcels, interpolation, and model time step. We evaluate the different model version based on a number of hydrologically relevant variables: continental evaporation recycling ratio (the percentage of evaporation that rains down over land), mean absolute latitudinal distance of the moisture transport, mean absolute longitudinal distance, and mean latitudinal and longitudinal change of the tracked moisture. We hypothesize that a Eulerian representation of the atmosphere at the resolution of ERA5 causes deviations in these variables from Lagrangian model versions. We also hypothesize that the improved resolution of vertical wind speeds allows for more accurate moisture recycling estimates, causing those estimates to deviate more with the vertical degradation of the data. Altogether, our analyses present model-dependent uncertainties in moisture recycling estimates across the globe. Based on our results we develop a moisture tracking model for ERA5 reanalysis data with optimal model assumptions and make it available on Github.

2 Methods

This paper tests the sensitivity in atmospheric moisture recycling to different assumptions in atmospheric moisture recycling models. In Section 2.1 we discuss the common principles of the model versions tested in this study and their differences regarding model structure and assumptions. In Section 2.2 we discuss the different simulation options that were tested.

2.1 Model descriptions

The offline atmospheric moisture recycling models used in this study are employed to determine the next precipitation location of evaporation that enters the atmosphere. This is done by using ERA5 atmospheric reanalysis as forcing data (Copernicus Climate Change Service), and effectively use the moisture tracking model as post-processing to this reanalysis. In general,

atmospheric moisture tracking is achieved by following moisture along its path through the atmosphere and keeping track of how much of that moisture rains out where.

The following stepwise procedure is employed to do the moisture tracking. At the starting location ~~For example~~, a given amount of moisture enters the atmosphere through evaporation ~~at some moment and location~~. This is the original amount of moisture to be tracked in a unit that we call parcel.

~~-~~Once the moisture is in the atmosphere, its downwind transport is tracked using ~~with~~ the local wind fields from the forcing data. These winds displace the parcel every time step, effectively creating a trajectory downstream from the original location. During every time step, the moisture budget over the parcel is made. Until precipitation has occurred at the location of the parcel~~moisture~~, all the original evaporated moisture remains in the parcel~~atmosphere~~. However, once there is precipitation at the location of the parcel, a fraction of the moisture (precipitation over precipitable water of the entire atmospheric column, $\frac{P}{PW}$) that is still present in the parcel ~~atmosphere~~ is allocated to rain out in that location. This assumes that all moisture in the atmospheric column has the same probability of raining out. Thus, the ~~fraction~~ amount of ~~the~~ original evaporation remaining ~~in the atmosphere~~ decreases with downwind moisture transport. In this study, the evaporated moisture is tracked until 99% of the moisture is allocated, or the moisture has been in the atmosphere for 30 days, whichever comes first.

The final step in the procedure is to determine the locations of all the allocated moisture. The map of the allocated water represents the downwind precipitation locations of the moisture that evaporated at the starting location. We call this the downwind precipitation footprint.

Despite the~~se~~ ~~communalities~~ commonalities between the model versions, several important assumptions are made that potentially affect the path of moisture through the atmosphere. These are discussed in the rest of this section.

2.1.1 Eulerian and Lagrangian model versions

Atmospheric moisture tracking models are used in either a Eulerian setting (Yoshimura et al., 2004; Dominguez et al., 2006; Van der Ent et al., 2010, 2013; Goessling and Reick, 2011; Singh et al., 2016) or a Lagrangian setting (Stohl et al., 2005; Dirmeyer and Brubaker, 2007; Tuinenburg et al., 2012). In ~~a~~ Eulerian models, the atmosphere through which the evaporated moisture is transported is divided into grid boxes, which may be the same size as the forcing data, but may also be ~~courser~~ coarser than the forcing data, such as in WAM-2layers (Van der Ent et al., 2014), which typically runs on 1.5° resolution. This means that moisture can only flow from one grid cell to one of its direct neighbours, which may be problematic if the time step is either too large or too small relative to the moisture flows between neighbouring cells. ~~If this time step is chosen too large, real moisture transport may occur faster than the simulation grid and time step allow for (i.e., if the Courant number $C = \frac{v\Delta t}{\Delta x} > 1$). If the time step is taken too small, numerical diffusion will occur, meaning that moisture transport in the model will be faster than in the forcing data.~~

In ~~a~~ Lagrangian models, the internal model state is not a model grid, but ~~instead~~ generally a collection of water ~~particle~~parcels. During the simulation, these water ~~particle~~parcels are released and advected with the forcing wind field. The location of the ~~particle~~parcels is not bound to the grid of the forcing data, which means that the Lagrangian model can accommodate large atmospheric moisture fluxes, i.e. ~~particle~~parcels can jump several grid cells of the forcing data in one model time step. The advantage of Lagrangian models is that these do not suffer from the potential numerical inaccuracies of the Eulerian models, and therefore better resemble the moisture transport in the forcing data. The simulation time of Lagrangian models scales with the number of ~~particle~~parcels released, which is low for point releases but high if evaporation from large areas is considered.

2.1.2 Two-dimensional vs. ~~Three~~three-dimensional simulations

For both the Eulerian and the Lagrangian model versions we perform simulations with two- and three-dimensional forcing data in order to test the influence of the vertical variability of atmospheric moisture flows on the moisture tracking results. When the model is forced with three-dimensional data, the horizontal (north/south, which is 'northward' in ERA5, and east/west, which is 'eastward' in ERA5) transport is driven by the wind speed at the pressure level of the ~~particle~~parcel (Lagrangian model) or grid cell (Eulerian model). For ~~both~~ the three-dimensional models, we distribute the released ~~the~~ moisture ~~in the lowest grid box or just above the surface~~over the atmospheric column according to its precipitable water content. During the simulations, there is perfect vertical mixing every 24 hours. For the Lagrangian simulations, this means that the ~~particle~~parcel will be displaced vertically to a random altitude, weighted with the local moisture profile ~~on average~~ every 24 hours (for details, see Section 2.~~1~~2.~~4~~8). For the Eulerian simulations, the tracked moisture is distributed vertically proportional to the local moisture profile every 24 hours.

In case of forcing with two-dimensional data, there is no vertical variability in horizontal transport. The horizontal transport is then driven by the vertical integral of eastward and northward moisture ~~transport~~ flux (unit: kg m^{-1} s^{-1}) divided by the ~~precipitable water times the grid cell length in the direction of transport~~amount of moisture present in the grid cell (unit: kg m^{-2}), resulting in the average moisture flow speed (unit: m s^{-1}) for the entire atmospheric column.

~~All following experiments were carried out with the three-dimensional Lagrangian model version.~~

2.~~2~~1.~~1~~ 3 Forcing data ~~and simulations~~

We force the moisture tracking models with ERA5 hourly atmospheric reanalysis data on 0.25 × 0.25° resolution. We use two-dimensional fields of Total Precipitation, Evaporation, Vertical integral of northward water vapour flux, Vertical integral of eastward water vapour flux and Total Column Water Vapour and three-dimensional fields of Specific Humidity, U and V components of wind speed and Vertical wind speed. For the three-dimensional fields, we use data on 25 pressure levels: every 25 hPa between 1000 hPa and 750 hPa, and every 50 hPa between 750 hPa and 50 hPa, except for the simulations with

vertically degraded forcing data (see Section 2.2.~~2~~5). For the Eulerian model setup, we use the same grid setup as the ERA5 forcing data, which is 0.25° spatial resolution and—for a three dimensional simulation—25 vertical layers.

2.2 Experimental set-up

2.2.1 ~~Forcing data and s~~Simulations and evaluation

For this study, we track evaporation that enters the atmosphere in the first five days of July 2012. All evaporation within this period is accounted for. We continue to track this moisture either until it has all been allocated~~,~~ or the simulation reaches the end of July 2012. We perform forward tracking from seven point sources around the world with different climates and topographies: Chendu in China (30.75°N, 103.5°E), Central Kansas in the USA (39.0°N, 86.0°W), Manaus in Brazil (3.0°S, 60.0°W), Nagpur in India (20.0°N, 80.0°E), Nairobi in Kenya (1.25°S, 36.75°E), Stockholm in Sweden (59.5°N, 18.0°E), and Utrecht in the Netherlands (52.0°N, 5.0°E). We carry out experiments in which we evaluate the model output based on a number of criteria: visual difference in footprint, the continental recycling ratio (the percentage of evaporation that rains down over land; CRR), mean absolute latitudinal distance of the moisture transport, mean absolute longitudinal distance, and mean latitudinal and longitudinal change of the moisture.

For some of the sensitivity tests, these criteria are evaluated against the simulation with the most detailed settings (most parcels, highest resolution, etc.), in which case there is a numerical true estimate. However, for some tests, there is no information to derive a true value. For these tests, the uncertainty remains higher and we derive the sensitivity of moisture recycling to the assumptions.

Despite the fact that simulation times are very much ~~CPU-~~CPU-dependent, we give an estimation of the simulation time necessary (excluding the reading of the forcing data from disk). We compare the results against a baseline model that incorporates as much detail as is possible given the available data: a ~~3D-~~three-dimensional Lagrangian model with interpolated wind speeds and directions, with the high amount of released 10,000 ~~particle~~parcels per mm of evaporation.

We show the results for Manaus in the main text and add figures for footprints of the other locations in the Supplementary Material.

Unless stated otherwise, experiments were carried out with the three-dimensional Lagrangian model version.

2.2.~~4~~ 2 Number of ~~particle~~parcels released per unit of evaporation

For the Lagrangian simulations, the trajectories of the moisture that enters the atmosphere ~~is~~ are simulated through a number of ~~particle~~parcels. This number ~~has needs~~should ~~to~~ be chosen carefully. If the moisture is simulated by a small number of

~~particle~~parcels, atmospheric moisture convergence and divergence cannot be simulated well enough. However, since the simulation times of the Lagrangian simulations scale~~s~~ approximately linearly with the number of ~~particle~~parcels, simulation times may increase too much if the number of ~~particle~~parcels chosen is too large. By default, we release 2,000 moisture ~~particle~~parcels per mm of evaporation for all simulations. However, to test for the effect of different number of ~~particle~~parcels, we performed simulations with 10, 50, 100, 500, 2,000, and 10,000 ~~particle~~parcels per mm and assess their differences. Note that these numbers of parcels are on the higher side of the range of the values typically used in moisture recycling studies (for example, Läderach and Sodemann, 2016; Sorí et al., 2017; García-Herrera et al., 2019).

2.~~1~~2.3 Release height of moisture entering the atmosphere

We also test the differences between releasing moisture from the surface and releasing it well-mixed in the atmospheric column. Naturally, actual evaporation occurs at the surface, but moisture tracking simulations generally assume a well-mixed starting condition, which may affect the precipitation footprints of evaporation sources (Bosilovich, 2002). ~~For the three-dimensional simulations, the initial vertical position of the moisture entering the atmosphere has to be determined. For the Eulerian simulation, we add the moisture to the lowest vertical level, just above the surface. For the Lagrangian simulations, there are~~We test two options~~. E~~: either the ~~particle~~parcels are released just above the surface ~~as in the Eulerian simulations~~, or the ~~particle~~parcels are released at a random vertical location weighted by the local vertical humidity profile, as in (Dirmeyer and Brubaker, 2007).

2.2.~~3~~ 4 Interpolation within the ERA5 space and time grid

If the internal model time step of the moisture tracking model is smaller than the one-hour temporal resolution of the ERA5 forcing data set, the forcing data need to be linearly interpolated in time. For the Lagrangian model, the same is true for the spatial grid: the ~~particle~~parcels may be present on different locations than the grid cell centres of the forcing data. Therefore, linear interpolation on the spatial grid is done as well. As a default, all simulations in this study use linear spatial interpolation, but this interpolation might be costly in terms of simulation time. Therefore, we test how much accuracy is lost if the simulation is run without linear interpolation and the nearest neighbour value of the forcing data is used instead.

2.2.~~2~~ 5 Vertical degradation of the forcing data

The number of vertical layers can have a strong effect on the outcome (Van der Ent et al., 2013), but this has never been tested with the large amount of vertical layers (137 model levels, but output is available on 37 pressure levels, of which this study uses 25) in ERA5. Since the size of the forcing data is substantial ~~on~~ at full resolution (around 200 Gb for one month of forcing data), we are interested in determining the degradation of the results if we degrade the vertical resolution of the forcing data. As alternatives to non-degraded data, we consider six degradations of the forcing data, consisting of two sets of three degradations. In the first set, we use the full atmospheric column, but reduce the vertical resolution to 50 hPa ('hpa50'), 100 hPa ('hpa100') and 200 hPa ('hpa200'). In the second set, we use only forcing data between 1000 hPa and 500 hPa, since this

is where the majority of the moisture is found. The vertical resolutions of this second set are 25 hPa ('5k25'), 50 hPa ('5k50'), and 100 hPa ('5k100').

2.2.6 Horizontal degradation of the forcing data

Similar to the experiments with degraded vertical data, we test the effects of a degraded horizontal resolution of the forcing data. Apart from those at 0.25° resolution, we perform simulations with data on 0.5°, 1.0°, and 1.5° resolution. Instead of interpolating the original forcing data as in the default simulations, for these simulations with horizontal degradations we average the forcing data at 0.25° to the respective degraded resolution.

2.2.~~5~~ 7 Integration time step

The internal time step of the moisture tracking model can influence the simulation result. In the default simulation, it is set at 0.1 h. If it is set at a high value, the simulation time is reduced, but the Lagrangian trajectories may become unrealistic, as the forcing data are assumed to be constant during the entire time step. However, if the time step is chosen very small, simulation times might increase too much with too limited improvement in accuracy. We perform simulations with internal time steps of 0.01 h, 0.05 h, 0.1 h, 0.5 h, ~~and~~ 1 h, 3 h and 6 h. Note that the latter two imply an effective degradation of the temporal resolution of the forcing data. For these cases we used instantaneous data ~~averaged hourly data~~ on wind speed and direction.

The internal time step of the Eulerian simulations is 0.1 h, ensuring numerical stability of the simulations. In ERA5, the absolute eastward wind speed divided by the grid cell size in the east-west direction can be higher than a grid cell length per hour (for July 2012, see Fig. S1). These values are typically larger at higher latitudes than near the equator, given the smaller east-west grid cell size near the poles. Moreover, these values are larger further away from the surface, as ~~the~~ wind speed tends to increase with altitude. The Courant numbers for vertically integrated eastward moisture transport divided by the precipitable water are generally lower than for the individual layers, but can be larger than one grid cell per hour in up to 40° of latitude away from the poles (Fig. S1). This means that if the simulation time step is too large, Courant numbers are larger than unity and moisture cannot be correctly transported on the Eulerian grid. Since decreasing the time step prohibitively increases the simulation time, Eulerian simulations were only done with a time step of 0.1 h.

2.1.~~4~~ 8 Vertical displacement during transport

For the ~~three~~ three-dimensional Lagrangian simulations, the vertical locations of the moisture ~~particle~~parcels ~~has~~ have to be updated during the atmospheric transport. We test several options for this vertical displacement. The first option is to use the ERA5 large-scale vertical wind speed, 'omega', for the vertical displacement. Due to all kinds of sub-grid processes, such as convection, turbulence etc., omega is almost certainly an underestimation of air mixing in the vertical direction. However, the extent to which this occurs and affects moisture recycling is unknown. Hence, apart from using omega as the input for vertical displacement, we also explore options where each parcel of moisture has a certain probability of being assigned a random new

vertical position scaled by the local vertical moisture profile. This is the same procedure used to determine the initial vertical position as in Dirmeyer and Brubaker (2007). This means that moisture ~~particle~~parcels can potentially have a quite strong vertical displacement in a short time. ~~However, this may be realistic if the particle is part of a convective up- or downdraft.~~ During every time step, there is a small probability (dt/mix-strength) of running the vertical displacement. We summarize these stochastic vertical displacement versions of the model by the mix-strength (unit: hours), or average time for one repositioning of one parcel, which is once per hour, once per six hours, once per 24 hours, and once per 120 hours. This procedure ensures that for each parcel, mixing happens on average once in the time period described by the mixing strength and that the mixing happens at random moments during the trajectory. Thus, no biases occur due to mixing at specific prescribed moments.

3 Results

3.1 Differences ~~between~~ among Eulerian and Lagrangian models in two and three dimensions

Comparing two-dimensional and three-dimensional Eulerian and Lagrangian models, we find considerable differences in the 'footprints' of evaporation during July 2012 from our point sources across the globe. The mean difference in continental recycling ratio (CRR) with the baseline model across the source locations was 13 percentage points for the two-dimensional Eulerian model, 11 percentage points for the three-dimensional Eulerian one, 14 percentage points for the two-dimensional Lagrangian one, and zero percentage points for the three-dimensional Lagrangian one. The mean difference in absolute latitudinal transport distance with the baseline model was 4.4° for the two-dimensional Eulerian model, 4.5° for the three-dimensional Eulerian one, 2.2° for the ~~three~~two-dimensional Lagrangian one, and 0.0° degrees for the three-dimensional Lagrangian one. Similarly, the mean difference in absolute longitudinal transport distance was 3.2° for the two-dimensional Eulerian model, 5.3° for the three-dimensional Eulerian one, 2.2° for the ~~three~~two-dimensional Lagrangian one, and 0.0° degrees for the three-dimensional Lagrangian one.

Relative to the baseline model, both the two-dimensional and three-dimensional Eulerian models underestimate atmospheric transport distances in both latitudinal and longitudinal directions (only the absolute longitudinal transport in the case of Nagpur for the two-dimensional model is higher). This relatively close transport does not, however, lead to a consistent overestimation of CRR: for Nagpur, Nairobi and Utrecht the CRR is lower than in the baseline model (Table 1), which is due to geographical reasons (e.g. increased local flow from Nairobi to Lake Victoria, which is not regarded as continental in the ERA5 land mask). The simple, two-dimensional Lagrangian model tends to track moisture flows too far and therefore underestimates CRR in all simulations (Table 1). The three-dimensional Lagrangian model practically performs the same as the baseline model: all CRR estimates are equal with one percentage point accuracy. Only the absolute latitudinal distance for Utrecht and Stockholm and the absolute longitudinal distance for Stockholm were 0.1° higher than that for the baseline model (with 0.1° accuracy) (Table 1).

The case of Manaus illustrates how differences ~~between~~ among models can cause divergent estimates for CRR (Fig. 3). The CRR varies from 38% in the two-dimensional Lagrangian model to 91% in the two-dimensional Eulerian model. The continental recycling ratios for the three-dimensional Eulerian (76%) and three-dimensional Lagrangian (68%) models are closer to that of the baseline model (68%). The ~~low~~ high value for the two-dimensional Eulerian model coincides with its failure to simulate moisture flows across the Andes (Fig. 3A). The two-dimensional Lagrangian model simulates a relatively large flow across the Andes (Fig. 3C) followed by the three-dimensional Lagrangian model (Fig. 4D). Differences in footprints from other sources than Manaus are also substantial (Figs. S2–S7). For example, both Lagrangian models simulate a remote flow from Nairobi up to India, which is entirely absent from the simulations of the Eulerian models (Fig. ~~S4~~S5).

Calculation times differ more among the four model versions than among the simulations in a single model version (Table 1). The simulations took (mean ± standard deviation) 2650 ± 538 CPU seconds with the two-dimensional Eulerian model, 20,470 ± 610 CPU seconds with the three-dimensional Eulerian model, 46 ± 16 CPU seconds with the two-dimensional Lagrangian model, 279 ± 108 CPU seconds with the three-dimensional Lagrangian model, and 1,384 ± 538 CPU seconds with the baseline model. In other words, for the point sources considered, the two-dimensional Lagrangian model is about 30 times faster than the baseline model, the three-dimensional Lagrangian model is five times faster, the two-dimensional Eulerian model is two times slower, and the three-dimensional Eulerian model is 15 times slower than the baseline model.

3.2 Effects of number of tracked ~~particle~~parcels

We compared the effects of tracking different amounts of ~~particle~~parcels in a three-dimensional Lagrangian model: 10, 50, 100, 500, 2,000 (i.e. the three-dimensional model in 3.1), and 10,000 mm^{-1} evaporation ~~h^{-1}~~ (i.e. the baseline model). The number of ~~particle~~parcels has a small effect on the level of detail. The runs with 500 and 2,000 ~~particle~~parcels mm^{-1} ~~h^{-1}~~ did not result in any differences with the baseline model regarding CRR, mean absolute latitudinal distance or mean absolute longitudinal distance. The runs with 100 ~~particle~~parcels mm^{-1} ~~h^{-1}~~ resulted in a difference of 0.1° for both mean absolute latitudinal distance and mean absolute longitudinal distance, but no difference in CRR. The runs with 50 parcels mm^{-1} resulted in a difference of 0.1° for both mean absolute latitudinal distance and mean absolute longitudinal distance, and a difference of one percentage point in CRR. The runs with 10 parcels mm^{-1} resulted in a difference of 0.2° for both mean absolute latitudinal distance and mean absolute longitudinal distance, and a difference of one percentage point in CRR. It can be seen for the simulations for Manaus (Fig. 4) and the other locations (Figs. S8–S13) that the smoothness of the footprints increases with the number of tracked ~~particle~~parcels, but the figures confirm that the patterns in the baseline model are already captured by the simulations with ~~100~~ a relatively small amount of tracked ~~particle~~parcels ~~$mm^{-1} h^{-1}$~~. The simulation times did differ considerably, because they scale ~~roughly~~ almost linearly with the number of tracked ~~particle~~parcels: the simulations with 2,000, 500, ~~and~~ 100, 50, and 10 ~~particle~~parcels mm^{-1} ~~h^{-1}~~ were on average five times, 19 times, ~~and~~ 83 times, 152 times, and 223 times faster than that with 10,000 ~~particle~~parcels mm^{-1} ~~h^{-1}~~.

3.3 Effects of release height

The two different ways of ~~tracked particle~~parcel release in the atmospheric column, moisture release at the surface and moisture release scaled with the vertical moisture profile, led to differences in evaporation footprints. Although the average difference in CRR between both model versions was zero percentage points, the model with moisture profile release produced more distant flows than that with surface release: for all locations it resulted in larger latitudinal flows, with an average of 0.2°; for all locations except Kansas it resulted in larger longitudinal flows as well, by 0.3° on average (both the mean difference and mean absolute difference).

The footprints for the simulations with moisture profile release and surface release are visually very similar (Figs. 5, S14–S19). However, the distance of moisture transport can differ substantially, as exemplified by the mean longitudinal distance of transport from Utrecht, which differed by as much as 0.8° (Fig. S19).

The average calculation time for surface release was 2% ~~faster~~ shorter than for moisture profile release.

3.4 Effects of interpolation

We find effects of interpolation of wind speed~~s~~ and direction in the three-dimensional Lagrangian model on evaporation footprints. The mean absolute difference in CRR between the interpolated and non-interpolated simulations was one percentage point. For Kansas and Nagpur, estimated CRR is lower without interpolation, but in the other cases it was higher without interpolation. Because of this lack of consistent difference, the mean CRR across locations was equal for both model versions (with an accuracy of one percentage point). The absolute latitudinal distance of moisture flows was lower without interpolation, except in the case of Kansas. Both the mean difference and mean absolute difference in latitudinal distance between the two model versions were 0.3°. The absolute longitudinal distance of moisture flows also tended to be lower without interpolation, except in the cases of Kansas and Utrecht. The mean difference in longitudinal distance was 0.1°, and the mean absolute longitudinal difference 0.3°, between the runs with the interpolated and non-interpolated data. The simulations with interpolation were on average 3% slower than those without interpolation. Visually, the differences in evaporation footprint are very small (Figs. 6, S20–S25).

3.5 Effects of degraded vertical atmospheric profile

The six versions of the three-dimensional Lagrangian model with a degraded vertical atmospheric profile ('hpa50', 'hpa100', 'hpa200', '5k25', '5k50', and '5k100') yielded considerable differences in evaporation footprints and their statistics: the output from 'hpa50' differed from that of the baseline model by an average of seven percentage points in CRR, by 1.7° in absolute latitudinal distance, and by 2.2° in absolute longitudinal distance. The average simulation time did not differ (with an accuracy of 1%) from that of the non-degraded model with 2,000 ~~particle~~parcels mm^{-1} ~~h^{-1}~~. The output from 'hpa100' differed from that

of the baseline model by an average of ten percentage points in CRR, by 2.2° in absolute latitudinal distance, and by 3.3° in absolute longitudinal distance. The average simulation time was 1% ~~higher~~ longer than that of the non-degraded model. The output from 'hpa200' differed from that of the baseline model by an average of 17 percentage points in CRR, by 3.7° in absolute latitudinal distance, and by 4.8° in absolute longitudinal distance. The average simulation time was 5% ~~higher~~ longer than that of the non-degraded model. The output from '5k25' differed from that of the baseline model by an average of one percentage point in CRR, by 0.6° in absolute latitudinal distance, and by 0.6° in absolute longitudinal distance. The average simulation time was 4% ~~lower~~ shorter than that of the non-degraded model. The output from '5k50' differed from that of the baseline model by an average of four percentage points in CRR, by 1.0° in absolute latitudinal distance, and by 1.3° in absolute longitudinal distance. The average simulation time was 1% ~~lower~~ shorter than that of the non-degraded model. Finally, the output from '5k100' differed from that of the baseline model by an average of nine percentage points in CRR, by 2.4° in absolute latitudinal distance, and by 3.1° in absolute longitudinal distance. The average simulation time did not differ from that of the non-degraded model.

The effects of adjustments to the vertical profile can also be seen from the evaporation footprints from Manaus, with larger flows southward and eastward (Fig. 7), and from those from the other locations (Figs. S26–S31).

3.6 Effects of degraded horizontal resolution

Degrading the horizontal resolution of the input data affected the results, but less than the degradation in the vertical direction did. The runs with a horizontal resolution of 0.5° differed from the baseline model by one percentage point in CRR, by 0.4° in absolute latitudinal distance, and by 0.5° in absolute longitudinal distance. The runs with a horizontal resolution of 1.0° differed from the baseline model by two percentage points in CRR, by 0.5° in absolute latitudinal distance, and by 0.6° in absolute longitudinal distance. The runs with a horizontal resolution of 1.5° differed from the baseline model by two percentage points in CRR, by 0.7° in absolute latitudinal distance, and by 0.8° in absolute longitudinal distance. Although the patterns of the footprints are not much affected by the horizontal degradations, their level of detail is, with a progressively pixelated output as the resolution becomes coarser (Figs. 8, S32−37). The runs with horizontal degradation were on average slower than without degradation: those at 0.5° were 19% slower than those at 0.25°, those at 1.0° were 32% slower, and those at 1.5° were 76% slower. The reason that the horizontal degradations slowed down the runs is that in this model version, the averaging of forcing data occurred during the simulations.

3.~~6~~ 7 Effect of time steps

We find a low sensitivity of the footprints to reducing the time step dt. For dt = 0.01 h and dt = 0.05 h, we find no difference in CRR, absolute latitudinal distance or absolute longitudinal distance with the baseline model, which has dt = 0.1 h. For dt = 0.5 h and dt = 1 h, we find no difference in CRR, but we do find a small difference of 0.1° in mean absolute longitudinal distance and mean absolute latitudinal difference with the baseline model. For the increase in time step to dt = 3 h, we find a

mean difference in CRR of one percentage point, in absolute latitudinal distance of 0.3°, and in absolute longitudinal distance of 0.4°. For dt = 6 h, we find a mean difference in CRR of two percentage points, in absolute latitudinal distance of 0.3° and in absolute longitudinal distance of 0.6°. The low sensitivity to the chosen time step is confirmed by the ~~practically indistinguishable~~similarity among footprints (Figs. ~~8~~9. ~~S32~~S38–~~S37~~S43).

The runs with dt = 0.01 h were nine times slower than those with dt = 0.1 h. The ones with dt = 0.05 were two times slower, the ones with dt = 0.5 h were four times faster, and the ones with dt = 1 h, dt = 3 h, and dt = 6h were each on average seven times faster.

3.~~7~~ 8 Effects of vertical mixing probabilities

Turbulence may cause considerable vertical mixing in the atmosphere, but ~~Because~~ because the rate of ~~vertical~~ this mixing ~~in the atmosphere~~ is unknown, there can be no baseline model to compare results against. However, we tested the sensitivity of downwind evaporation footprint to eight different rates of vertical mixing. These eight rates consist of those with and without accounting for large-scale vertical flow in the ERA5 reanalysis data (called 'omega') and of four different randomized mixing probabilities: that at which full vertical mixing takes place on average every hour, every six hours, every 24 hours, and every 120 hours.

In the simulations in which we did not account for omega, CRR decreased slightly with average mixing time (i.e. with lower mixing probability): averaged across the source locations, CRR decreases by one percentage point at each stepwise decrease in mixing probability, i.e. from hourly to six-hourly mixing, from six-hourly mixing to daily mixing, and from daily mixing to 120-hourly mixing. The absolute latitudinal transport distance increased from hourly to six-hourly mixing by an average of 0.7°. From six-hourly mixing to 24-hourly mixing this increased by another 0.2°, but from 24-hourly to 120-hourly mixing it decreased by 0.3°. The absolute longitudinal transport distance increased from hourly to six-hourly mixing by an average of 0.5°, increased from six-hourly mixing to 24-hourly mixing by 0.1°, and decreased from 24-hourly mixing to 120-hourly mixing by 0.5°. The larger spread of rainfall locations from the point sources is also clearly visible from the footprints (Figs. ~~9~~10, ~~S38~~S44–~~S43~~S49).

In the simulations in which we did account for omega, CRR decreased much more rapidly with increasing mixing time than in the simulations without omega: from one-hourly to six-hourly mixing, mean CRR decreased by ten percentage points, from six-hourly to daily mixing it decreased by nine percentage points, and from daily to 120-hourly mixing by four percentage points. The absolute latitudinal transport distance increased monotonically with mixing time: from hourly to six-hourly mixing by an average of 2.1°, from six-hourly to daily mixing by 0.6°, and from daily to 120-hourly mixing by 0.1°. The absolute longitudinal transport distance increased from hourly to six-hourly mixing by an average of 2.3°, increased from six-hourly mixing to 24-hourly mixing by 0.8°, and increased from 24-hourly mixing to 120-hourly mixing by 0.4°. Also here, the figures

show that slower vertical mixing increases the area where rainfall depends on evaporation from the studied sources. However, with omega, the rainfall from the sources is more equally distributed within the footprints than without omega. In other words, with omega the footprints show a pattern that is less influenced by diffusion (Figs. ~~9~~10, ~~S38~~S44–~~S43~~S49).

CRR was higher without omega than with omega, a difference that increased with mixing time. At hourly mixing, the mean difference was four percentage points, at six-hourly mixing 13 percentage points, at daily mixing 21 percentage points, and at 120-hourly mixing 25 percentage points. Absolute latitudinal transport distance was higher with omega than without omega, and also this difference increased with mixing time: at hourly mixing, the mean difference was 1.1°, at six-hourly mixing 2.5°, at daily mixing 2.9°, and at 120-hourly mixing 3.3°. Similarly, absolute longitudinal transport distance was consistently higher with omega than without omega: at hourly mixing, the mean difference was 1.5°, at six-hourly mixing 3.3°, at daily mixing 3.9°, and at 120-hourly mixing 4.8°.

When omega was not accounted for, the simulations ran consistently faster with larger mixing times: from hourly to six-hourly mixing by 7%, from six-hourly to daily mixing by 4%, and from daily to 120-hourly mixing by 3%. With omega included, the simulation times did not show a consistent pattern: from hourly to six-hourly mixing it decreased by 2%, but from six-hourly to daily mixing it increased by 2%, and from daily to 120-hourly mixing it increased by another 1%. Averaged across all simulations, the calculations without omega ran 11% faster than those with omega.

4 Discussion

Our aim was to identify an optimal model to track the global flows of atmospheric moisture accurately and efficiently given the best available data. Therefore, we tested how different types of moisture tracking models and their assumptions, forced with the high-resolution ERA5 reanalysis data, produced different 'footprints' of evaporation from source locations. Below, we evaluate our results and use them to propose such an optimal model for which we publish the code.

~~We f~~First, we tested the performance of the two main classes of moisture tracking models, Eulerian and Lagrangian, implemented in two and three spatial dimensions. Eulerian models are grid-based, meaning that at each time step moisture is exchanged between neighbouring grid cells. Lagrangian models track moisture ~~particle~~parcels in continuous space, meaning that at each time step the coordinates of the ~~particle~~parcels are updated. In both cases, the moisture budget is also updated at each time step based on the local precipitation, evaporation and precipitable water. Under the premise that tracking moisture flows becomes more accurate by processing more detailed atmospheric information, we compared our results to a three-dimensional Lagrangian model that is based on as much information as possible and tracks the very large amount of 10,000 ~~particle~~parcels mm^{-1} evaporation~~ h^{-1}~~. For both the Eulerian models and the two-dimensional Lagrangian model, we found large errors (>10 percentage points) in the hydrologically important variable of continental evaporation recycling ratio (CRR), which

is the proportion of evaporated moisture that precipitates on land. Also the distances of moisture transport differed by several degrees for each of these models. For many purposes, such errors are too large, while no benefit was reached regarding simulation time: both the two- and three-dimensional Eulerian models were considerably slower (58 and 73 times) than their Lagrangian equivalents. Thus, for point sources, it can be concluded that Eulerian models, on the resolution of the ERA5 data, are not efficient compared to Lagrangian models. Although a two-dimensional Lagrangian model is fastest, the errors that result from the simplification from three to two dimensions will generally be considered too large. Therefore, we argue that an optimal moisture tracking model using ERA5 data should be a three-dimensional Lagrangian one.

We found that the accuracy of the output of the Lagrangian model was not very sensitive to the amount of ~~particle~~parcels that were tracked for each mm of evaporation ~~per hour~~, while much simulation time can be saved by minimising that amount. At 500 ~~particle~~parcels mm^{-1} ~~h-1~~, the model performance was always as good as when more ~~particle~~parcels were tracked, so we conclude that this is a sufficiently large amount of ~~particle~~parcels to track from point sources for one month. When the moisture is tracked from an area rather than a source, or when a longer study period is concerned, it may be justified to track even fewer ~~particle~~parcels. This is especially the case when one is interested in mean moisture flows rather than highly detailed spatial or temporal differences. The reason is that when a larger amount of evaporation is being considered (i.e. due to an expansion of study area or period), the total amount of ~~particle~~parcels that is tracked can be kept equal with a corresponding reduction of amount of ~~particle~~parcels mm^{-1} ~~h-1~~.

The effect of the height in the atmospheric column at which moisture was released at the start of the simulation resulted in small but measurable differences in the distance of the flows, where moisture release according to the vertical moisture profile yielded longer distances than moisture release at the surface. However, eventually, which model is most suitable depends on the aim of the simulation. Generally, one would want to track evaporation rather than already-present atmospheric moisture. Because evaporation occurs at the surface, and following a similar assessment by Van der Ent et al. (2013), surface release will be the default in our model.

The level of detail of the atmospheric moisture profile matters. We found that especially the degradation of this information introduced significant errors, so we advise against doing that. Similarly, our optimal model does nor reduce the horizontal resolution of the forcing data; although it affected the results to a lesser extent than reducing the vertical resolution, it affected their level of detail. In addition, interpolation of the ERA5 reanalysis data (in three spatial dimensions and the temporal dimension) affected the footprints of evaporation, while its effect on simulation time was marginal. Therefore, we conclude that, even when all available atmospheric layers in ERA5 are used, interpolating the data is still advisable, as did previous studies using Lagrangian models (Tuinenburg et al., 2012, 2014; Van der Ent et al., 2013; Van der Ent and Tuinenburg, 2017; Tuinenburg and van der Ent, 2019).

~~The~~ Smaller time steps for calculation (dt) ~~that we evaluated~~ had little effect on the evaporation footprints and their statistics, but did affect the simulation times significantly. A value of dt = 0.1 h, the time step chosen in the baseline model, gave the same results as smaller values of dt, while increasing it above that did introduce some errors. Therefore, dt = 0.1 h seems optimal.

We tested the effects of eight different assumptions on the speed of mixing in the vertical direction. In this case there is no ideal (baseline) model to compare results ~~against~~with, because the real vertical mixing speed in the atmosphere is unknown, leaving only a relative comparison. Atmospheric reanalysis data do include vertical wind speeds ('omega'), but these are only grid-scale flows and do not include turbulence and convection, which have a large influence on the vertical mixing. However, while it is known that omega underestimates vertical mixing, the extent to which it does is not. Therefore, moisture tracking models may complement the omega-based vertical displacement by using a mixing scheme based on turbulent mixing (Stohl et al., 2005), or disregard omega and either choose another method to account for vertical mixing, such as based on ~~on turbulent mixing,~~ transporting ~~particle~~parcels on isentropic levels (Dirmeyer and Brubaker, 2007), or distribute the moisture budget errors over the vertical layers (WAM-2layers; Van der Ent et al., 2014). In our case, at each time step each moisture ~~particle~~parcel had a certain probability of being relocated within the atmospheric column (randomly, but scaled with the humidity content of the atmosphere). These probabilities were chosen such that on average every hour, six hours, 24 hours, or 120 hours full mixing will have occurred. All four options were assessed with and without additionally accounting for ~~large~~ large-scale vertical wind speed. We found that whether or not omega was accounted for had a large effect on the results. This is to be expected especially when many vertical layers are used between which flows take place. The effect of omega declines with more rapid randomized mixing. Because of the uncertainties related to vertical mixing, we leave the mixing time and inclusion of omega as an option in the model. As default we take a mixing time of 24 h without omega. The rationale for choosing 24 h is twofold: first, it is within the range (6−24 h) where the results are relatively robust to the choice of mixing time; second, atmospheric mixing follows a diurnal cycle (Tuinenburg and van der Ent, 2019), which is averaged out by mixing continuously with a full mixing every 24 hours. While w~~W~~e assume that this speed of mixing is rapid enough to supersede larger-scale vertical flows so as to simplify the model and exclude omega, the moisture tracking results can be very sensitive to vertical mixing. This study does not use a true reference to compare the vertical mixing assumptions against. This means that it is hard to justify a definitive choice. Experiments using tracers could be devised to constrain the uncertainty regarding the vertical transport further and may lead to inclusion of omega or a more physically based mixing.

The uncertainty regarding the process of vertical mixing combined with the sensitivity of moisture recycling to the vertical mixing introduces a corresponding uncertainty in any moisture recycling result. Based on our sensitivity analysis, it can be expected that in this respect alone, the uncertainty in transport distance is limited to several tenths of degrees in both latitudinal and longitudinal directions. Continental recycling ratios differed only by a few percentage points depending on mixing assumptions. In case randomized mixing, representing turbulence, would need to be complemented by omega, the uncertainty

becomes very sensitive to the level of turbulence. We found that continental recycling ratios could differ in the range of ten percentage points and transport distances by several degrees. These are large uncertainties, so we argue that a better constraint of vertical mixing could greatly improve the accuracy of moisture tracking models in the future.

We used a selection of point sources and tracked the destinations of their evaporation for a single arbitrary month (July 2012). Although moisture recycling can strongly vary both spatially and temporally (Brubaker et al., 1993; Gimeno et al., 2012), we chose to focus on the spatial variation to cover a range of terrains, latitudes, and wind patterns, as the effects of different model assumptions may become apparent especially by studying different regions ~~especially~~ (Goessling and Reick, 2013). ~~The~~ Here the purpose ~~here~~ was to compare the performance of different models and their assumptions for a range of hydrological statistics as well as simulation time. Thus, the footprints may differ in their representativeness for the respective locations, but they are helpful in visualising the consequences of different assumptions in atmospheric moisture tracking.

Many moisture recycling studies have used low-spatial-resolution Eulerian models (typically 1.5° with one or two vertical layers) forced with ERA-Interim reanalysis data (Dee et al., 2011). When Eulerian models are run on coarse spatial scales, the risk of numerical instability due to large Courant numbers is contained. However, we ~~advise to be cautious~~recommend caution when developing Eulerian models based on the resolution of ERA5 data, because of the large moisture fluxes compared to the grid cell size and the numerical dispersion when this is mitigated by using smaller time steps. Downgrading the data to coarser resolutions such as 1.5° would circumvent the problem, but comes at the cost of ~~large~~ loss~~es~~ of information. The Lagrangian model we present here does not suffer from numerical issues caused by a grid-based approach, and can be expected to become more accurate with the availability of more accurate atmospheric data.

The facts that the errors in moisture recycling estimates depend~~ed~~ on the study area and that we tracked only moisture for one month that evaporated during five days mean~~s~~ that one should be cautious with generalizing the implications of these outcomes. An example of moisture flow above complex terrain is ~~the evaporation~~that from Manaus in the Amazon, where westward moisture flows are blocked by the Andes and partially diverted southward, but also partially pass over the mountain range and precipitate over the Pacific Ocean. We argue that for areas with relatively complex terrain in particular, three-dimensional Lagrangian models are most suitable because these describe atmospheric moisture transport better under situations with strong vertical variability in horizontal moisture transport.

5 Conclusions

Moisture recycling science has a long history, with gradually improved models depending on the state-of-the-art data, from early one-dimensional work to explicit moisture tracking in two-dimensional and three-dimensional Eulerian and Lagrangian models. This model development has gone hand-in-hand with improved data development. With the development of the new

ERA5 reanalysis data, data limitations have ~~reduced~~ decreased considerably. We evaluated the performance of different model types given these new data. Our comprehensive sensitivity analysis led us to propose an optimal three-dimensional Lagrangian moisture tracking model – one that is able to produce highly detailed 'footprints' of evaporation and that is devoid of unnecessary complexity. It therefore runs relatively fast with negligible loss of information. Furthermore, we conclude that in our and any other moisture tracking method, the vertical mixing assumptions are the most significant. Therefore, we recommend to focus further research on this vertical moisture transport. Finally, w~~W~~e make the code for our ~~this~~ model freely available.

Code and data availability

The model code is available at: https://github.com/ObbeTuinenburg/U-Track. The ERA5 data are available at: https://cds.climate.copernicus.eu/cdsapp#!/home.

Author contributions

OAT conceived and designed the study. Both authors carried out the study, interpreted the results and wrote the paper.

Acknowledgments

We thank Ruud van der Ent, Ingo Fetzer, Line Gordon and Lan Wang-Erlandsson for useful discussions. We thank both reviewers and Jolanda Theeuwen for helpful comments on the manuscript. We thank the Bolin Centre for Climate Research for funding the stay of OAT at the Stockholm Resilience Centre. OAT acknowledges support from the research program Innovational Research Incentives Scheme Veni (016.veni.171.019), funded by the Netherlands Organisation for Scientific Research (NWO). AS acknowledges support from the European Research Council project Earth Resilience in the Anthropocene (743080 ERA).

References

Bosilovich, M. G.: On the vertical distribution of local and remote sources of water for precipitation, Meteorology and Atmospheric Physics, 80(1), 31–41, doi:10.1007/s007030200012, 2002.

Brubaker, K. L., Entekhabi, D. and Eagleson, P. S.: Estimation of continental precipitation recycling, Journal of Climate, 6(6), 1077–1089, doi:10.1175/1520-0442(1993)006<1077:EOCPR>2.0.CO;2, 1993.

Burde, G. I. and Zangvil, A.: The estimation of regional precipitation recycling. Part I: review of recycling models, J. Climate, 14(12), 2497–2508, doi:10.1175/1520-0442(2001)014<2497:TEORPR>2.0.CO;2, 2001.

Copernicus Climate Change Service (C3S): ERA5: Fifth generation of ECMWF atmospheric reanalyses of the global climate, Copernicus Climate Change Service Climate Data Store (CDS), doi:https://cds.climate.copernicus.eu/cdsapp#!/home, n.d.

Dee, D. P., Uppala, S. M., Simmons, A. J., Berrisford, P., Poli, P., Kobayashi, S., Andrae, U., Balmaseda, M. A., Balsamo, G. and Bauer, P.: The ERA-Interim reanalysis: configuration and performance of the data assimilation system, Quarterly Journal of the Royal Meteorological Society, 137(656), 553–597, doi:10.1002/qj.828, 2011.

Dirmeyer, P. A. and Brubaker, K. L.: Characterization of the global hydrologic cycle from a back-trajectory analysis of atmospheric water vapor, Journal of Hydrometeorology, 8(1), 20–37, doi:10.1175/JHM557.1, 2007.

Dominguez, F., Kumar, P., Liang, X.-Z. and Ting, M.: Impact of atmospheric moisture storage on precipitation recycling, Journal of Climate, 19(8), 1513–1530, doi:10.1175/JCLI3691.1, 2006.

García-Herrera, R., Garrido-Perez, J. M., Barriopedro, D., Ordóñez, C., Vicente-Serrano, S. M., Nieto, R., Gimeno, L., Sorí, R. and Yiou, P.: The European 2016/17 drought, Journal of Climate, 32(11), 3169–3187, doi:10.1175/JCLI-D-18-0331.1, 2019.

Gimeno, L., Stohl, A., Trigo, R. M., Dominguez, F., Yoshimura, K., Yu, L., Drumond, A., Durán-Quesada, A. M. and Nieto, R.: Oceanic and terrestrial sources of continental precipitation, Reviews of Geophysics, 50(4), doi:10.1029/2012RG000389, 2012.

Goessling, H. F. and Reick, C. H.: What do moisture recycling estimates tell us? Exploring the extreme case of non-evaporating continents, Hydrology and Earth System Sciences, 15, 3217–3235, 2011.

Goessling, H. F. and Reick, C. H.: On the "well-mixed" assumption and numerical 2-D tracing of atmospheric moisture, Atmospheric Chemistry and Physics, 13, 5567–5585, doi:10.5194/acp-13-5567-2013, 2013.

Keys, P. W., Wang-Erlandsson, L. and Gordon, L. J.: Revealing invisible water: moisture recycling as an ecosystem service, PloS ONE, 11(3), e0151993, doi:10.1371/journal.pone.0151993, 2016.

Keys, P. W., Wang-Erlandsson, L. and Gordon, L. J.: Megacity precipitationsheds reveal tele-connected water security challenges, PLoS ONE, 13(3), e0194311, doi:10.1371/journal.pone.0194311, 2018.

Läderach, A. and Sodemann, H.: A revised picture of the atmospheric moisture residence time, Geophysical Research Letters, 43(2), 924–933, doi:10.1002/2015GL067449, 2016.

Singh, H. A., Bitz, C. M., Nusbaumer, J. and Noone, D. C.: A mathematical framework for analysis of water tracers: Part 1: Development of theory and application to the preindustrial mean state, Journal of Advances in Modeling Earth Systems, 8(2), 991–1013, doi:10.1002/2016MS000649, 2016.

Sorí, R., Nieto, R., Vicente-Serrano, S. M., Drumond, A. and Gimeno, L.: A Lagrangian perspective of the hydrological cycle in the Congo River basin, Earth System Dynamics, 8(3), 653–675, doi:10.5194/esd-8-653-2017, 2017.

Spracklen, D. V., Baker, J. C. A., Garcia-Carreras, L. and Marsham, J.: The effects of tropical vegetation on rainfall, Annual Review of Environment and Resources, 43(1), 193–218, doi:10.1146/annurev-environ-102017-030136, 2018.

Staal, A., Tuinenburg, O. A., Bosmans, J. H. C., Holmgren, M., van Nes, E. H., Scheffer, M., Zemp, D. C. and Dekker, S. C.: Forest-rainfall cascades buffer against drought across the Amazon, Nature Climate Change, 8(6), 539–543, doi:10.1038/s41558-018-0177-y, 2018.

Staal, A., Flores, B. M., Aguiar, A. P. D., Bosmans, J. H. C., Fetzer, I. and Tuinenburg, O. A.: Feedback between drought and deforestation in the Amazon, Environmental Research Letters, doi:10.1088/1748-9326/ab738e, 2020.

Stohl, A., Forster, C., Frank, A., Seibert, P. and Wotawa, G.: The Lagrangian particle dispersion model FLEXPART version 6.2, Atmospheric Chemistry and Physics, 5(9), 2461–2474, doi:10.5194/acp-5-2461-2005, 2005.

Tuinenburg, O. A. and van der Ent, R. J.: Land surface processes create patterns in atmospheric residence time of water, Journal of Geophysical Research: Atmospheres, 124(2), 583–600, doi:10.1029/2018JD028871, 2019.

Tuinenburg, O. A., Hutjes, R. W. A. and Kabat, P.: The fate of evaporated water from the Ganges basin, Journal of Geophysical Research: Atmospheres, 117(D1), D01107, doi:10.1029/2011JD016221, 2012.

Tuinenburg, O. A., Hutjes, R. W. A., Stacke, T., Wiltshire, A. and Lucas-Picher, P.: Effects of irrigation in India on the atmospheric water budget, Journal of Hydrometeorology, 15(3), 1028–1050, doi:10.1175/JHM-D-13-078.1, 2014.

Van der Ent, R. J. and Savenije, H. H. G.: Length and time scales of atmospheric moisture recycling, Atmospheric Chemistry and Physics, 11(5), 1853–1863, doi:10.5194/acp-11-1853-2011, 2011.

Van der Ent, R. J. and Tuinenburg, O. A.: The residence time of water in the atmosphere revisited, Hydrology and Earth System Sciences, 21(2), 779–790, doi:10.5194/hess-21-779-2017, 2017, 2017.

Van der Ent, R. J., Savenije, H. H. G., Schaefli, B. and Steele-Dunne, S. C.: Origin and fate of atmospheric moisture over continents, Water Resources Research, 46, W09525, doi:10.1029/2010WR009127, 2010.

Van der Ent, R. J., Tuinenburg, O. A., Knoche, H. R., Kunstmann, H. and Savenije, H. H. G.: Should we use a simple or complex model for moisture recycling and atmospheric moisture tracking?, Hydrology and Earth System Sciences, 17(12), 4869–4884, doi:10.5194/hess-17-4869-2013, 2013.

Van der Ent, R. J., Wang-Erlandsson, L., Keys, P. W. and Savenije, H. H. G.: Contrasting roles of interception and transpiration in the hydrological cycle-Part 2: Moisture recycling, Earth System Dynamics, 5(2), 471–489, 2014.

Wang-Erlandsson, L., Fetzer, I., Keys, P. W., van der Ent, R. J., Savenije, H. H. G. and Gordon, L. J.: Remote land use impacts on river flows through atmospheric teleconnections, Hydrology and Earth System Sciences, 22(8), 4311–4328, doi:10.5194/hess-22-4311-2018, 2018.

Yoshimura, K., Oki, T., Ohte, N. and Kanae, S.: Colored moisture analysis estimates of variations in 1998 Asian monsoon water sources, Journal of the Meteorological Society of Japan. Ser. II, 82(5), 1315–1329, doi:10.2151/jmsj.2004.1315, 2004.

Zemp, D. C., Schleussner, C. F., Barbosa, H. M. J., van der Ent, R. J., Donges, J. F., Heinke, J., Sampaio, G. and Rammig, A.: On the importance of cascading moisture recycling in South America, Atmospheric Chemistry and Physics, 14(23), 13337–13359, doi:10.5194/acp-14-13337-2014, 2014.

Zemp, D. C., Schleussner, C. F., Barbosa, H. M. J., Hirota, M., Montade, V., Sampaio, G., Staal, A., Wang-Erlandsson, L. and Rammig, A.: Self-amplified Amazon forest loss due to vegetation-atmosphere feedbacks, Nature Communications, 8, 14681, doi:10.1038/ncomms14681, 2017.

Tables and Figures

Table 1: Continental recycling ratio (%), absolute latitudinal distance (°), absolute longitudinal distance (°), mean latitudinal change (°), mean longitudinal change (°), and calculation time (CPU seconds) for the baseline, two-dimensional Eulerian, three-dimensional Eulerian, two-dimensional Lagrangian, and three-dimensional Lagrangian model versions for each of the seven point sources ~~considered~~ in July 2012. For continental recycling ratio, absolute latitudinal distance, absolute longitudinal distance, mean latitudinal change, and mean longitudinal change, the absolute differences with the baseline model are also given.

	Baseline	2D Eulerian	3D Eulerian	2D Lagrangian	3D Lagrangian
			Continental recycling ratio (%)		
Chendu	94	99	96	72	94
Kansas	44	51	47	38	44
Manaus	68	91	76	38	68
Nagpur	94	78	80	77	94
Nairobi	87	73	62	75	87
Stockholm	63	83	80	51	63
Utrecht	45	35	34	42	44
Mean diff.	–	13	11	14	0
			Absolute latitudinal distance (°)		
Chendu	2.6	1.1	1.0	5.8	2.6
Kansas	7.2	1.7	2.8	7.6	7.2
Manaus	4.8	0.8	1.4	6.6	4.8
Nagpur	5.1	1.7	1.2	5.9	5.1
Nairobi	7.3	4.0	2.3	14.8	7.3
Stockholm	7.4	2.6	2.5	8.1	7.5
Utrecht	11.4	2.9	3.1	12.4	11.5
Mean diff.	–	4.4	4.5	2.2	0.0
			Absolute longitudinal distance (°)		
Chendu	3.4	0.8	1.7	6.2	3.4
Kansas	19.6	9.2	9.3	20.6	19.6
Manaus	15.0	8.6	7.5	14.3	15.0
Nagpur	5.1	5.7	4.3	6.6	5.1
Nairobi	6.1	1.9	2.4	11.0	6.1
Stockholm	15.0	7.0	6.0	16.8	15.1

Utrecht	16.0	13.7	11.7	18.2	16.0
Mean diff.	–	3.2	5.3	2.2	0.0
		Mean latitudinal change (°)			
Chendu	2.3	0.6	0.1	5.6	2.3
Kansas	4.0	1.3	1.8	4.5	4.0
Manaus	1.5	0.4	0.0	4.3	1.5
Nagpur	4.9	1.3	1.3	5.8	4.9
Nairobi	7.2	4.0	2.2	14.8	7.2
Stockholm	1.3	2.6	2.3	0.0	1.3
Utrecht	6.1	2.8	3.1	8.5	6.0
Mean diff.	–				
		Mean longitudinal change (°)			
Chendu	2.4	0.6	0.9	6.0	2.4
Kansas	15.2	9.2	8.5	14.6	15.2
Manaus	–14.3	–8.6	–7.4	–14.3	–14.4
Nagpur	3.6	5.7	3.8	5.2	3.6
Nairobi	3.0	–1.6	0.8	6.2	3.0
Stockholm	11.1	–0.6	–1.4	13.3	11.1
Utrecht	15.3	11.3	9.8	17.9	15.4
Mean diff.	–	5.1	4.8	2.0	0.0
		Calculation time (CPU seconds)			
Chendu	821	2612	20366	35	166
Kansas	2182	2601	20229	69	439
Manaus	1553	2670	21713	53	313
Nagpur	808	2655	20275	25	163
Nairobi	924	2663	20733	31	186
Stockholm	1623	2611	20140	52	327
Utrecht	1774	2741	19836	57	357

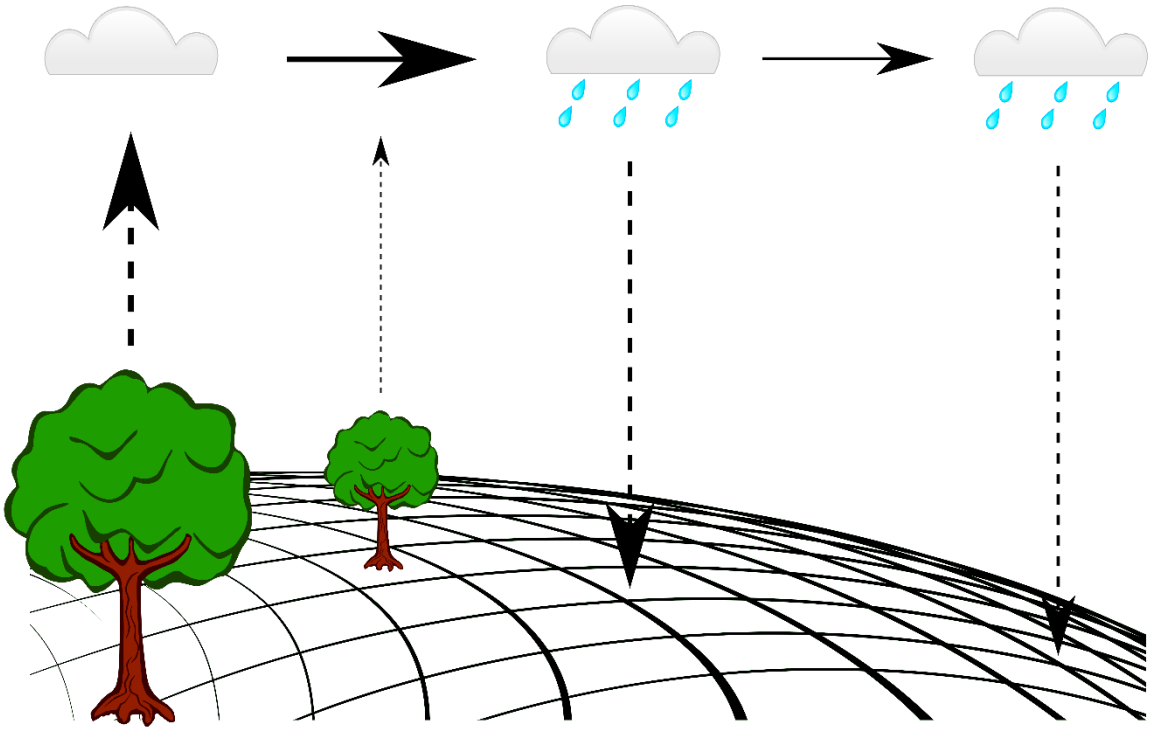

Figure 1: Moisture tracking from source to sink. All moisture tracking models use atmospheric reanalysis data to simulate the locations of moisture. At each time step, moisture budgets are updated based on wind speed and directions (horizontal arrows), evaporation (dashed arrows up) and precipitation (dashed arrows down). This leads to source-to-sink estimates of atmospheric moisture flows, such as the evaporation footprints and basin recycling ratios in this study.

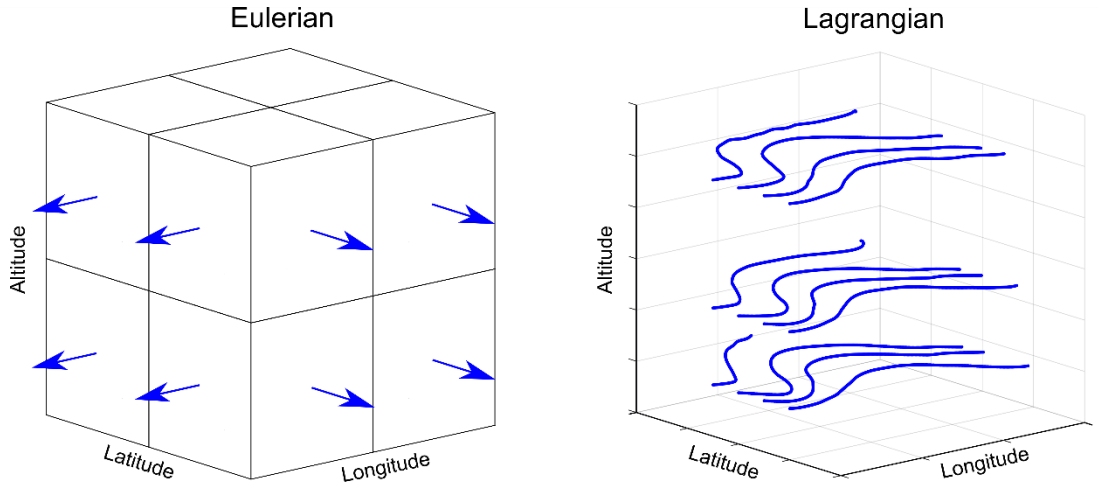

Figure 2: The difference between Eulerian and Lagrangian moisture tracking models. A) Eulerian models are grid-based, meaning that the study area is divided into a two- or three-dimensional grid of cells. At each time step, the tracked moisture content of each grid cell is updated based on estimated cell-to-cell winds, precipitation, and evaporation. B) Lagrangian models are trajectory-based, meaning that a number of moisture parcels have coordinates. At each time step, the coordinates and the tracked moisture content of the parcels are updated based on point-based wind flows, precipitation, and evaporation.

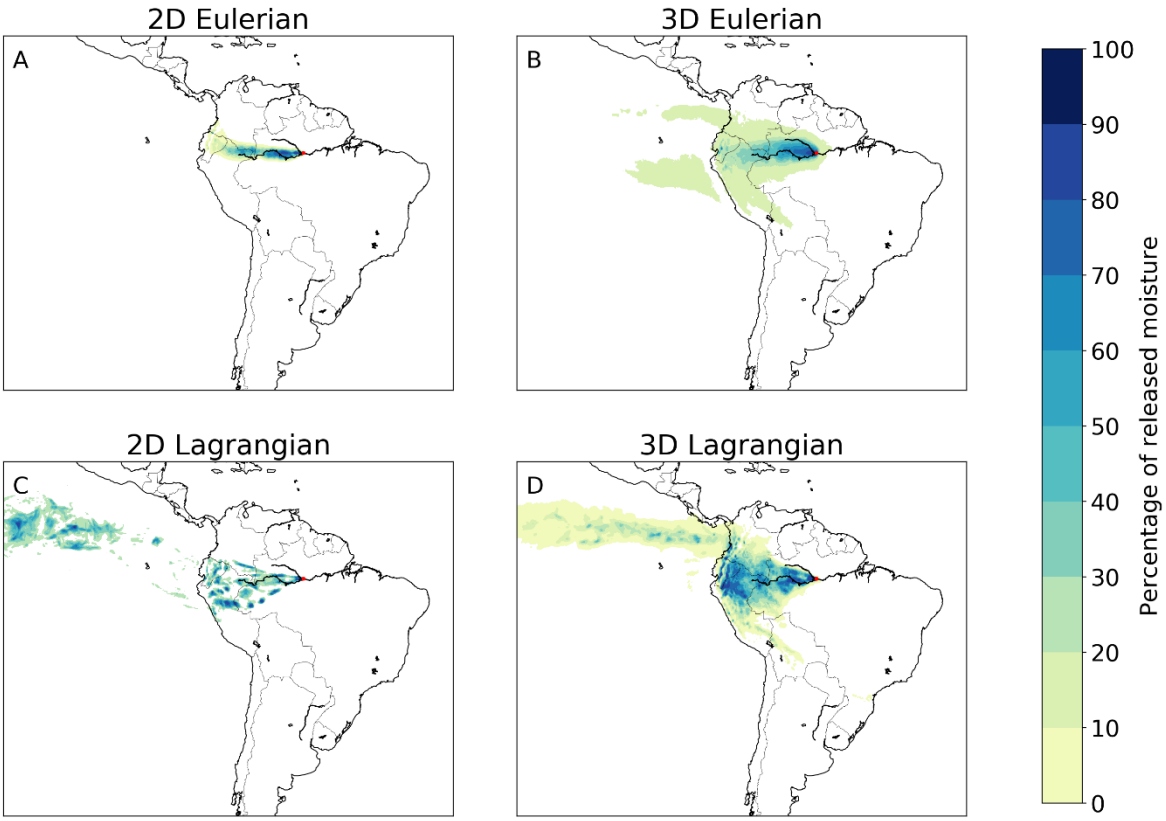

Figure 3: Different footprints of moisture releases from Manaus in July 2012 in two-dimensional and three-dimensional Eulerian and Lagrangian models. A) Two-dimensional Eulerian, with a mean latitudinal moisture flow of 0.4° in northerly direction and mean longitudinal flow of 8.6° in westerly direction; B) Three-dimensional Eulerian, with a mean latitudinal moisture flow of 0.0° in northerly/southerly direction and mean longitudinal flow of 7.4° in westerly direction; C) Two-dimensional Lagrangian, with a mean latitudinal moisture flow of 4.3° in northerly direction and mean longitudinal flow of 14.3° in westerly direction; D) Three-dimensional Lagrangian, with a mean latitudinal moisture flow of 1.5° in northerly direction and mean longitudinal flow of 14.4° in westerly direction.

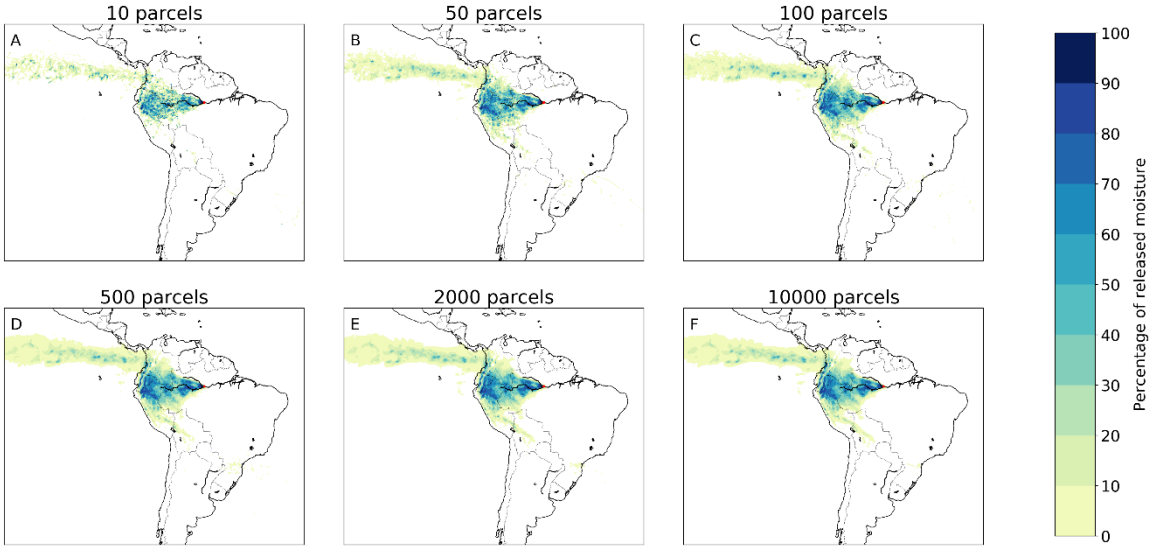

Figure 4: Different footprints of moisture releases from Manaus in July 2012 in a three-dimensional Lagrangian model with 10, 50, 100, 500, 2,000, and 10,000 tracked ~~particle~~parcels mm^{-1}~~ h-1~~). A) 10 parcels, with a mean latitudinal moisture flow of 1.3° in northerly direction and mean longitudinal flow of 14.2° in westerly direction; B) 50 parcels, with a mean latitudinal moisture flow of 1.6° in northerly direction and mean longitudinal flow of 14.3° in westerly direction; ~~A~~C) 100 ~~particle~~parcels, with a mean latitudinal moisture flow of 1.4° in northerly direction and mean longitudinal flow of 14.2° in westerly direction; ~~B~~D) 500 ~~particle~~parcels, with a mean latitudinal moisture flow of 1.4° in northerly direction and mean longitudinal flow of 14.3° in westerly direction; ~~C~~E) 2,000 ~~particle~~parcels, with a mean latitudinal moisture flow of 1.5° in northerly direction and mean longitudinal flow of 14.4° in westerly direction; ~~D~~F) 10,000 ~~particle~~parcels, with a mean latitudinal moisture flow of 1.5° in northerly direction and mean longitudinal flow of 14.3° in westerly direction.

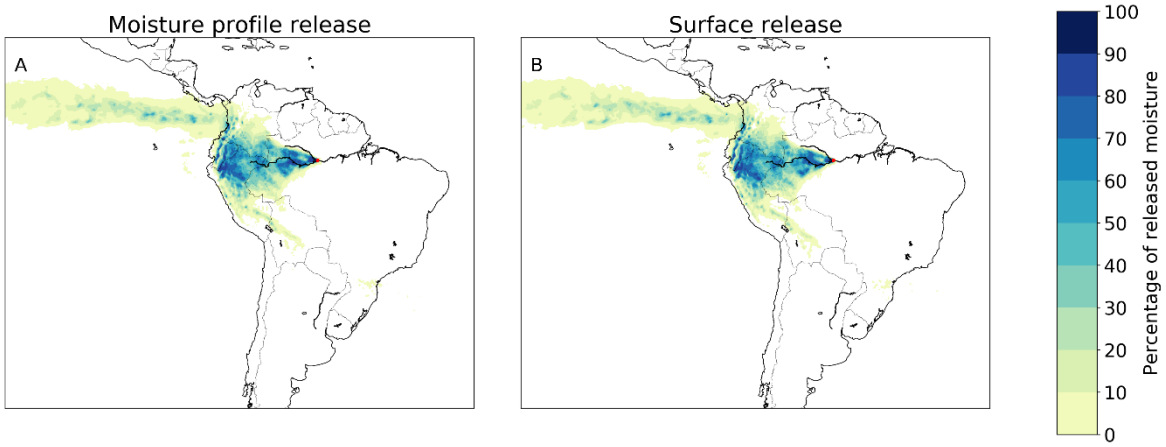

Figure 5: Different footprints of moisture releases from Manaus in July 2012 in a three-dimensional Lagrangian model with moisture released according to the vertical moisture profile of the atmosphere and moisture released at the surface. A) Release according to the moisture profile, with a mean latitudinal moisture flow of 1.5° in northerly direction and mean longitudinal flow of 14.4° in westerly direction; B) Release at the surface, with a mean latitudinal moisture flow of 1.3° in northerly direction and mean longitudinal flow of 14.2° in westerly direction.

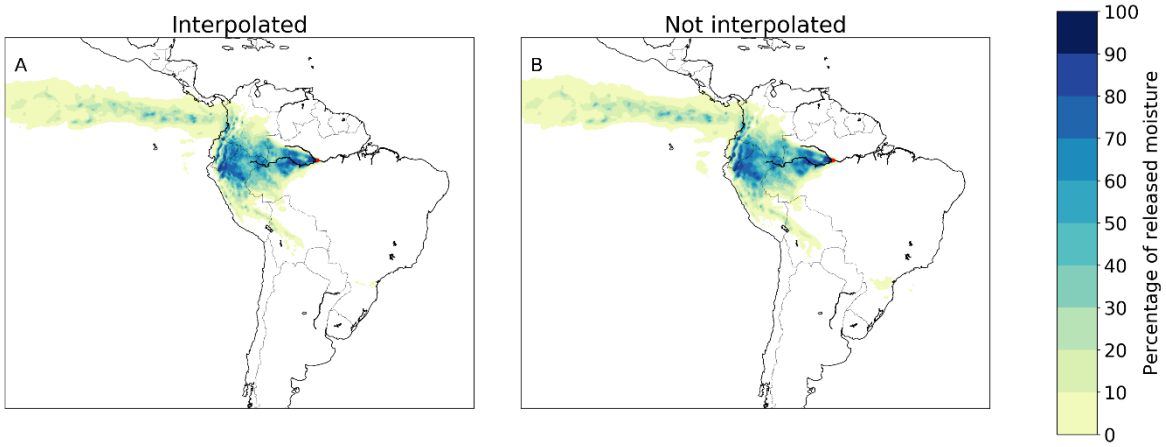

Figure 6: Different footprints of moisture releases from Manaus in July 2012 in a three-dimensional Lagrangian model with and without interpolation of wind speed and directions. A) Interpolated, with a mean latitudinal moisture flow of 1.5° in northerly direction and mean longitudinal flow of 14.4° in westerly direction; B) Not interpolated, with a mean latitudinal moisture flow of 1.4° in northerly direction and mean longitudinal flow of 14.3° in westerly direction.

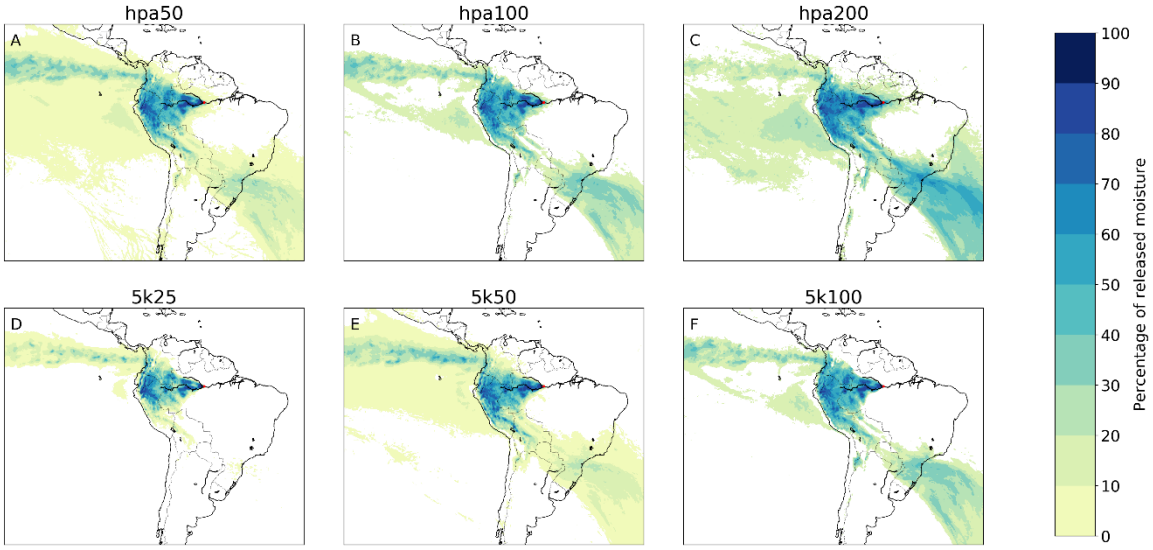

Figure 7: Different footprints of moisture releases from Manaus in July 2012 in a three-dimensional Lagrangian model with different degradations of the vertical moisture profile. A) hpa50, with a mean latitudinal moisture flow of 2.8° in southerly direction and mean longitudinal flow of 11.0° in westerly direction; B) hpa100, with a mean latitudinal moisture flow of 5.3° in southerly direction and mean longitudinal flow of 9.2° in westerly direction; C) hpa200, with a mean latitudinal moisture flow of 17.6° in southerly direction and mean longitudinal flow of 1.8° in westerly direction; D) 5k25, with a mean latitudinal moisture flow of 1.7° in northerly direction and mean longitudinal flow of 14.4° in westerly direction; E) 5k50, with a mean latitudinal moisture flow of 2.8° in southerly direction and mean longitudinal flow of 11.6° in westerly direction; F) 5k100, with a mean latitudinal moisture flow of 5.1° in southerly direction and mean longitudinal flow of 9.6° in westerly direction.

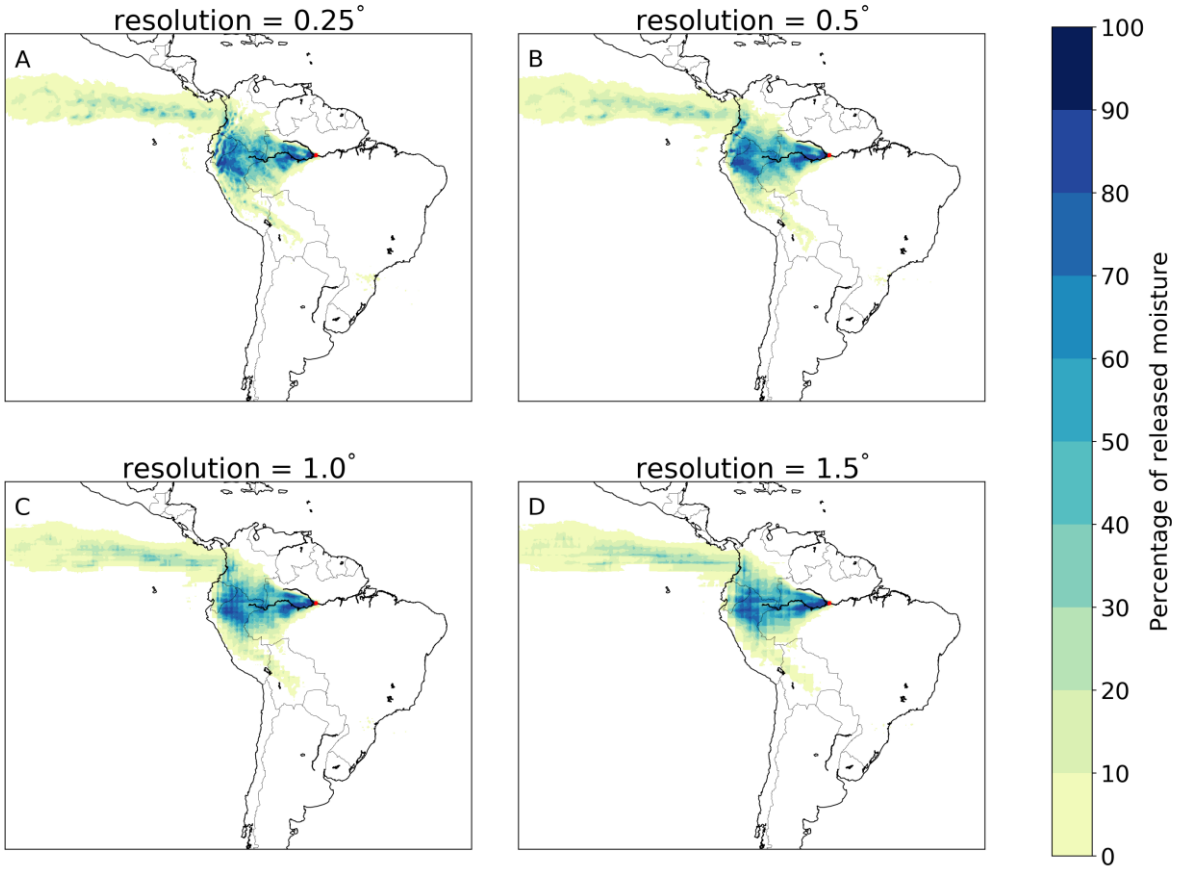

Figure 8: Different footprints of moisture releases from Manaus in July 2012 in a three-dimensional Lagrangian model with different horizontal resolutions. A) 0.25°, with a mean latitudinal moisture flow of 1.5° in northerly direction and mean longitudinal flow of 14.4° in westerly direction; B) 0.5°, with a mean latitudinal moisture flow of 1.6° in northerly direction and mean longitudinal flow of 14.3° in westerly direction; C) 1.0°, with a mean latitudinal moisture flow of 1.7° in northerly direction and mean longitudinal flow of 14.2° in westerly direction; D) 1.5°, with a mean latitudinal moisture flow of 1.7° in northerly direction and mean longitudinal flow of 14.2° in westerly direction.

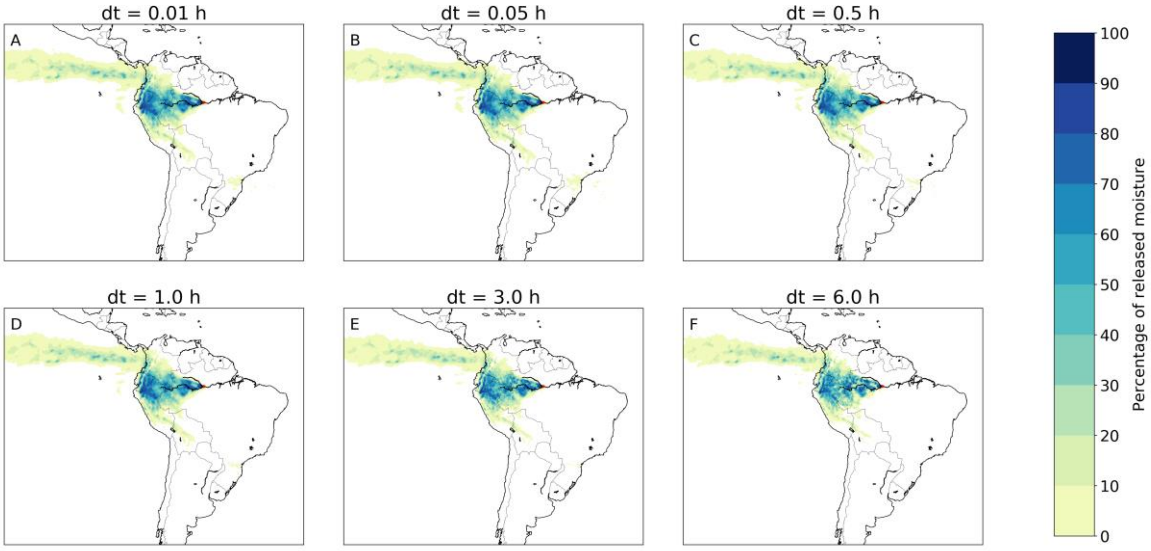

Figure ~~89~~: Different footprints of moisture releases from Manaus in July 2012 in a three-dimensional Lagrangian model with different time steps (dt): 0.01 hours, 0.05 hours, 0.5 hours, ~~and~~ 1.0 hours, 3.0 hours, and 6.0 hours. A) 0.01 h, with a mean latitudinal moisture flow of 1.4° in northerly direction and mean longitudinal flow of 14.3° in westerly direction; B) 0.05 h, with a mean latitudinal moisture flow of 1.3° in northerly direction and mean longitudinal flow of 14.2° in westerly direction; C) 0.5 h, with a mean latitudinal moisture flow of 1.5° in northerly direction and mean longitudinal flow of 14.4° in westerly direction; D) 1.0 h, with a mean latitudinal moisture flow of 1.5° in northerly direction and mean longitudinal flow of 14.5° in westerly direction~~.~~; E) 3.0 h, with a mean latitudinal moisture flow of 1.6° in northerly direction and mean longitudinal flow of 14.3° in westerly direction; F) 6.0 h, with a mean latitudinal moisture flow of 1.7° in northerly direction and mean longitudinal flow of 14.2° in westerly direction.

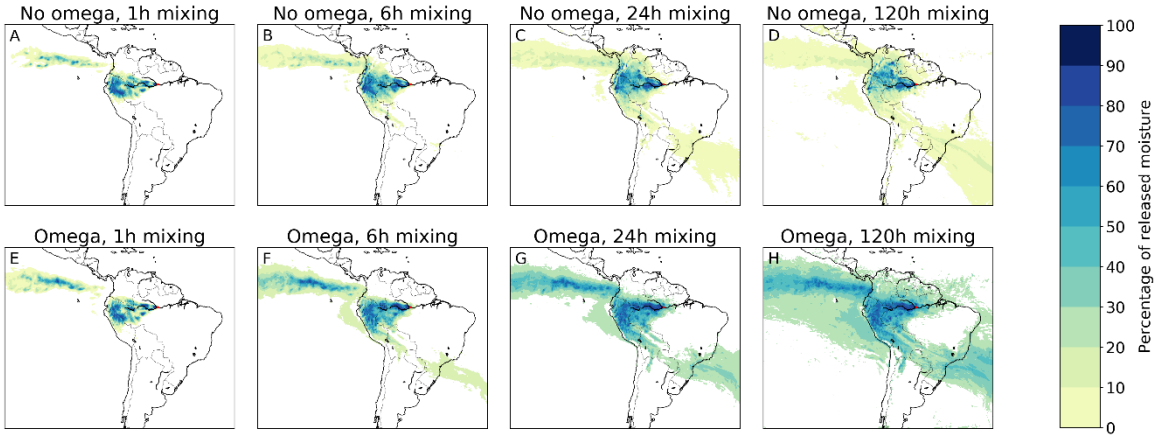

Figure ~~9~~10: Different footprints of moisture releases from Manaus in July 2012 in a three-dimensional Lagrangian model with different mixing assumptions: without and with accounting for the three-dimensional moisture flows in the ERA5 data (termed omega), and with different assumptions of additional vertical mixing speed (full mixing every 1 h, every 6 h, every 24 h, and every 120 h). A) Without omega, every 1 h mixing, with a mean latitudinal moisture flow of 2.4° in northerly direction and mean longitudinal flow of 16.4° in westerly direction; B) Without omega, every 6 h mixing, with a mean latitudinal moisture flow of 1.4° in northerly direction and mean longitudinal flow of 14.3° in westerly direction; C) Without omega, every 24 h mixing, with a mean latitudinal moisture flow of 0.1° in northerly direction and mean longitudinal flow of 11.6° in westerly direction; D) Without omega, every 120 h mixing, with a mean latitudinal moisture flow of 1.2° in northerly direction and mean longitudinal flow of 9.0° in westerly direction; E) With omega, every 1 h mixing, with a mean latitudinal moisture flow of 3.0° in northerly direction and mean longitudinal flow of 16.7° in westerly direction; F) With omega, every 6 h mixing, with a mean latitudinal moisture flow of 0.3° in northerly direction and mean longitudinal flow of 14.5° in westerly direction; G) With omega, every 24 h mixing, with a mean latitudinal moisture flow of 5.0° in northerly direction and mean longitudinal flow of 12.3° in westerly direction; H) With omega, every 120 h mixing, with a mean latitudinal moisture flow of 6.9° in northerly direction and mean longitudinal flow of 11.5° in westerly direction.

Supplementary Material

Tracking the global flows of atmospheric moisture

Obbe A. Tuinenburg[1,2,3], Arie Staal[2,3]

[1] Copernicus Institute for Sustainable Development, Utrecht University, Utrecht, 3508 TC, the Netherlands

[2] Stockholm Resilience Centre, Stockholm University, Stockholm, SE-10691, Sweden

[3] Bolin Centre for Climate Research, Stockholm, SE-10691, Sweden

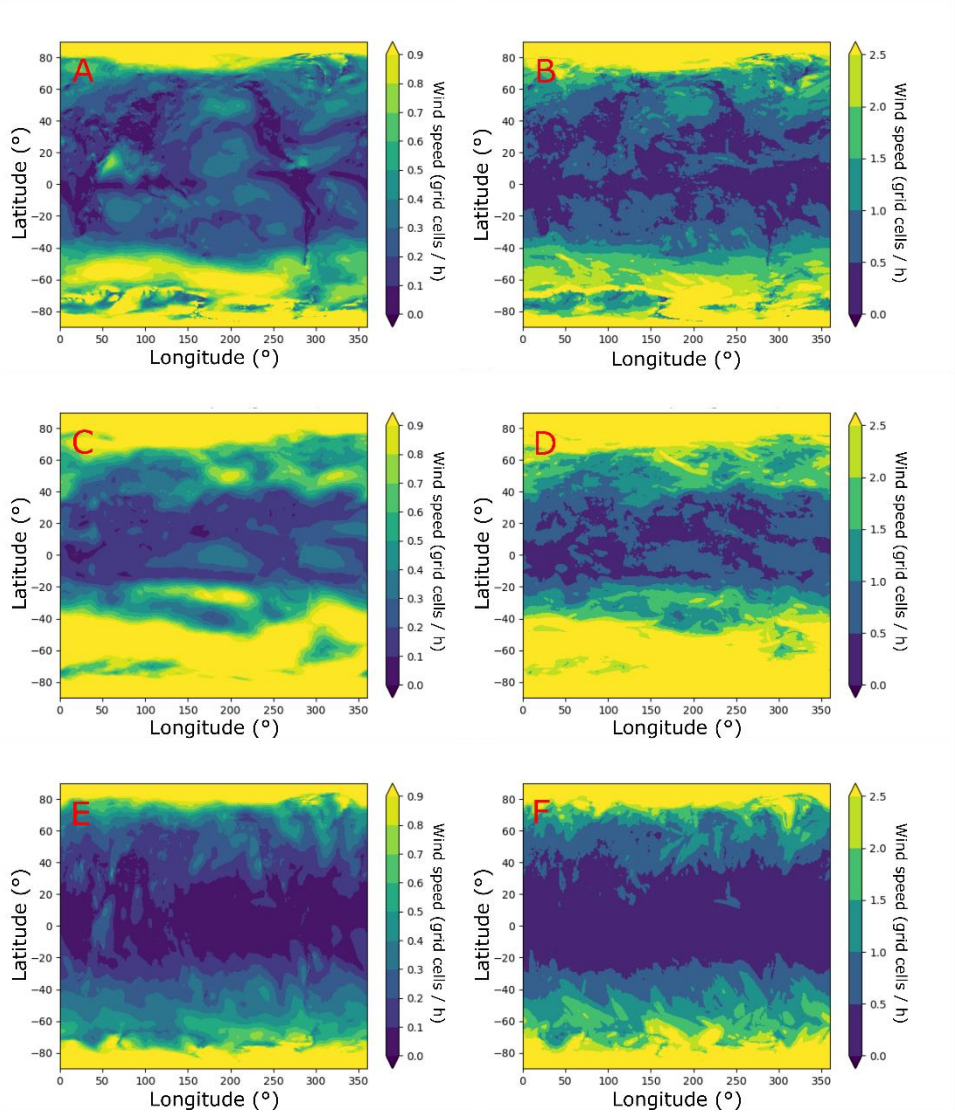

Figure S1: Eastward wind speeds in July 2012 across the globe, given in ERA5 grid cells / h (Courant number). A) Mean eastward wind speeds at 900 hPa; B) Maximum eastward wind speeds at 900 hPa; C) Mean eastward wind speeds at 500 hPa; D) Maximum eastward wind speeds at 500 hPa; E) Mean eastward wind speeds, vertically integrated divided by the precipitable water; F) Maximum eastward wind speeds, vertically integrated divided by the precipitable water.

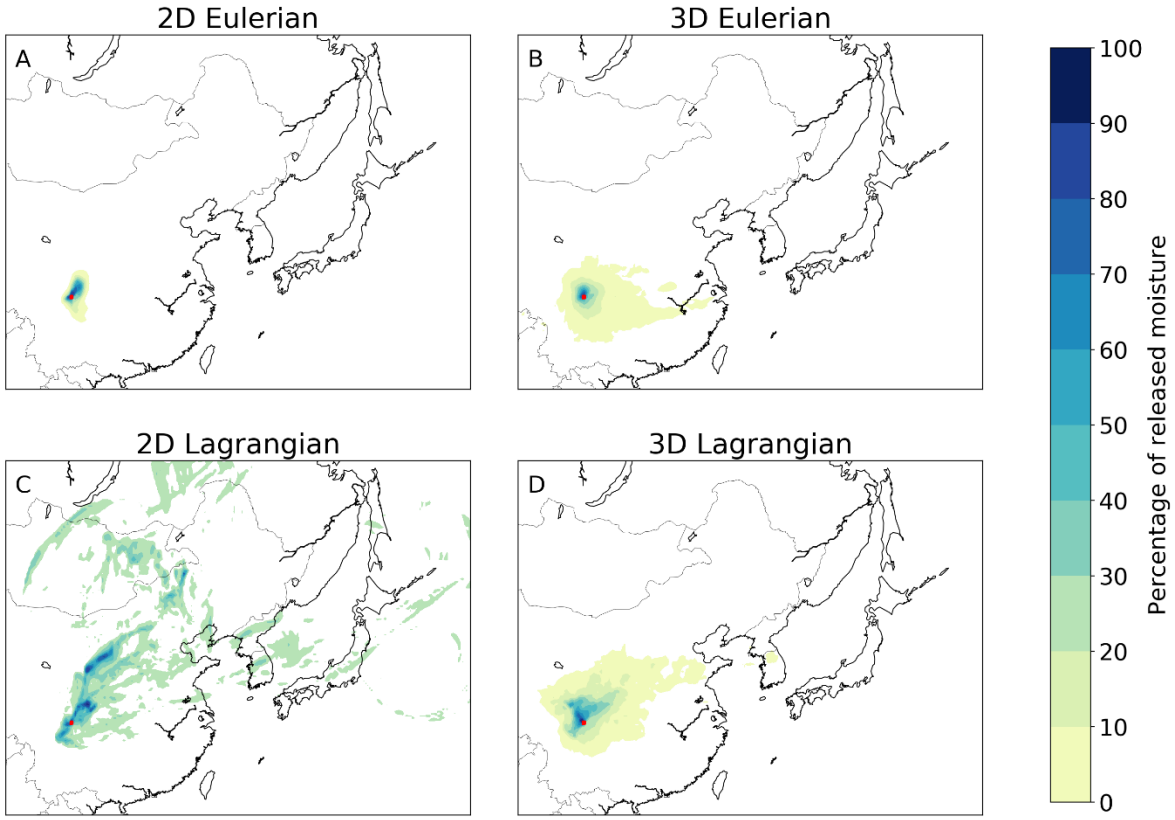

Figure S2: Different footprints of moisture releases from Chendu in July 2012 in two-dimensional and three-dimensional Eulerian and Lagrangian models. A) Two-dimensional Eulerian, with a mean latitudinal moisture flow of 0.6° in northerly direction and mean longitudinal flow of 0.6° in easterly direction; B) Three-dimensional Eulerian, with a mean latitudinal moisture flow of 0.1° in northerly direction and mean longitudinal flow of 0.9° in easterly direction; C) Two-dimensional Lagrangian, with a mean latitudinal moisture flow of 6.5° in northerly direction and mean longitudinal flow of 5.6° in easterly direction; D) Three-dimensional Lagrangian, with a mean latitudinal moisture flow of 1.8° in northerly direction and mean longitudinal flow of 1.7° in easterly direction.

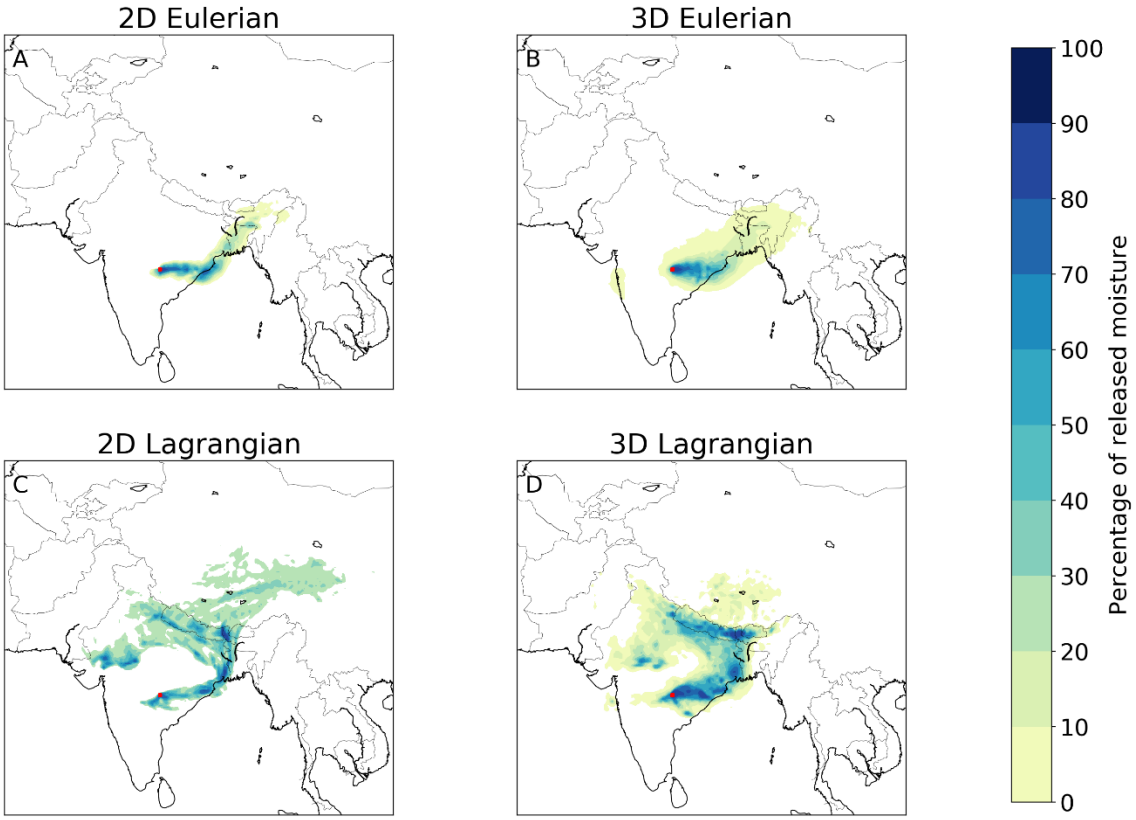

Figure S3: Different footprints of moisture releases from Nagpur in July 2012 in two-dimensional and three-dimensional Eulerian and Lagrangian models. A) Two-dimensional Eulerian, with a mean latitudinal moisture flow of 1.3° in northerly direction and mean longitudinal flow of 5.7° in easterly direction; B) Three-dimensional Eulerian, with a mean latitudinal moisture flow of 0.6° in northerly direction and mean longitudinal flow of 3.8° in easterly direction; C) Two-dimensional Lagrangian, with a mean latitudinal moisture flow of 5.5° in northerly direction and mean longitudinal flow of 4.8° in easterly direction; D) Three-dimensional Lagrangian, with a mean latitudinal moisture flow of 4.7° in northerly direction and mean longitudinal flow of 3.6° in easterly direction.

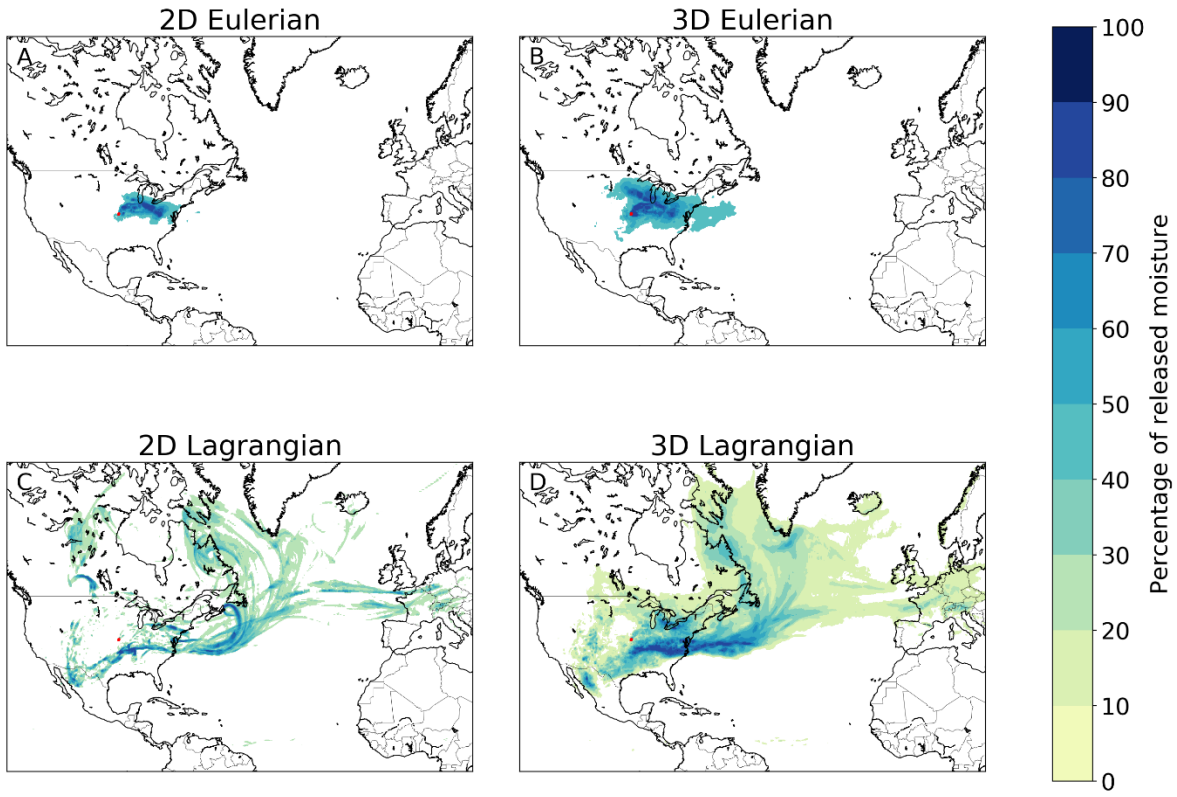

Figure S4: Different footprints of moisture releases from Central Kansas in July 2012 in two-dimensional and three-dimensional Eulerian and Lagrangian models. A) Two-dimensional Eulerian, with a mean latitudinal moisture flow of 1.8° in northerly direction and mean longitudinal flow of 8.5° in easterly direction; B) Three-dimensional Eulerian, with a mean latitudinal moisture flow of 1.3° in southerly direction and mean longitudinal flow of 7.1° in easterly direction; C) Two-dimensional Lagrangian, with a mean latitudinal moisture flow of 5.4° in northerly direction and mean longitudinal flow of 14.4° in easterly direction; D) Three-dimensional Lagrangian, with a mean latitudinal moisture flow of 4.1° in northerly direction and mean longitudinal flow of 15.6° in easterly direction.

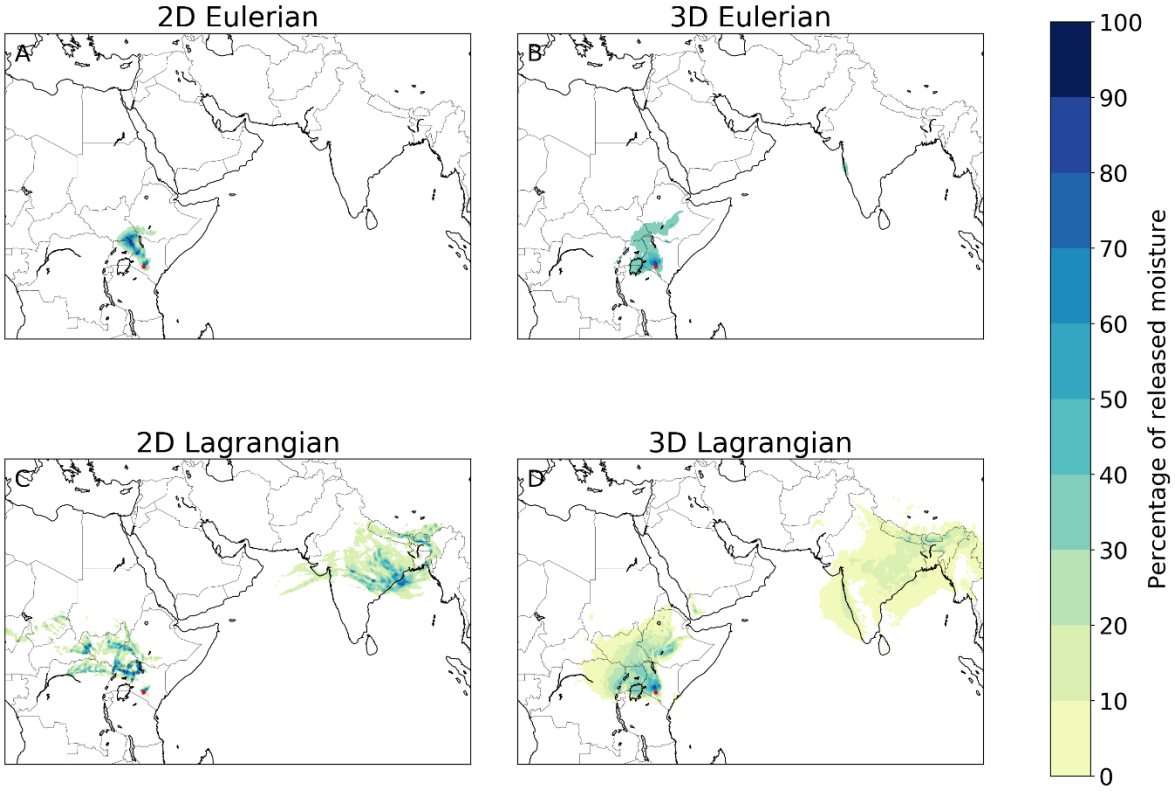

Figure S5: Different footprints of moisture releases from Nairobi in July 2012 in two-dimensional and three-dimensional Eulerian and Lagrangian models. A) Two-dimensional Eulerian, with a mean latitudinal moisture flow of 4.0° in northerly direction and mean longitudinal flow of 1.6° in westerly direction; B) Three-dimensional Eulerian, with a mean latitudinal moisture flow of 2.2° in northerly direction and mean longitudinal flow of 0.8° in easterly direction; C) Two-dimensional Lagrangian, with a mean latitudinal moisture flow of 14.0° in northerly direction and mean longitudinal flow of 3.9° in easterly direction; D) Three-dimensional Lagrangian, with a mean latitudinal moisture flow of 6.6° in northerly direction and mean longitudinal flow of 2.9° in easterly direction.

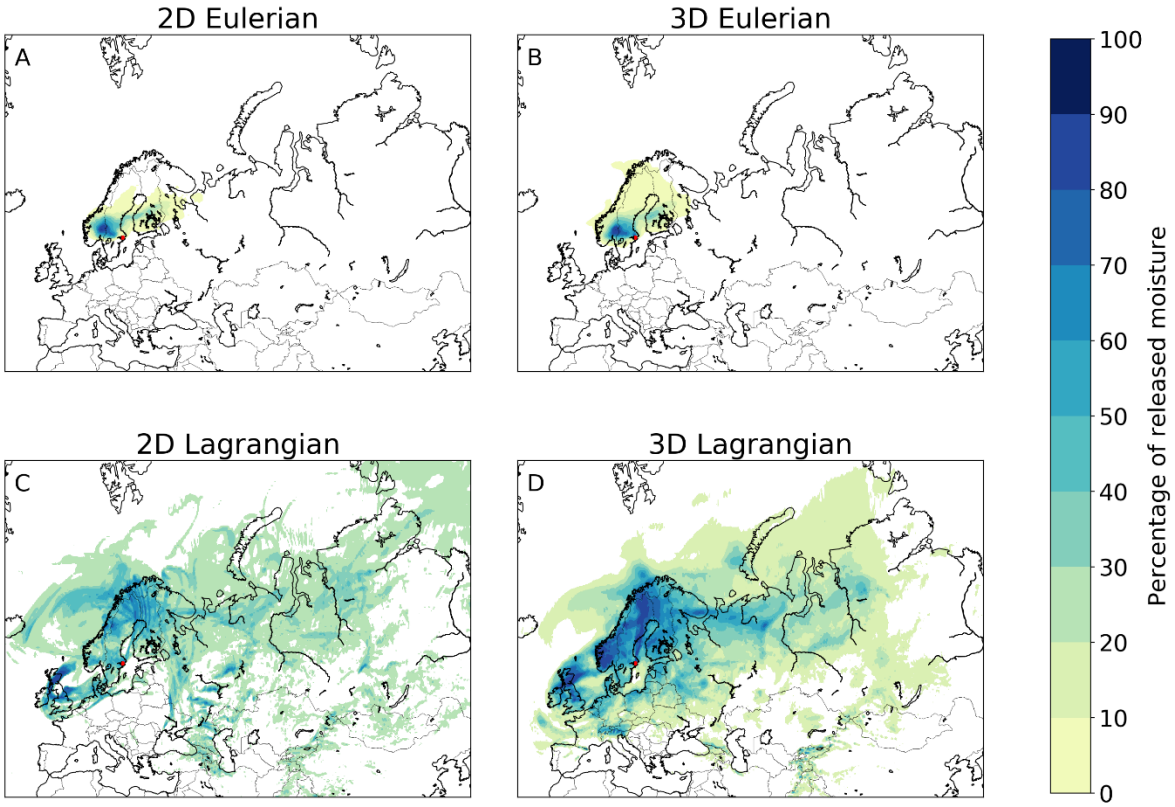

Figure S6: Different footprints of moisture releases from Stockholm in July 2012 in two-dimensional and three-dimensional Eulerian and Lagrangian models. A) Two-dimensional Eulerian, with a mean latitudinal moisture flow of 2.6° in northerly direction and mean longitudinal flow of 0.6° in westerly direction; B) Three-dimensional Eulerian, with a mean latitudinal moisture flow of 2.3° in northerly direction and mean longitudinal flow of 1.4° in westerly direction; C) Two-dimensional Lagrangian, with a mean latitudinal moisture flow of 0.0° in northerly/southerly direction and mean longitudinal flow of 13.9° in easterly direction; D) Three-dimensional Lagrangian, with a mean latitudinal moisture flow of 1.4° in northerly direction and mean longitudinal flow of 11.0° in easterly direction.

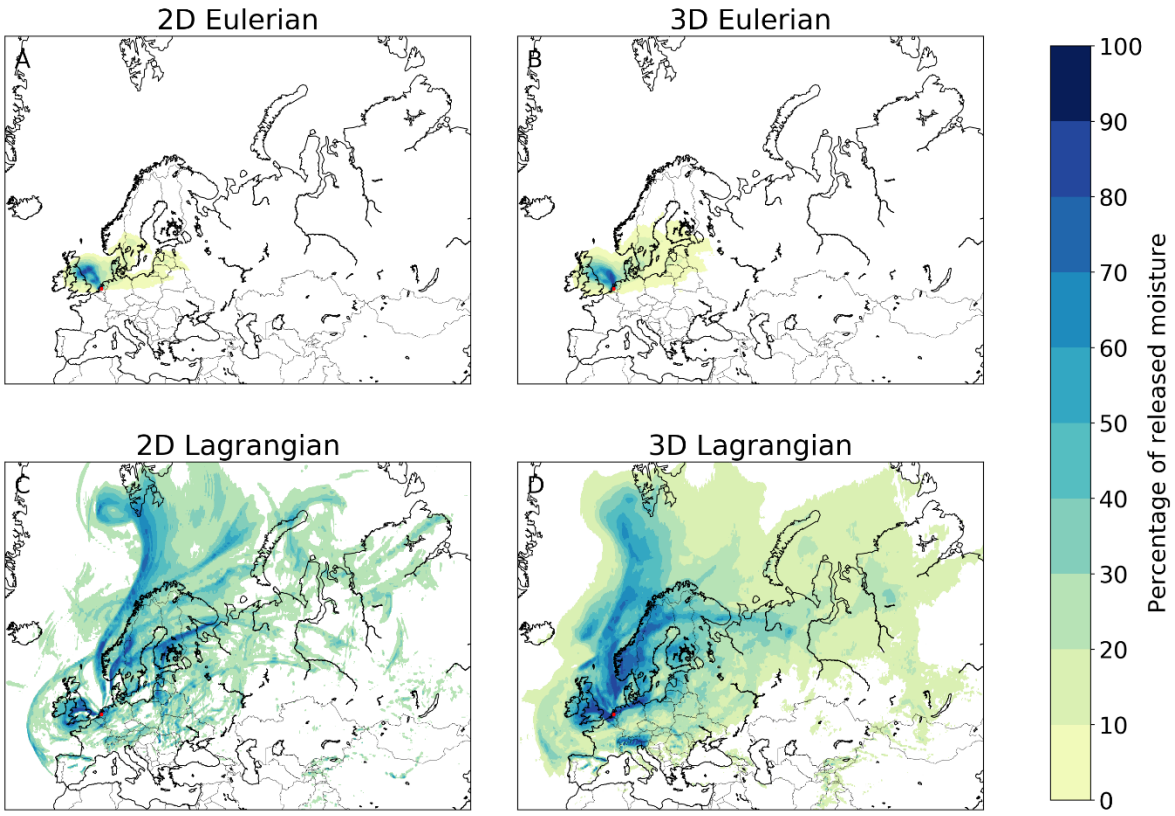

Figure S7: Different footprints of moisture releases from Utrecht in July 2012 in two-dimensional and three-dimensional Eulerian and Lagrangian models. A) Two-dimensional Eulerian, with a mean latitudinal moisture flow of 2.8° in northerly direction and mean longitudinal flow of 11.3° in easterly direction; B) Three-dimensional Eulerian, with a mean latitudinal moisture flow of 3.1° in northerly direction and mean longitudinal flow of 9.8° in easterly direction; C) Two-dimensional Lagrangian, with a mean latitudinal moisture flow of 8.7° in northerly direction and mean longitudinal flow of 18.1° in easterly direction; D) Three-dimensional Lagrangian, with a mean latitudinal moisture flow of 6.2° in northerly direction and mean longitudinal flow of 15.4° in easterly direction.

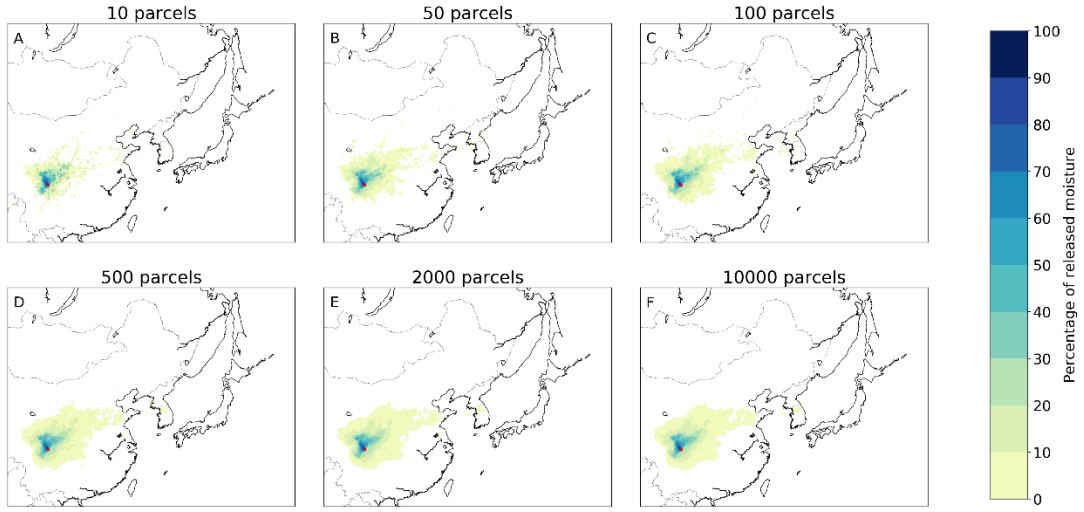

Figure S8: Different footprints of moisture releases from Chendu in July 2012 in a three-dimensional Lagrangian model with 10, 50, 100, 500, 2,000, and 10,000 tracked ~~particle~~parcels mm^{-1} ~~h^{-1}~~). A) 10 parcels, with a mean latitudinal moisture flow of 2.4° in northerly direction and mean longitudinal flow of 2.5° in easterly direction; B) 50 parcels, with a mean latitudinal moisture flow of 2.3° in northerly direction and mean longitudinal flow of 2.6° in easterly direction; ~~A~~C) 100 ~~particle~~parcels, with a mean latitudinal moisture flow of 1.9° in northerly direction and mean longitudinal flow of 1.8° in easterly direction; ~~B~~D) 500 ~~particle~~parcels, with a mean latitudinal moisture flow of 1.9° in northerly direction and mean longitudinal flow of 1.7° in easterly direction; ~~C~~E) 2,000 ~~particle~~parcels, with a mean latitudinal moisture flow of 1.8° in northerly direction and mean longitudinal flow of 1.7° in easterly direction; ~~D~~F) 10,000 ~~particle~~parcels, with a mean latitudinal moisture flow of 1.8° in northerly direction and mean longitudinal flow of 1.7° in easterly direction.

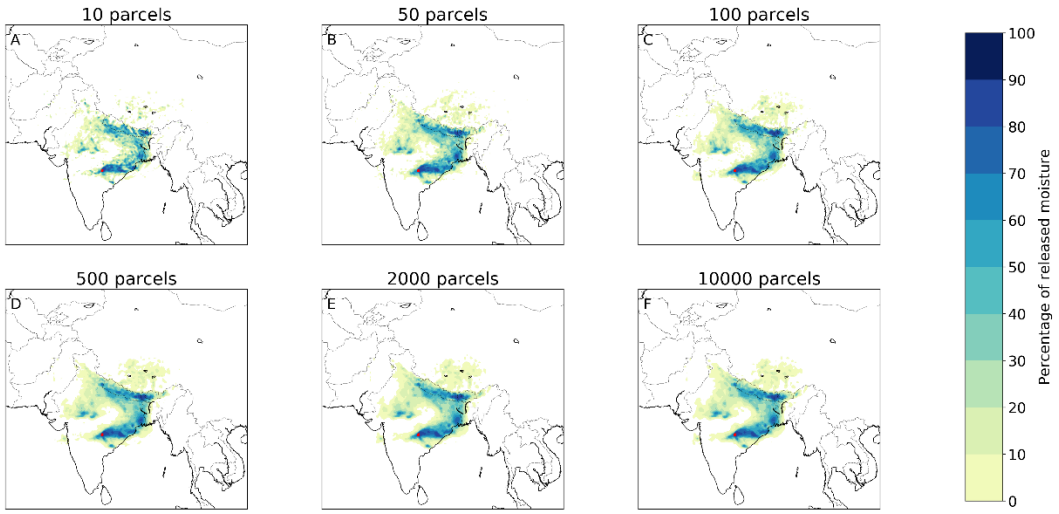

Figure S9: Different footprints of moisture releases from Nagpur in July 2012 in a three-dimensional Lagrangian model with 10, 50, 100, 500, 2,000, and 10,000 tracked ~~particle~~parcels mm^{-1} ~~h^{-1}~~). A) 10 parcels, with a mean latitudinal moisture flow of 5.0° in northerly direction and mean longitudinal flow of 3.7° in easterly direction; B) 50 parcels, with a mean latitudinal moisture flow of 4.9° in northerly direction and mean longitudinal flow of 3.7° in easterly direction; ~~A~~C) 100 ~~particle~~parcels, with a mean latitudinal moisture flow of 4.7° in northerly direction and mean longitudinal flow of 3.5° in easterly direction; ~~B~~D) 500 ~~particle~~parcels, with a mean latitudinal moisture flow of 4.7° in northerly direction and mean longitudinal flow of 3.6° in easterly direction; ~~C~~E) 2,000 ~~particle~~parcels, with a mean latitudinal moisture flow of 4.7° in northerly direction and mean longitudinal flow of 3.6° in easterly direction; ~~D~~F) 10,000 ~~particle~~parcels, with a mean latitudinal moisture flow of 4.7° in northerly direction and mean longitudinal flow of 3.6° in easterly direction.

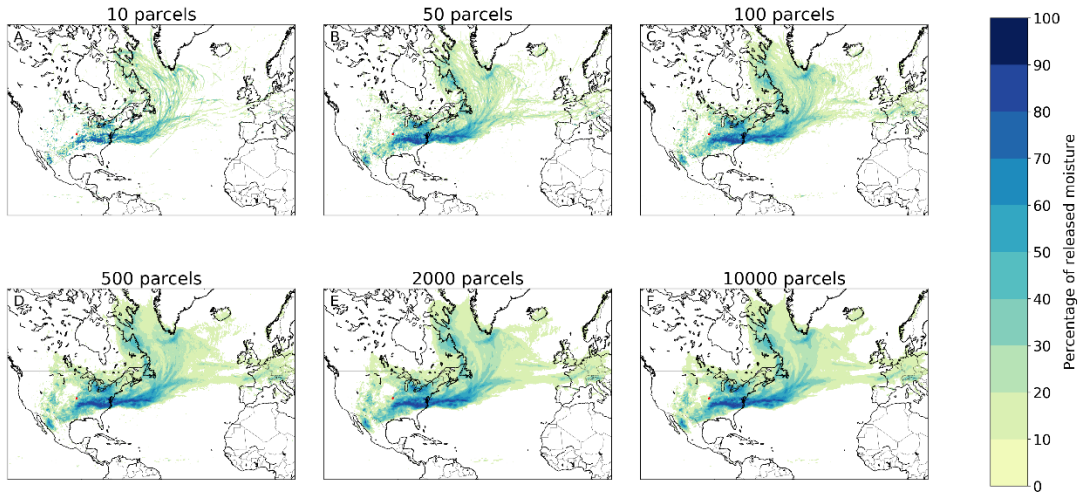

Figure S10: Different footprints of moisture releases from Central Kansas in July 2012 in a three-dimensional Lagrangian model with 10, 50, 100, 500, 2,000, and 10,000 tracked ~~particle~~parcels mm^{-1} ~~h^{-1}~~). A) 10 parcels, with a mean latitudinal moisture flow of 4.0° in northerly direction and mean longitudinal flow of 15.2° in easterly direction; B) 50 parcels, with a mean latitudinal moisture flow of 3.9° in northerly direction and mean longitudinal flow of 15.2° in easterly direction; ~~A~~C) 100 ~~particle~~parcels, with a mean latitudinal moisture flow of 4.2° in northerly direction and mean longitudinal flow of 15.4° in easterly direction; ~~B~~D) 500 ~~particle~~parcels, with a mean latitudinal moisture flow of 4.1° in northerly direction and mean longitudinal flow of 15.6° in easterly direction; ~~C~~E) 2,000 ~~particle~~parcels, with a mean latitudinal moisture flow of 4.1° in northerly direction and mean longitudinal flow of 15.6° in easterly direction; ~~D~~F) 10,000 ~~particle~~parcels, with a mean latitudinal moisture flow of 4.1° in northerly direction and mean longitudinal flow of 15.6° in easterly direction.

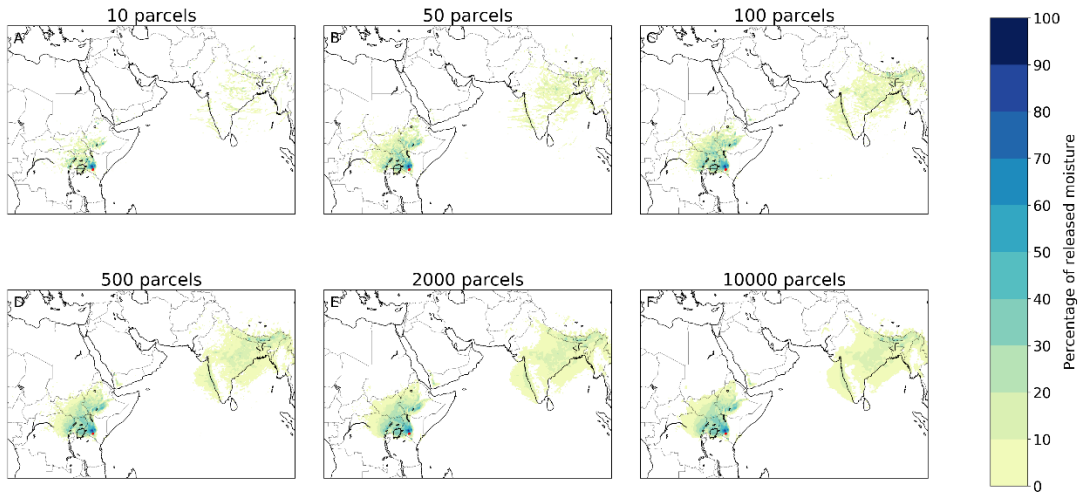

Figure S11: Different footprints of moisture releases from Nairobi in July 2012 in a three-dimensional Lagrangian model with 10, 50, 100, 500, 2,000, and 10,000 tracked ~~particle~~parcels mm^{-1} ~~h^{-1}~~). A) 10 parcels, with a mean latitudinal moisture flow of 7.2° in northerly direction and mean longitudinal flow of 3.1° in easterly direction; B) 50 parcels, with a mean latitudinal moisture flow of 7.5° in northerly direction and mean longitudinal flow of 3.1° in easterly direction; ~~A~~C) 100 ~~particle~~parcels, with a mean latitudinal moisture flow of 6.7° in northerly direction and mean longitudinal flow of 2.9° in easterly direction; ~~B~~D) 500 ~~particle~~parcels, with a mean latitudinal moisture flow of 6.9° in northerly direction and mean longitudinal flow of 3.1° in easterly direction; ~~C~~E) 2,000 ~~particle~~parcels, with a mean latitudinal moisture flow of 6.5° in northerly direction and mean longitudinal flow of 2.8° in easterly direction; ~~D~~F) 10,000 ~~particle~~parcels, with a mean latitudinal moisture flow of 6.6° in northerly direction and mean longitudinal flow of 2.9° in easterly direction.

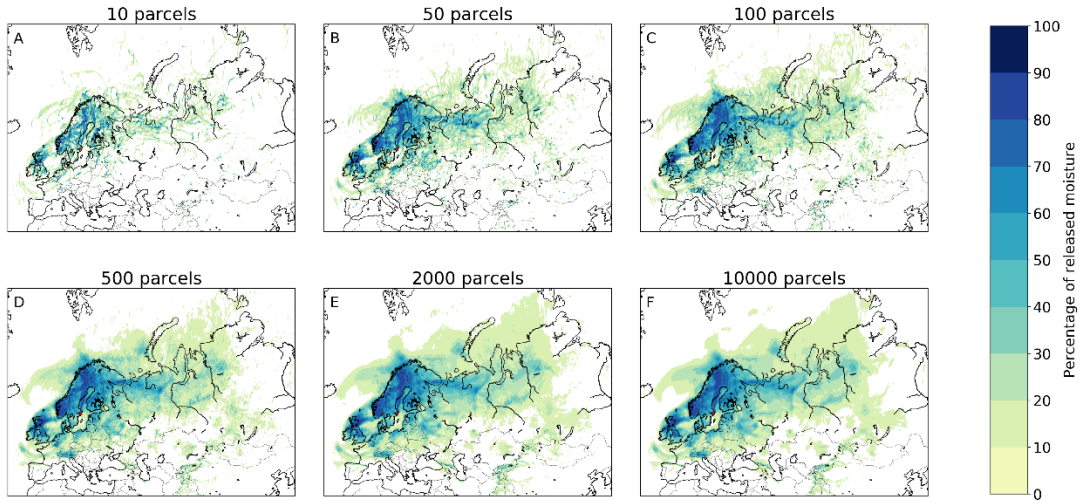

Figure S12: Different footprints of moisture releases from Stockholm in July 2012 in a three-dimensional Lagrangian model with 10, 50, 100, 500, 2,000, and 10,000 tracked ~~particle~~parcels mm^{-1} ~~h^{-1}~~). A) 10 parcels, with a mean latitudinal moisture flow of 1.8° in northerly direction and mean longitudinal flow of 11.5° in easterly direction; B) 50 parcels, with a mean latitudinal moisture flow of 0.9° in northerly direction and mean longitudinal flow of 11.0° in easterly direction; ~~A~~C) 100 ~~particle~~parcels, with a mean latitudinal moisture flow of 1.3° in northerly direction and mean longitudinal flow of 11.1° in easterly direction; ~~B~~D) 500 ~~particle~~parcels, with a mean latitudinal moisture flow of 1.5° in northerly direction and mean longitudinal flow of 11.1° in easterly direction; ~~C~~E) 2,000 ~~particle~~parcels, with a mean latitudinal moisture flow of 1.5° in northerly direction and mean longitudinal flow of 11.0° in easterly direction; ~~D~~F) 10,000 ~~particle~~parcels, with a mean latitudinal moisture flow of 1.4° in northerly direction and mean longitudinal flow of 11.0° in easterly direction.

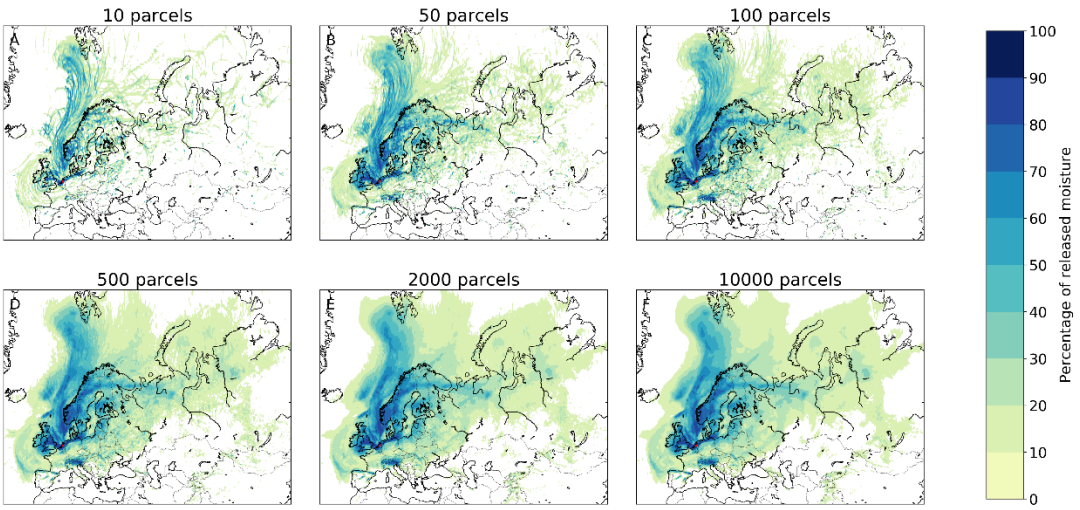

Figure S13: Different footprints of moisture releases from Utrecht in July 2012 in a three-dimensional Lagrangian model with 10, 50, 100, 500, 2,000, and 10,000 tracked ~~particle~~parcels mm^{-1} ~~h^{-1}~~). A) 10 parcels, with a mean latitudinal moisture flow of 6.8° in northerly direction and mean longitudinal flow of 15.5° in easterly direction; B) 50 parcels, with a mean latitudinal moisture flow of 6.4° in northerly direction and mean longitudinal flow of 15.3° in easterly direction; ~~A~~C) 100 ~~particle~~parcels, with a mean latitudinal moisture flow of 6.1° in northerly direction and mean longitudinal flow of 15.5° in easterly direction; ~~B~~D) 500 ~~particle~~parcels, with a mean latitudinal moisture flow of 6.4° in northerly direction and mean longitudinal flow of 15.5° in easterly direction; ~~C~~E) 2,000 ~~particle~~parcels, with a mean latitudinal moisture flow of 6.3° in northerly direction and mean longitudinal flow of 15.4° in easterly direction; ~~D~~F) 10,000 ~~particle~~parcels, with a mean latitudinal moisture flow of 6.2° in northerly direction and mean longitudinal flow of 15.4° in easterly direction.

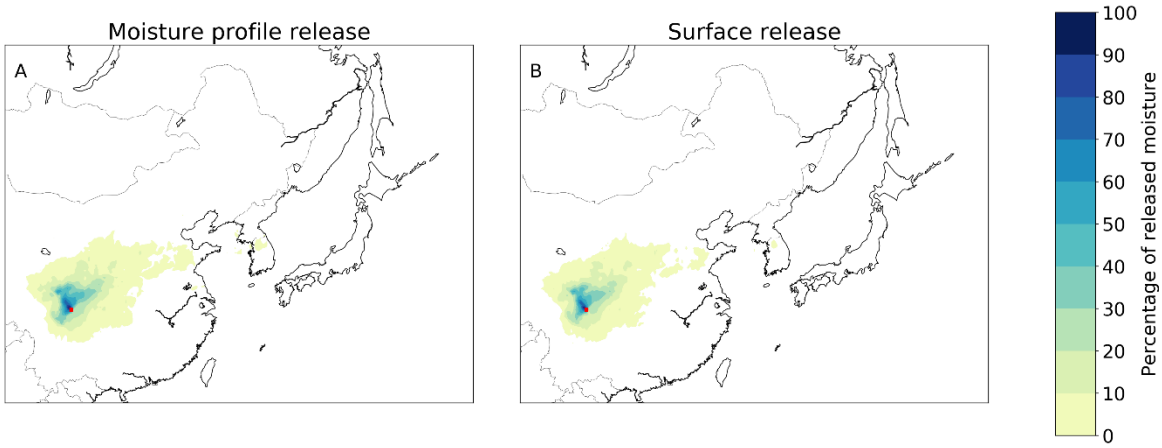

Figure S14: Different footprints of moisture releases from Chendu in July 2012 in a three-dimensional Lagrangian model with moisture released according to the vertical moisture profile of the atmosphere and moisture released at the surface. A) Release according to the moisture profile, with a mean latitudinal moisture flow of 2.3° in northerly direction and mean longitudinal flow of 2.4° in easterly direction; B) Release at the surface, with a mean latitudinal moisture flow of 2.0° in northerly direction and mean longitudinal flow of 2.1° in easterly direction.

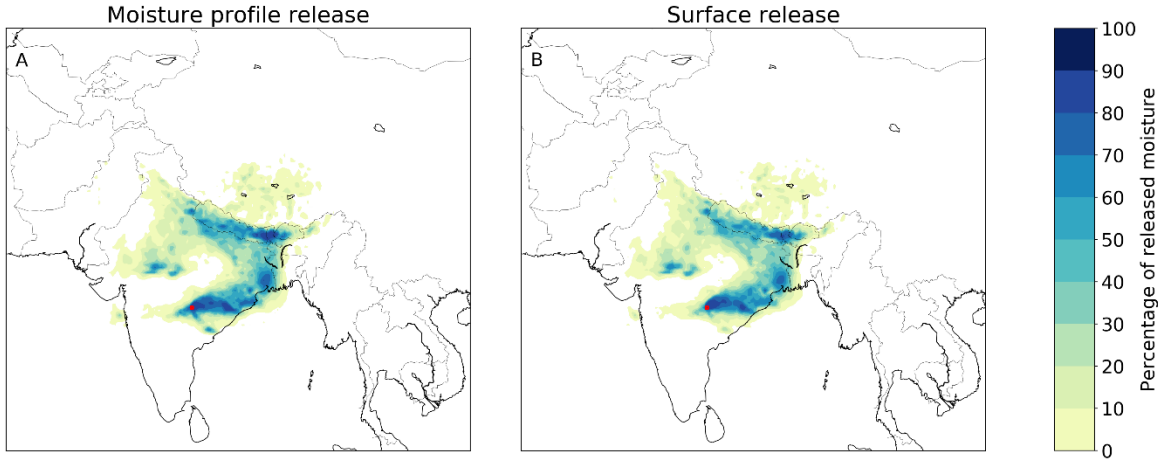

Figure S15: Different footprints of moisture releases from Nagpur in July 2012 in a three-dimensional Lagrangian model with moisture released according to the vertical moisture profile of the atmosphere and moisture released at the surface. A) Release according to the moisture profile, with a mean latitudinal moisture flow of 4.9° in northerly direction and mean longitudinal flow of 3.6° in easterly direction; B) Release at the surface, with a mean latitudinal moisture flow of 4.7° in northerly direction and mean longitudinal flow of 3.3° in easterly direction.

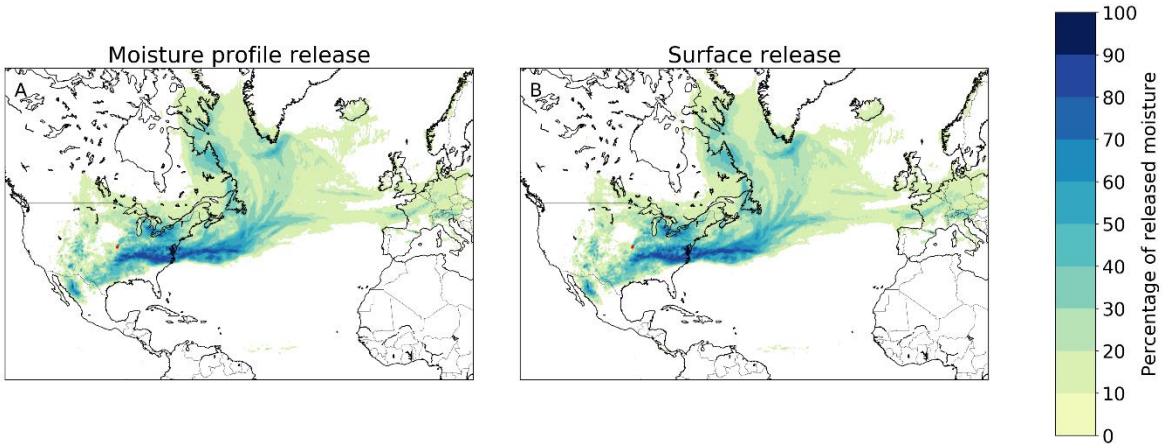

Figure S16: Different footprints of moisture releases from Central Kansas in July 2012 in a three-dimensional Lagrangian model with moisture released according to the vertical moisture profile of the atmosphere and moisture released at the surface. A) Release according to the moisture profile, with a mean latitudinal moisture flow of 4.0° in northerly direction and mean longitudinal flow of 15.2° in easterly direction; B) Release at the surface, with a mean latitudinal moisture flow of 4.0° in northerly direction and mean longitudinal flow of 15.3° in easterly direction.

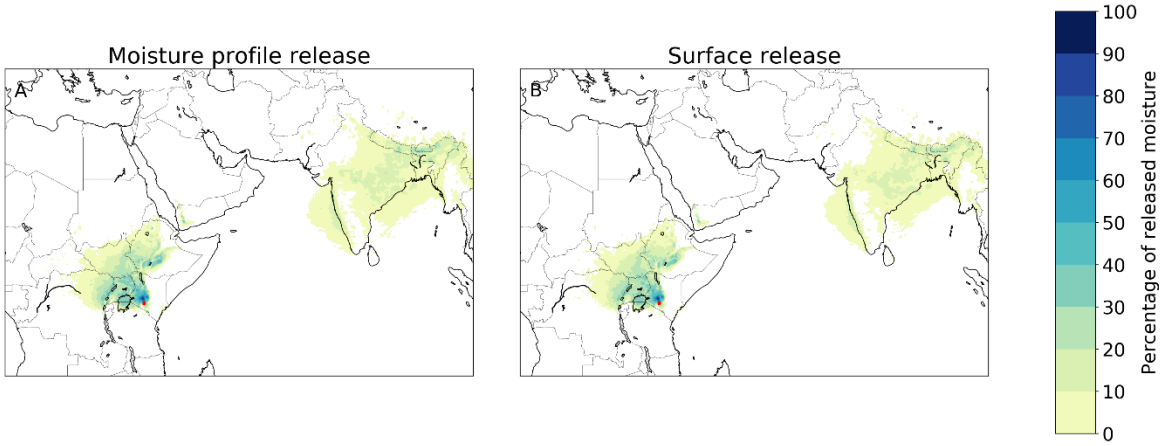

Figure S17: Different footprints of moisture releases from Nairobi in July 2012 in a three-dimensional Lagrangian model with moisture released according to the vertical moisture profile of the atmosphere and moisture released at the surface. A) Release according to the moisture profile, with a mean latitudinal moisture flow of 7.2° in northerly direction and mean longitudinal flow of 3.0° in easterly direction; B) Release at the surface, with a mean latitudinal moisture flow of 6.7° in northerly direction and mean longitudinal flow of 2.6° in easterly direction.

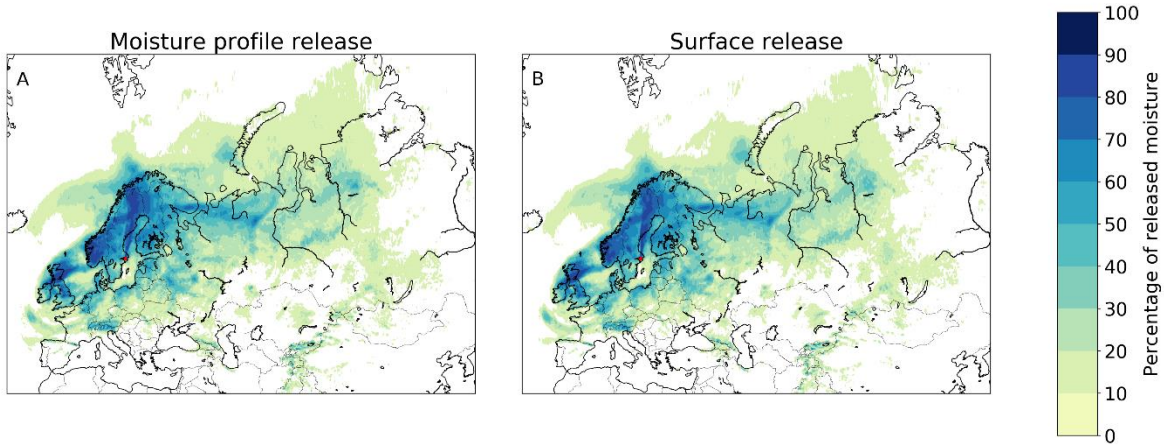

Figure S18: Different footprints of moisture releases from Stockholm in July 2012 in a three-dimensional Lagrangian model with moisture released according to the vertical moisture profile of the atmosphere and moisture released at the surface. A) Release according to the moisture profile, with a mean latitudinal moisture flow of 1.3° in northerly direction and mean longitudinal flow of 11.1° in easterly direction; B) Release at the surface, with a mean latitudinal moisture flow of 1.3° in northerly direction and mean longitudinal flow of 10.8° in easterly direction.

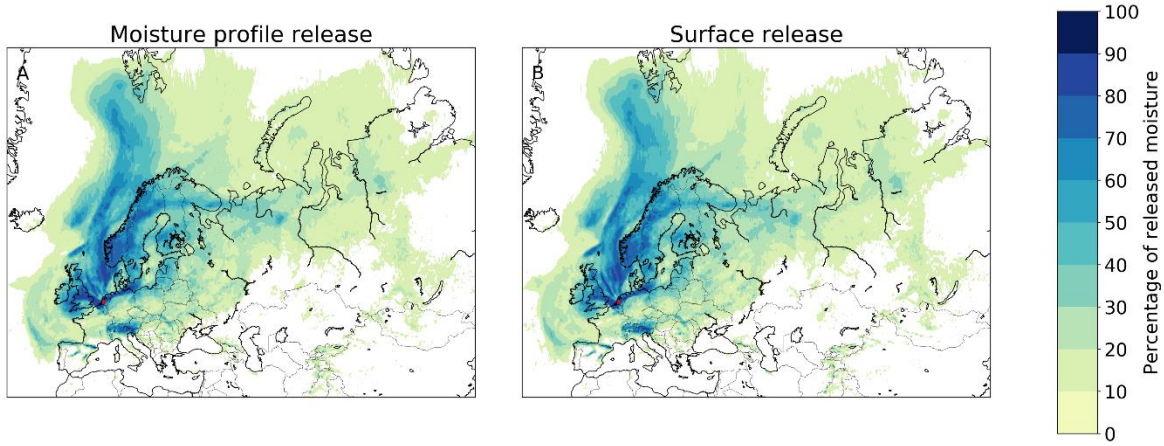

Figure S19: Different footprints of moisture releases from Utrecht in July 2012 in a three-dimensional Lagrangian model with moisture released according to the vertical moisture profile of the atmosphere and moisture released at the surface. A) Release according to the moisture profile, with a mean latitudinal moisture flow of 6.0° in northerly direction and mean longitudinal flow of 15.4° in easterly direction; B) Release at the surface, with a mean latitudinal moisture flow of 5.8° in northerly direction and mean longitudinal flow of 14.6° in easterly direction.

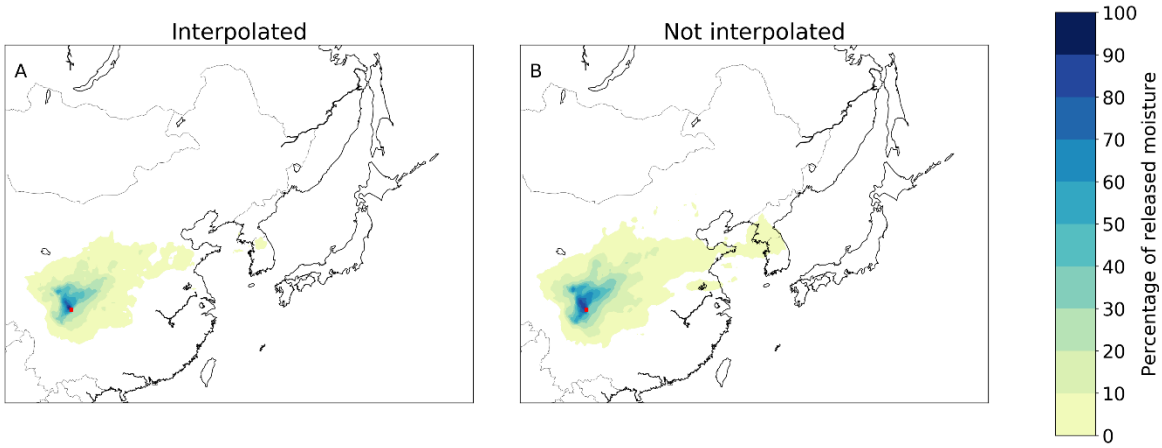

Figure S20: Different footprints of moisture releases from Chendu in July 2012 in a three-dimensional Lagrangian model with and without interpolation of wind speed and directions. A) Interpolated, with a mean latitudinal moisture flow of 1.8° in northerly direction and mean longitudinal flow of 1.7° in easterly direction; B) Not interpolated, with a mean latitudinal moisture flow of 2.3° in northerly direction and mean longitudinal flow of 2.4° in easterly direction.

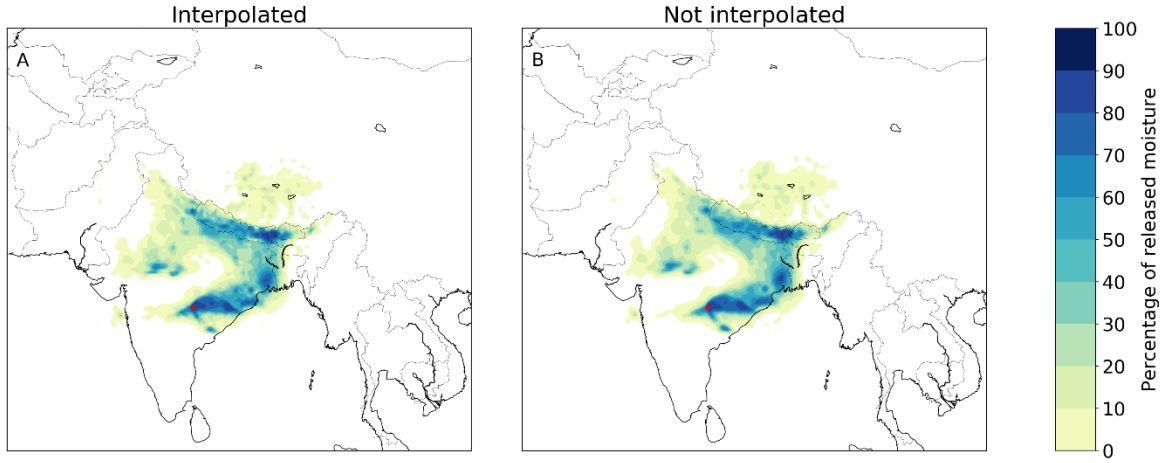

Figure S21: Different footprints of moisture releases from Nagpur in July 2012 in a three-dimensional Lagrangian model with and without interpolation of wind speed and directions. A) Interpolated, with a mean latitudinal moisture flow of 4.7° in northerly direction and mean longitudinal flow of 3.6° in easterly direction; B) Not interpolated, with a mean latitudinal moisture flow of 4.9° in northerly direction and mean longitudinal flow of 3.6° in easterly direction.

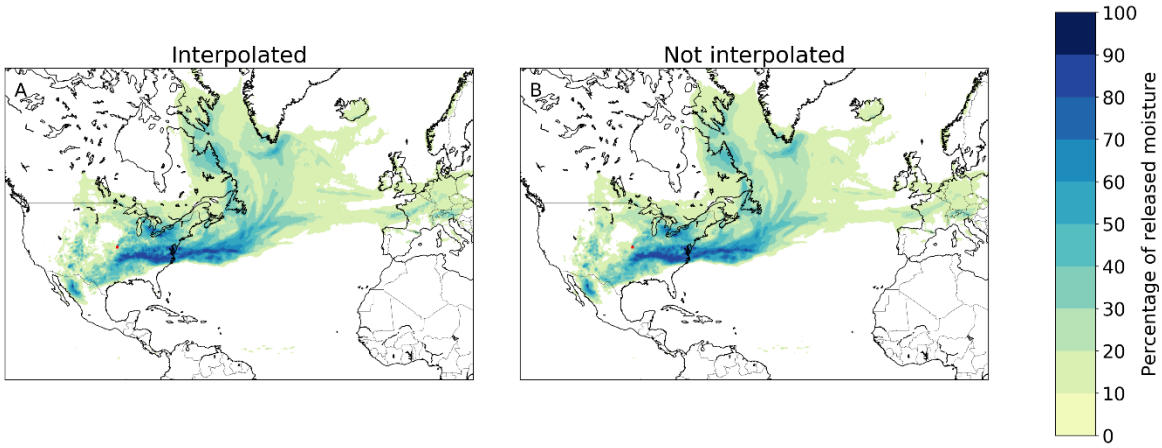

Figure S22: Different footprints of moisture releases from Central Kansas in July 2012 in a three-dimensional Lagrangian model with and without interpolation of wind speed and directions. A) Interpolated, with a mean latitudinal moisture flow of 4.1° in northerly direction and mean longitudinal flow of 15.6° in easterly direction; B) Not interpolated, with a mean latitudinal moisture flow of 4.0° in northerly direction and mean longitudinal flow of 15.2° in easterly direction.

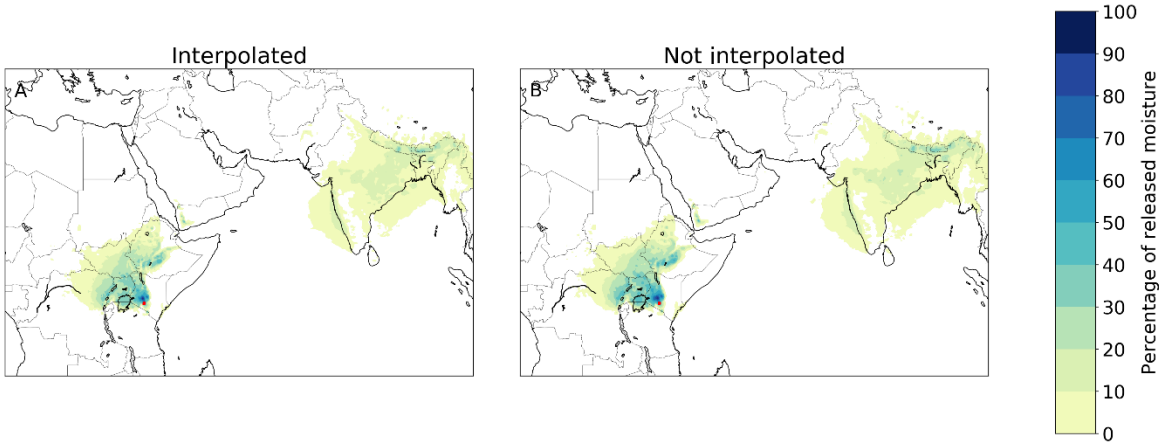

Figure S23: Different footprints of moisture releases from Nairobi in July 2012 in a three-dimensional Lagrangian model with and without interpolation of wind speed and directions. A) Interpolated, with a mean latitudinal moisture flow of 6.6° in northerly direction and mean longitudinal flow of 2.9° in easterly direction; B) Not interpolated, with a mean latitudinal moisture flow of 7.2° in northerly direction and mean longitudinal flow of 3.0° in easterly direction.

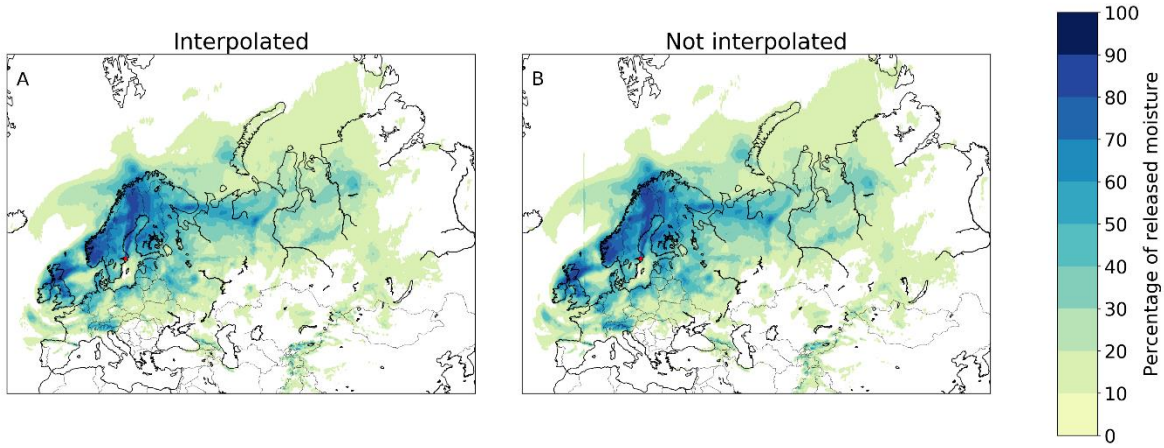

Figure S24: Different footprints of moisture releases from Stockholm in July 2012 in a three-dimensional Lagrangian model with and without interpolation of wind speed and directions. A) Interpolated, with a mean latitudinal moisture flow of 1.4° in northerly direction and mean longitudinal flow of 11.0° in easterly direction; B) Not interpolated, with a mean latitudinal moisture flow of 1.3° in northerly direction and mean longitudinal flow of 11.1° in easterly direction.

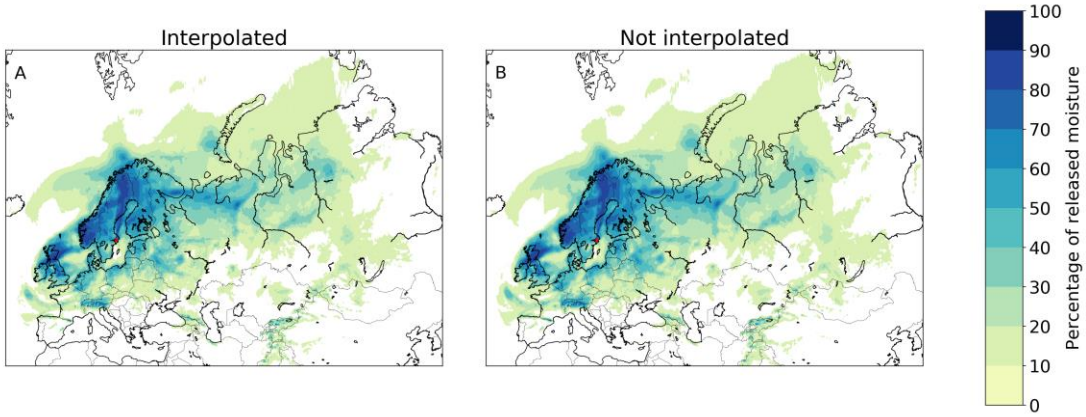

Figure S25: Different footprints of moisture releases from Utrecht in July 2012 in a three-dimensional Lagrangian model with and without interpolation of wind speed and directions. A) Interpolated, with a mean latitudinal moisture flow of 6.2° in northerly direction and mean longitudinal flow of 15.4° in easterly direction; B) Not interpolated, with a mean latitudinal moisture flow of 6.1° in northerly direction and mean longitudinal flow of 15.3° in easterly direction.

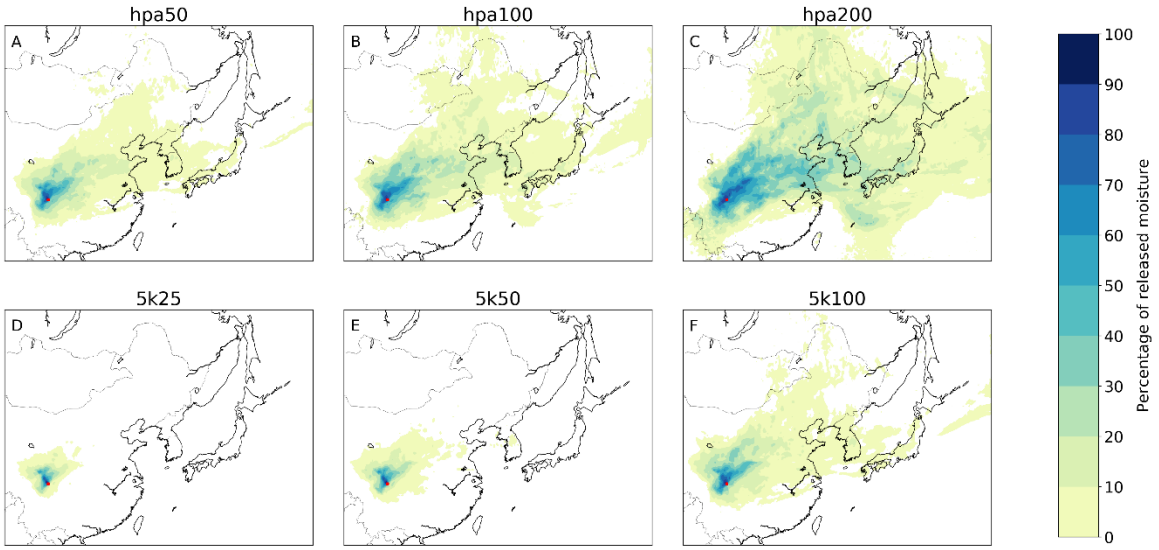

Figure S26: Different footprints of moisture releases from Chendu in July 2012 in a three-dimensional Lagrangian model with different degradations of the vertical moisture profile. A) hpa50, with a mean latitudinal moisture flow of 3.1° in northerly direction and mean longitudinal flow of 4.0° in easterly direction; B) hpa100, with a mean latitudinal moisture flow of 3.8° in northerly direction and mean longitudinal flow of 5.7° in easterly direction; C) hpa200, with a mean latitudinal moisture flow of 4.9° in northerly direction and mean longitudinal flow of 9.2° in easterly direction; D) 5k25, with a mean latitudinal moisture flow of 1.6° in northerly direction and mean longitudinal flow of 0.3° in easterly direction; E) 5k50, with a mean latitudinal moisture flow of 2.2° in northerly direction and mean longitudinal flow of 1.4° in easterly direction; F) 5k100, with a mean latitudinal moisture flow of 3.5° in northerly direction and mean longitudinal flow of 3.6° in easterly direction.

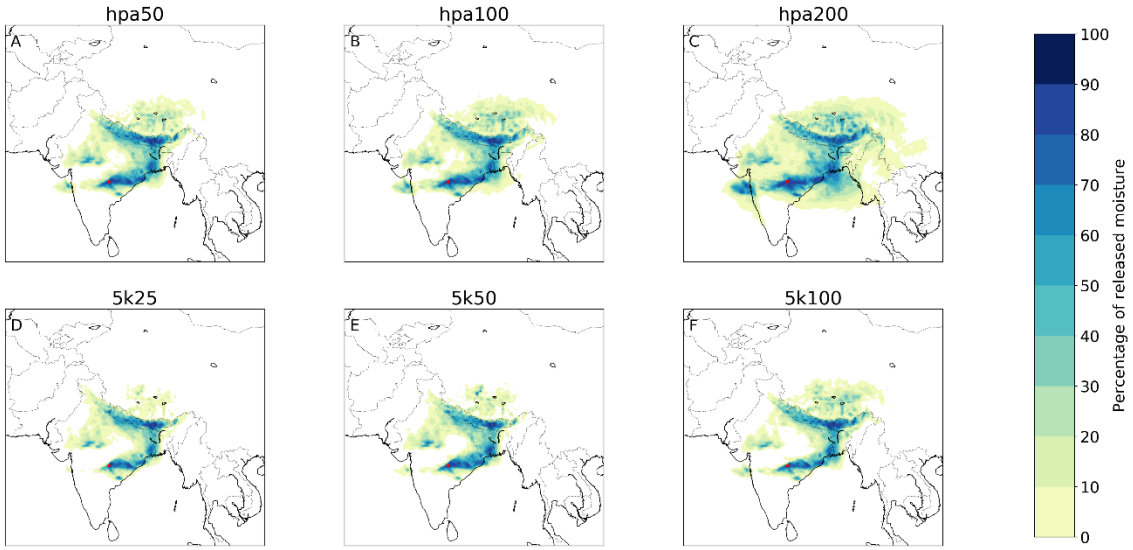

Figure S27: Different footprints of moisture releases from Nagpur in July 2012 in a three-dimensional Lagrangian model with different degradations of the vertical moisture profile. A) hpa50, with a mean latitudinal moisture flow of 4.9° in northerly direction and mean longitudinal flow of 4.6° in easterly direction; B) hpa100, with a mean latitudinal moisture flow of 4.8° in northerly direction and mean longitudinal flow of 5.1° in easterly direction; C) hpa200, with a mean latitudinal moisture flow of 3.1° in northerly direction and mean longitudinal flow of 5.1° in easterly direction; D) 5k25, with a mean latitudinal moisture flow of 5.0° in northerly direction and mean longitudinal flow of 4.0° in easterly direction; E) 5k50, with a mean latitudinal moisture flow of 4.8° in northerly direction and mean longitudinal flow of 3.8° in easterly direction; F) 5k100, with a mean latitudinal moisture flow of 5.4° in northerly direction and mean longitudinal flow of 5.6° in easterly direction.

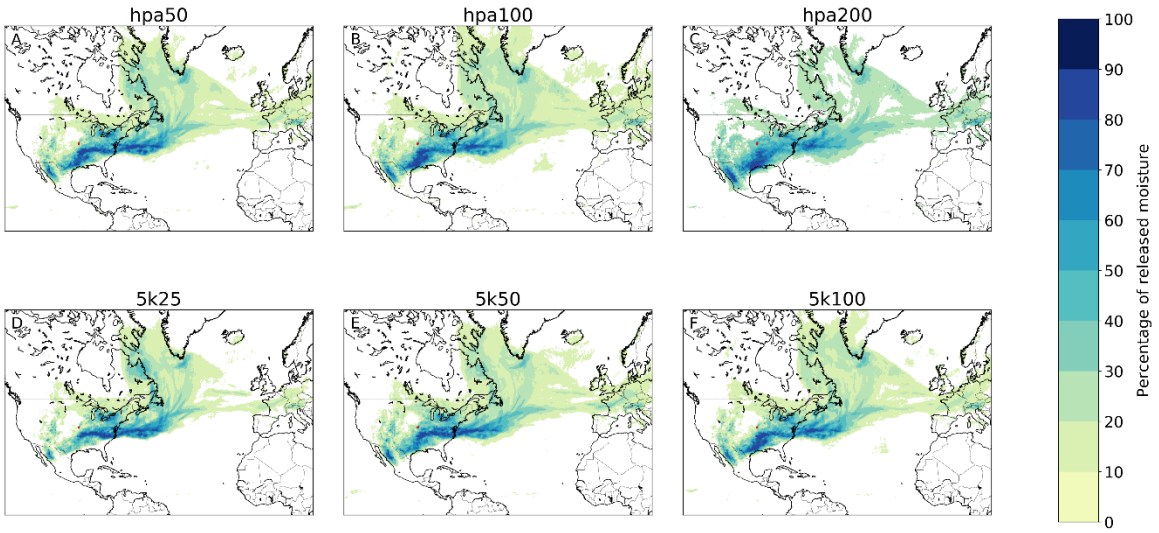

Figure S28: Different footprints of moisture releases from Central Kansas in July 2012 in a three-dimensional Lagrangian model with different degradations of the vertical moisture profile. A) hpa50, with a mean latitudinal moisture flow of 2.8° in northerly direction and mean longitudinal flow of 13.8° in easterly direction; B) hpa100, with a mean latitudinal moisture flow of 1.8° in northerly direction and mean longitudinal flow of 11.2° in easterly direction; C) hpa200, with a mean latitudinal moisture flow of 0.2° in southerly direction and mean longitudinal flow of 6.6° in easterly direction; D) 5k25, with a mean latitudinal moisture flow of 4.1° in northerly direction and mean longitudinal flow of 16.7° in easterly direction; E) 5k50, with a mean latitudinal moisture flow of 2.4° in northerly direction and mean longitudinal flow of 11.9° in easterly direction; F) 5k100, with a mean latitudinal moisture flow of 2.2° in northerly direction and mean longitudinal flow of 12.0° in easterly direction.

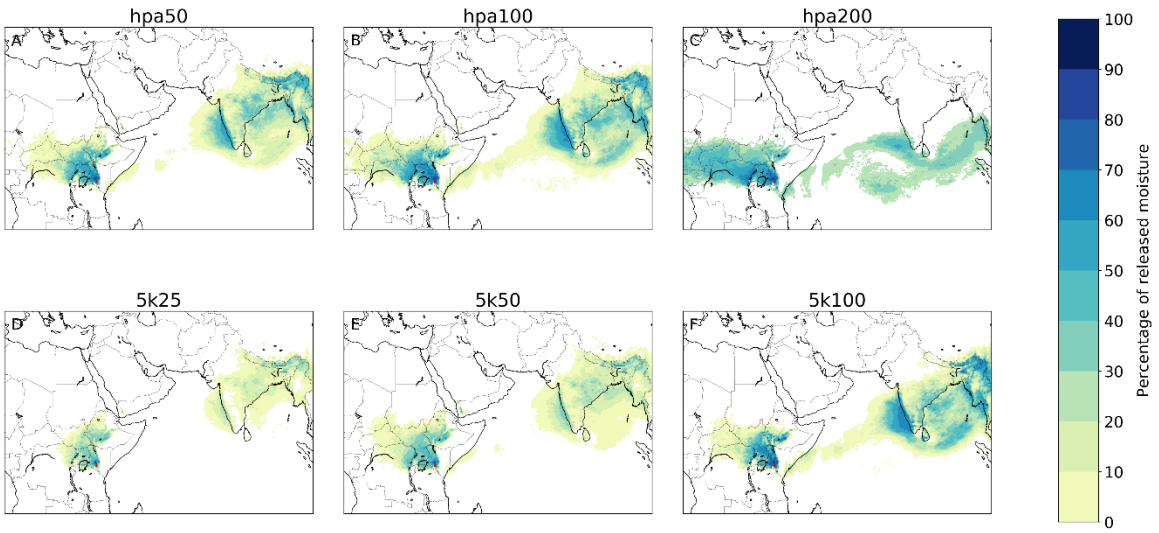

Figure S29: Different footprints of moisture releases from Nairobi in July 2012 in a three-dimensional Lagrangian model with different degradations of the vertical moisture profile. A) hpa50, with a mean latitudinal moisture flow of 11.3° in northerly direction and mean longitudinal flow of 9.8° in easterly direction; B) hpa100, with a mean latitudinal moisture flow of 11.0° in northerly direction and mean longitudinal flow of 11.0° in easterly direction; C) hpa200, with a mean latitudinal moisture flow of 4.3° in northerly direction and mean longitudinal flow of 2.7° in easterly direction; D) 5k25, with a mean latitudinal moisture flow of 8.6° in northerly direction and mean longitudinal flow of 5.4° in easterly direction; E) 5k50, with a mean latitudinal moisture flow of 8.5° in northerly direction and mean longitudinal flow of 5.9° in easterly direction; F) 5k100, with a mean latitudinal moisture flow of 13.2° in northerly direction and mean longitudinal flow of 14.1° in easterly direction.

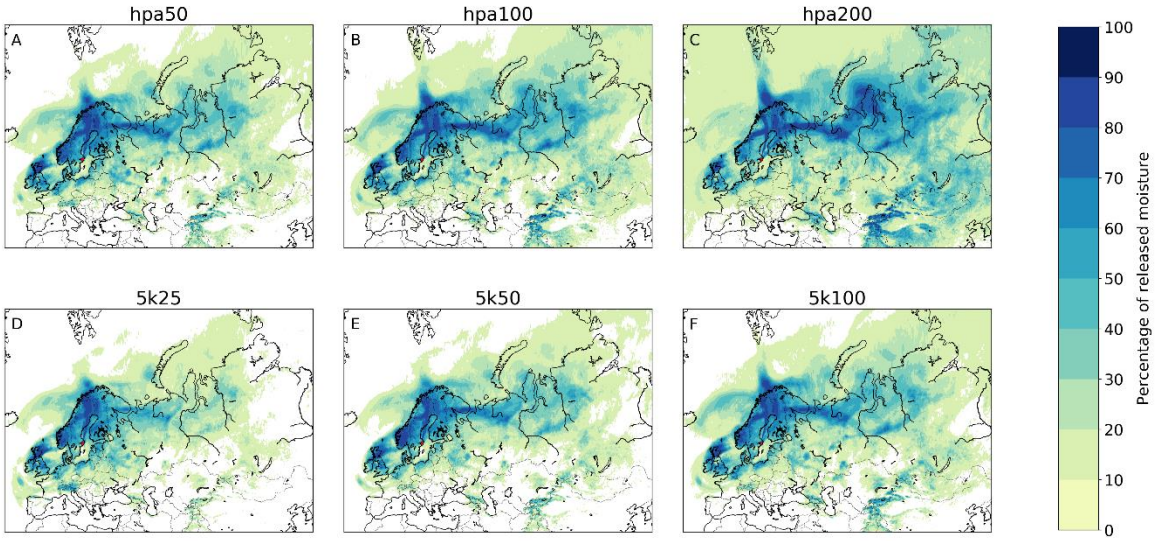

Figure S30: Different footprints of moisture releases from Stockholm in July 2012 in a three-dimensional Lagrangian model with different degradations of the vertical moisture profile. A) hpa50, with a mean latitudinal moisture flow of 1.7° in northerly direction and mean longitudinal flow of 14.0° in easterly direction; B) hpa100, with a mean latitudinal moisture flow of 1.3° in northerly direction and mean longitudinal flow of 15.4° in easterly direction; C) hpa200, with a mean latitudinal moisture flow of 0.0° in northerly/southerly direction and mean longitudinal flow of 18.1° in easterly direction; D) 5k25, with a mean latitudinal moisture flow of 1.1° in northerly direction and mean longitudinal flow of 11.1° in easterly direction; E) 5k50, with a mean latitudinal moisture flow of 2.5° in northerly direction and mean longitudinal flow of 12.9° in easterly direction; F) 5k100, with a mean latitudinal moisture flow of 1.4° in northerly direction and mean longitudinal flow of 14.4° in easterly direction.

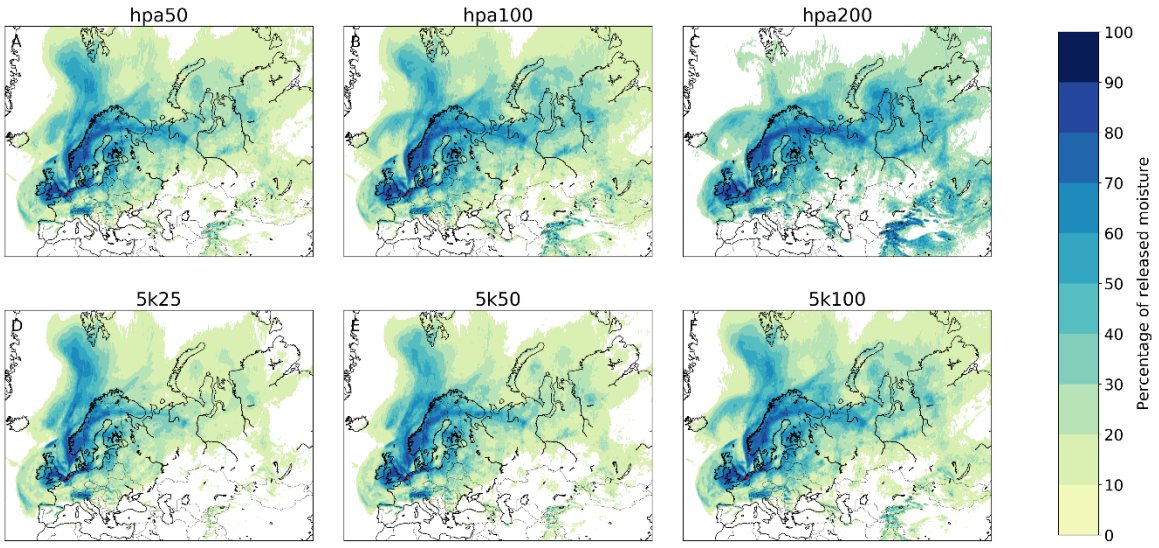

Figure S31: Different footprints of moisture releases from Utrecht in July 2012 in a three-dimensional Lagrangian model with different degradations of the vertical moisture profile. A) hpa50, with a mean latitudinal moisture flow of 7.0° in northerly direction and mean longitudinal flow of 17.9° in easterly direction; B) hpa100, with a mean latitudinal moisture flow of 6.3° in northerly direction and mean longitudinal flow of 19.1° in easterly direction; C) hpa200, with a mean latitudinal moisture flow of 3.8° in northerly direction and mean longitudinal flow of 21.0° in easterly direction; D) 5k25, with a mean latitudinal moisture flow of 6.7° in northerly direction and mean longitudinal flow of 15.7° in easterly direction; E) 5k50, with a mean latitudinal moisture flow of 7.2° in northerly direction and mean longitudinal flow of 17.0° in easterly direction; F) 5k100, with a mean latitudinal moisture flow of 6.7° in northerly direction and mean longitudinal flow of 18.7° in easterly direction.

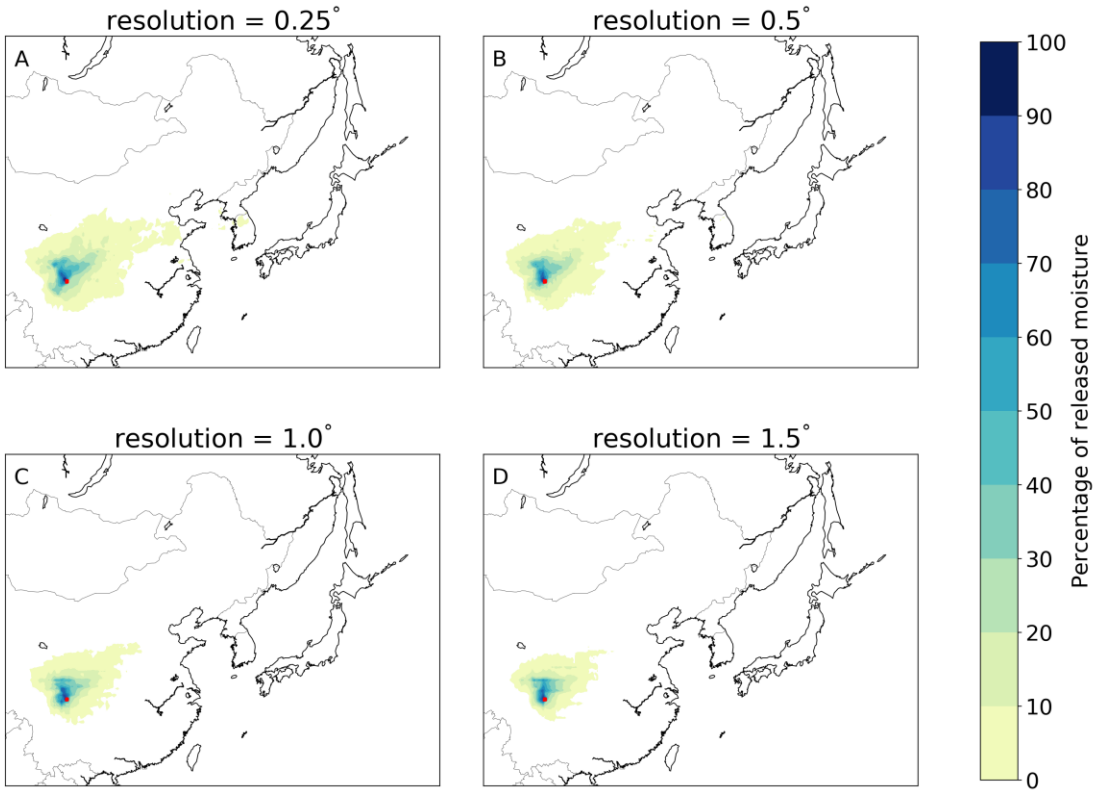

Figure S32: Different footprints of moisture releases from Chendu in July 2012 in a three-dimensional Lagrangian model with different horizontal resolutions. A) 0.25°, with a mean latitudinal moisture flow of 1.8° in northerly direction and mean longitudinal flow of 1.7° in easterly direction; B) 0.5°, with a mean latitudinal moisture flow of 1.7° in northerly direction and mean longitudinal flow of 1.4° in easterly direction; C) 1.0°, with a mean latitudinal moisture flow of 1.6° in northerly direction and mean longitudinal flow of 1.2° in easterly direction; D) 1.5°, with a mean latitudinal moisture flow of 1.6° in northerly direction and mean longitudinal flow of 1.1° in easterly direction.

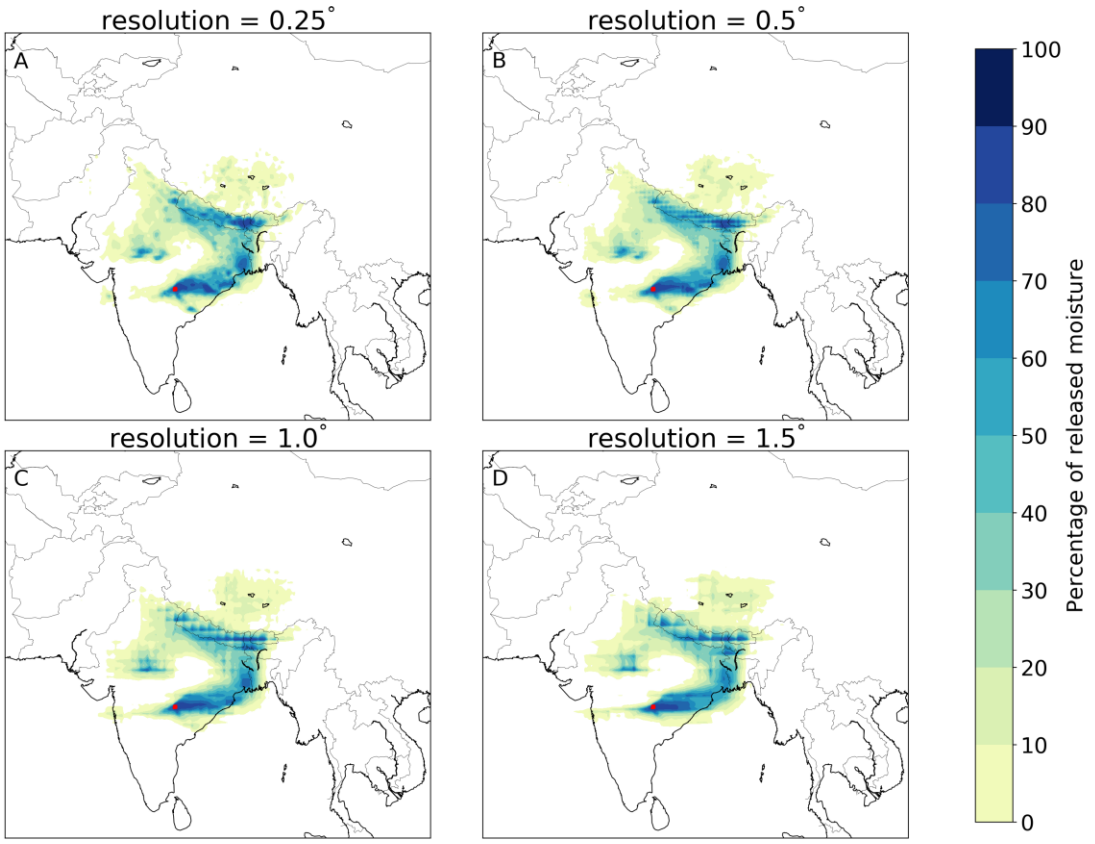

Figure S33: Different footprints of moisture releases from Nagpur in July 2012 in a three-dimensional Lagrangian model with different horizontal resolutions. A) 0.25°, with a mean latitudinal moisture flow of 4.7° in northerly direction and mean longitudinal flow of 3.6° in easterly direction; B) 0.5°, with a mean latitudinal moisture flow of 4.7° in northerly direction and mean longitudinal flow of 3.7° in easterly direction; C) 1.0°, with a mean latitudinal moisture flow of 4.7° in northerly direction and mean longitudinal flow of 3.9° in easterly direction; D) 1.5°, with a mean latitudinal moisture flow of 4.6° in northerly direction and mean longitudinal flow of 4.1° in easterly direction.

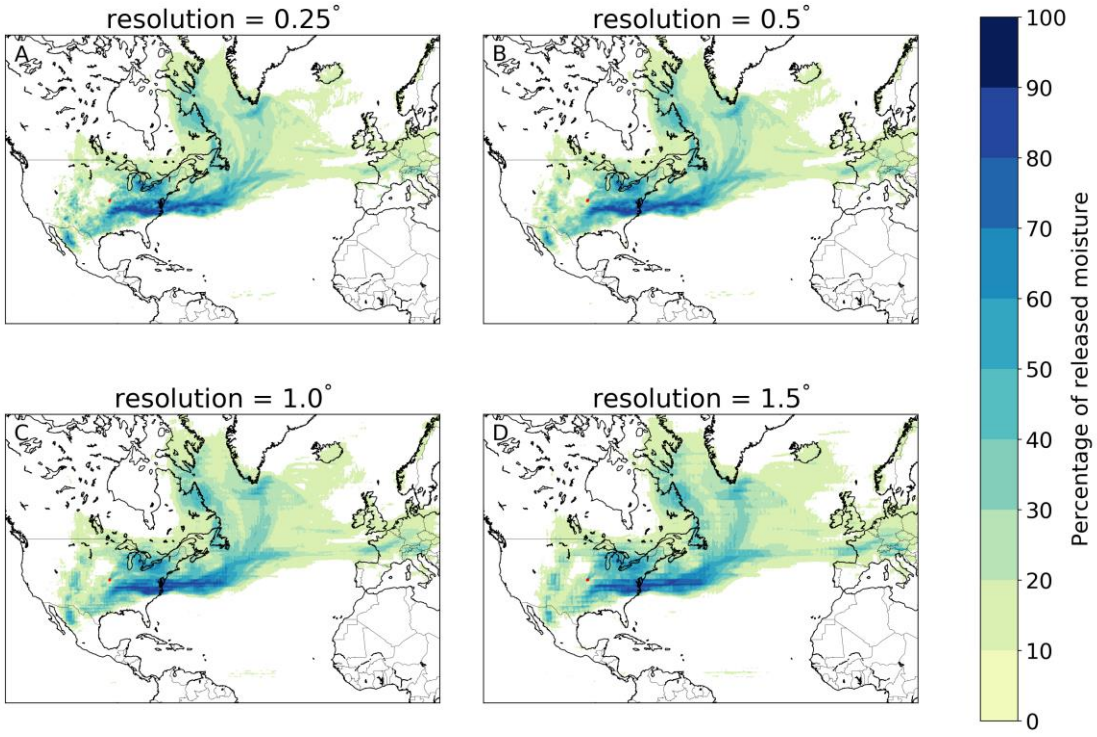

Figure S34: Different footprints of moisture releases from Central Kansas in July 2012 in a three-dimensional Lagrangian model with different horizontal resolutions. A) 0.25°, with a mean latitudinal moisture flow of 4.1° in northerly direction and mean longitudinal flow of 15.6° in easterly direction; B) 0.5°, with a mean latitudinal moisture flow of 4.3° in northerly direction and mean longitudinal flow of 15.9° in easterly direction; C) 1.0°, with a mean latitudinal moisture flow of 4.6° in northerly direction and mean longitudinal flow of 16.2° in easterly direction; D) 1.5°, with a mean latitudinal moisture flow of 4.9° in northerly direction and mean longitudinal flow of 16.3° in easterly direction.

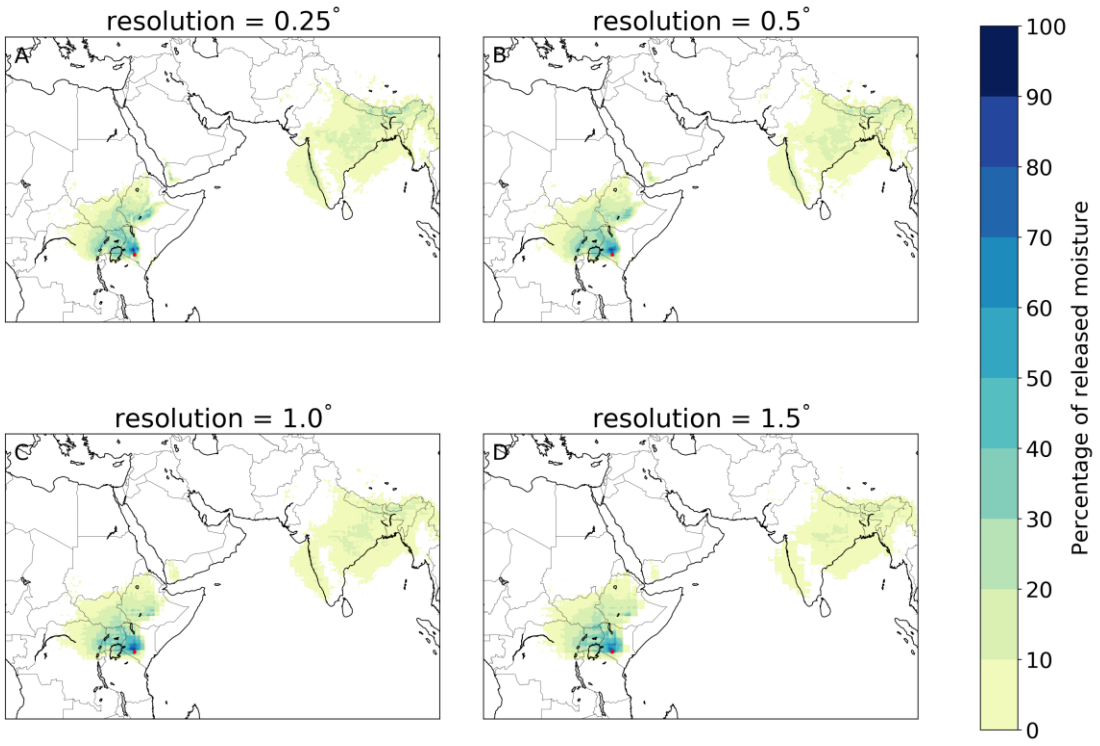

Figure S35: Different footprints of moisture releases from Nairobi in July 2012 in a three-dimensional Lagrangian model with different horizontal resolutions. A) 0.25°, with a mean latitudinal moisture flow of 6.6° in northerly direction and mean longitudinal flow of 2.9° in easterly direction; B) 0.5°, with a mean latitudinal moisture flow of 5.9° in northerly direction and mean longitudinal flow of 2.2° in easterly direction; C) 1.0°, with a mean latitudinal moisture flow of 5.4° in northerly direction and mean longitudinal flow of 1.5° in easterly direction; D) 1.5°, with a mean latitudinal moisture flow of 5.0° in northerly direction and mean longitudinal flow of 1.2° in easterly direction.

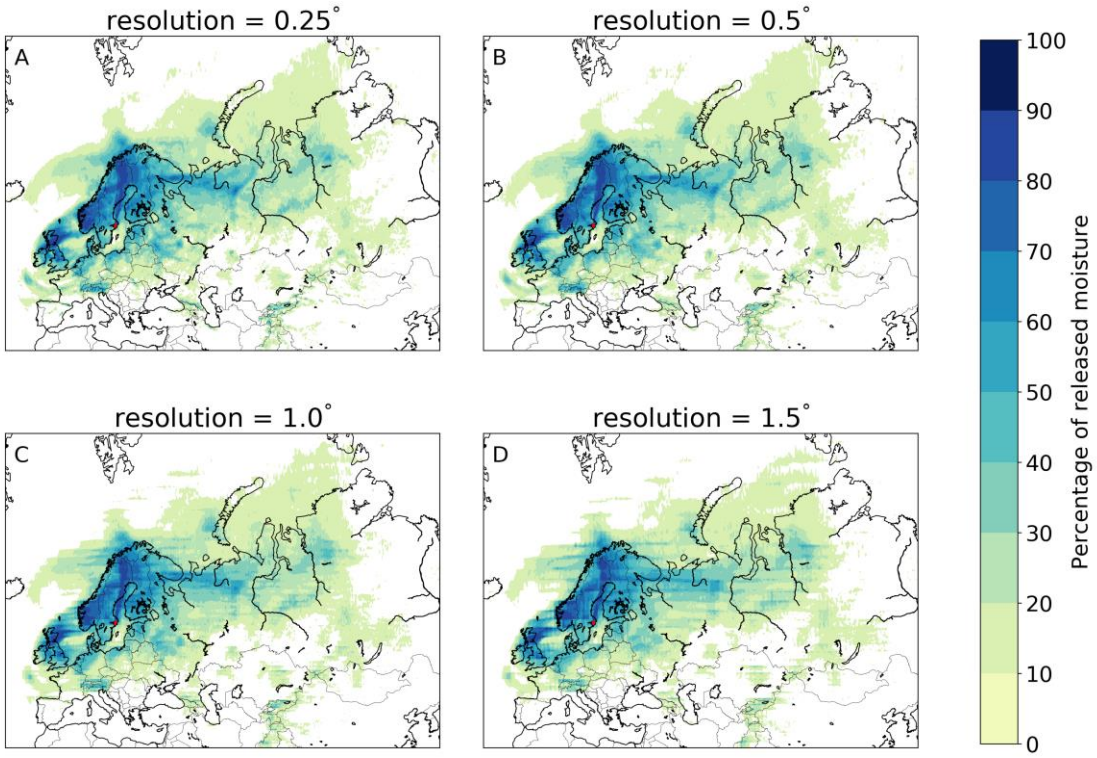

Figure S36: Different footprints of moisture releases from Stockholm in July 2012 in a three-dimensional Lagrangian model with different horizontal resolutions. A) 0.25°, with a mean latitudinal moisture flow of 1.4° in northerly direction and mean longitudinal flow of 11.0° in easterly direction; B) 0.5°, with a mean latitudinal moisture flow of 1.6° in northerly direction and mean longitudinal flow of 11.0° in easterly direction; C) 1.0°, with a mean latitudinal moisture flow of 1.8° in northerly direction and mean longitudinal flow of 10.9° in easterly direction; D) 1.5°, with a mean latitudinal moisture flow of 2.1° in northerly direction and mean longitudinal flow of 10.6° in easterly direction.

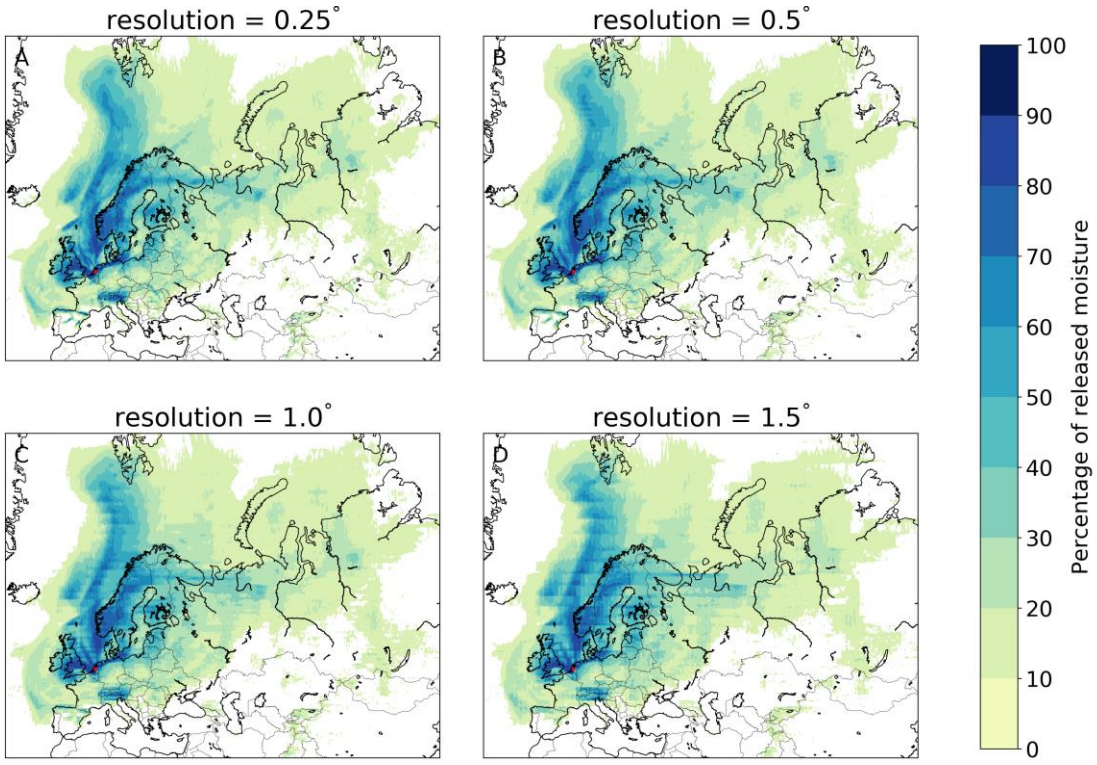

Figure S37: Different footprints of moisture releases from Utrecht in July 2012 in a three-dimensional Lagrangian model with different horizontal resolutions. A) 0.25°, with a mean latitudinal moisture flow of 6.2° in northerly direction and mean longitudinal flow of 15.4° in easterly direction; B) 0.5°, with a mean latitudinal moisture flow of 6.2° in northerly direction and mean longitudinal flow of 15.4° in easterly direction; C) 1.0°, with a mean latitudinal moisture flow of 6.6° in northerly direction and mean longitudinal flow of 15.4° in easterly direction; D) 1.5°, with a mean latitudinal moisture flow of 6.6° in northerly direction and mean longitudinal flow of 15.5° in easterly direction.

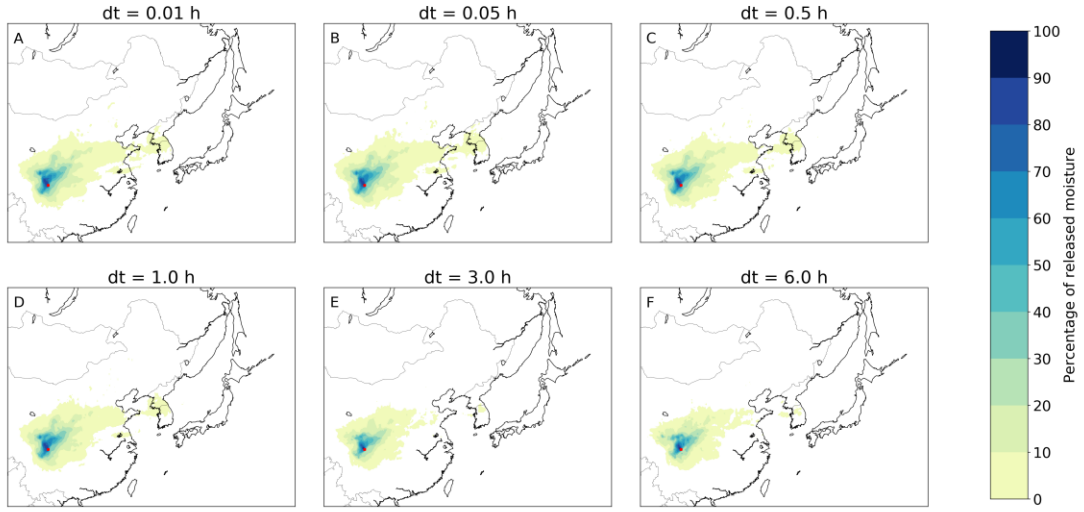

Figure ~~S32~~S38: Different footprints of moisture releases from Chendu in July 2012 in a three-dimensional Lagrangian model with different time steps (dt): 0.01 hours, 0.05 hours, 0.5 hours, ~~and~~ 1.0 hours, 3.0 hours, and 6.0 hours. A) 0.01 h, with a mean latitudinal moisture flow of 2.3° in northerly direction and mean longitudinal flow of 2.4° in easterly direction; B) 0.05 h, with a mean latitudinal moisture flow of 2.3° in northerly direction and mean longitudinal flow of 2.5° in easterly direction; C) 0.5 h, with a mean latitudinal moisture flow of 2.2° in northerly direction and mean longitudinal flow of 2.3° in easterly direction; D) 1.0 h, with a mean latitudinal moisture flow of 2.2° in northerly direction and mean longitudinal flow of 2.3° in easterly direction~~.~~; E) 3.0 h, with a mean latitudinal moisture flow of 1.8° in northerly direction and mean longitudinal flow of 1.6° in easterly direction; F) 6.0 h, with a mean latitudinal moisture flow of 1.9° in northerly direction and mean longitudinal flow of 1.7° in easterly direction.

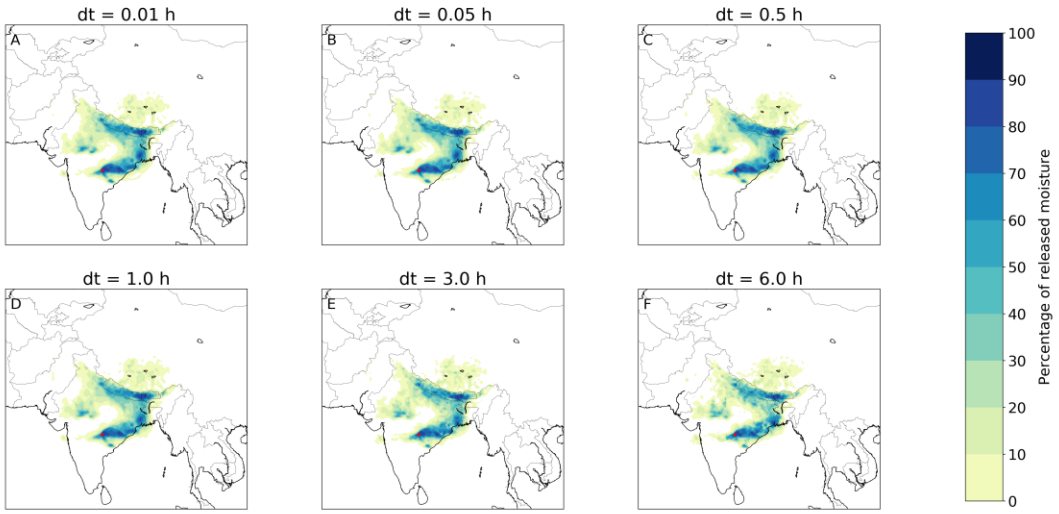

Figure ~~S33~~S39: Different footprints of moisture releases from Nagpur in July 2012 in a three-dimensional Lagrangian model with different time steps (dt): 0.01 hours, 0.05 hours, 0.5 hours, ~~and~~ 1.0 hours, 3.0 hours, and 6.0 hours. A) 0.01 h, with a mean latitudinal moisture flow of 4.9° in northerly direction and mean longitudinal flow of 3.6° in easterly direction; B) 0.05 h, with a mean latitudinal moisture flow of 4.9° in northerly direction and mean longitudinal flow of 3.6° in easterly direction; C) 0.5 h, with a mean latitudinal moisture flow of 4.9° in northerly direction and mean longitudinal flow of 3.7° in easterly direction; D) 1.0 h, with a mean latitudinal moisture flow of 4.9° in northerly direction and mean longitudinal flow of 3.8° in easterly direction~~.~~; E) 3.0 h, with a mean latitudinal moisture flow of 4.8° in northerly direction and mean longitudinal flow of 3.7° in easterly direction; F) 6.0 h, with a mean latitudinal moisture flow of 4.7° in northerly direction and mean longitudinal flow of 3.7° in easterly direction.

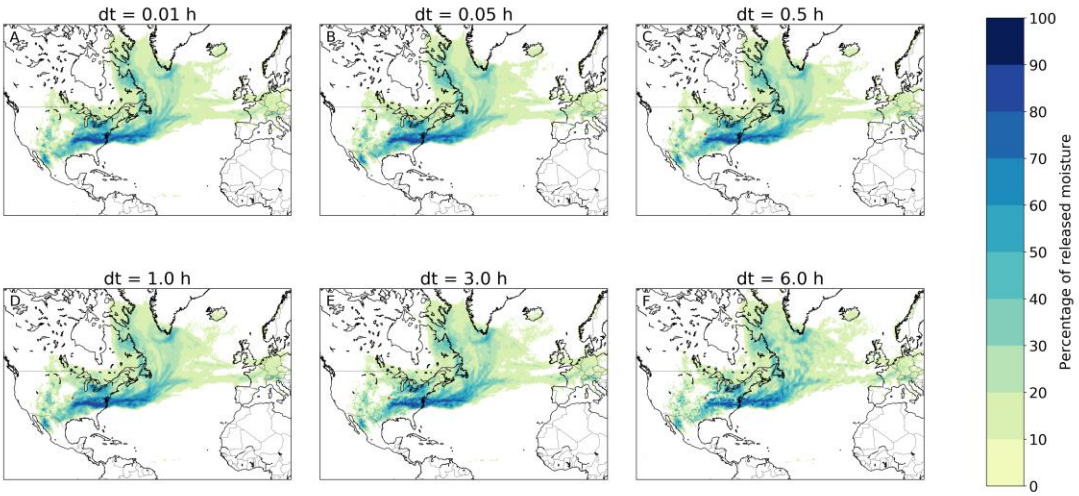

Figure ~~S34~~S40: Different footprints of moisture releases from Central Kansas in July 2012 in a three-dimensional Lagrangian model with different time steps (dt): 0.01 hours, 0.05 hours, 0.5 hours, ~~and~~ 1.0 hours, 3.0 hours, and 6.0 hours. A) 0.01 h, with a mean latitudinal moisture flow of 4.0° in northerly direction and mean longitudinal flow of 15.3° in easterly direction; B) 0.05 h, with a mean latitudinal moisture flow of 3.9° in northerly direction and mean longitudinal flow of 15.3° in easterly direction; C) 0.5 h, with a mean latitudinal moisture flow of 3.9° in northerly direction and mean longitudinal flow of 15.3° in easterly direction; D) 1.0 h, with a mean latitudinal moisture flow of 4.0° in northerly direction and mean longitudinal flow of 15.3° in easterly direction~~.~~; E) 3.0 h, with a mean latitudinal moisture flow of 4.2° in northerly direction and mean longitudinal flow of 16.1° in easterly direction; F) 6.0 h, with a mean latitudinal moisture flow of 4.5° in northerly direction and mean longitudinal flow of 16.7° in easterly direction.

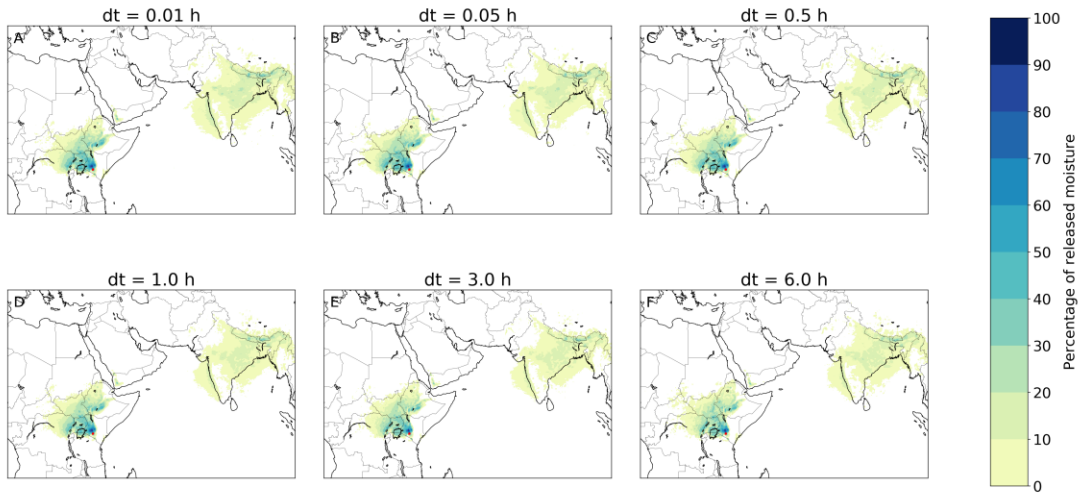

Figure ~~S35~~S41: Different footprints of moisture releases from Nairobi in July 2012 in a three-dimensional Lagrangian model with different time steps (dt): 0.01 hours, 0.05 hours, 0.5 hours, ~~and~~ 1.0 hours, 3.0 hours, and 6.0 hours. A) 0.01 h, with a mean latitudinal moisture flow of 7.4° in northerly direction and mean longitudinal flow of 3.2° in easterly direction; B) 0.05 h, with a mean latitudinal moisture flow of 7.2° in northerly direction and mean longitudinal flow of 3.0° in easterly direction; C) 0.5 h, with a mean latitudinal moisture flow of 7.1° in northerly direction and mean longitudinal flow of 2.8° in easterly direction; D) 1.0 h, with a mean latitudinal moisture flow of 6.9° in northerly direction and mean longitudinal flow of 2.5° in easterly direction.~~;~~ E) 3.0 h, with a mean latitudinal moisture flow of 6.6° in northerly direction and mean longitudinal flow of 2.5° in easterly direction; F) 6.0 h, with a mean latitudinal moisture flow of 6.6° in northerly direction and mean longitudinal flow of 2.5° in easterly direction.

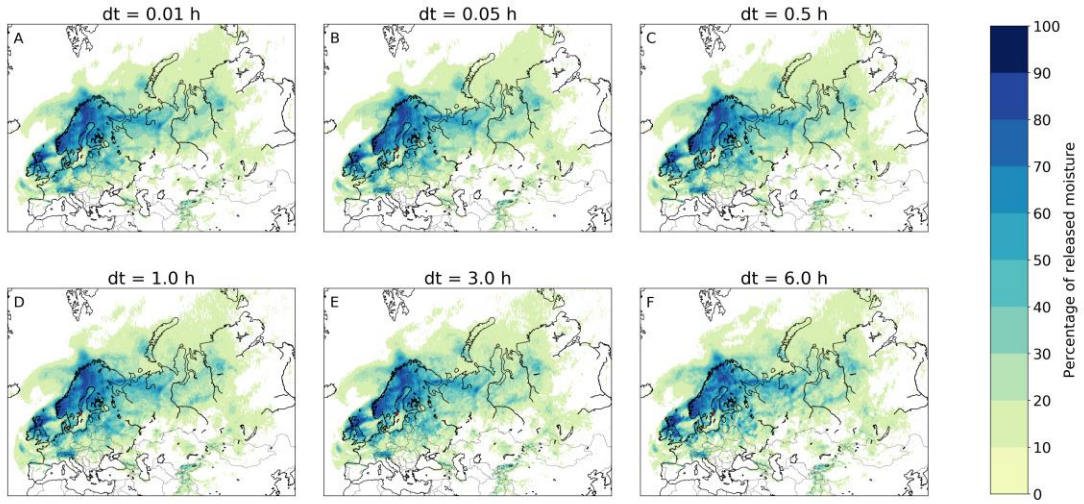

Figure ~~S36~~S42: Different footprints of moisture releases from Stockholm in July 2012 in a three-dimensional Lagrangian model with different time steps (dt): 0.01 hours, 0.05 hours, 0.5 hours, ~~and~~ 1.0 hours, 3.0 hours, and 6.0 hours. A) 0.01 h, with a mean latitudinal moisture flow of 1.3° in northerly direction and mean longitudinal flow of 11.0° in easterly direction; B) 0.05 h, with a mean latitudinal moisture flow of 1.3° in northerly direction and mean longitudinal flow of 11.1° in easterly direction; C) 0.5 h, with a mean latitudinal moisture flow of 1.1° in northerly direction and mean longitudinal flow of 11.1° in easterly direction; D) 1.0 h, with a mean latitudinal moisture flow of 0.8° in northerly direction and mean longitudinal flow of 11.2° in easterly direction~~.~~; E) 3.0 h, with a mean latitudinal moisture flow of 1.1° in northerly direction and mean longitudinal flow of 11.0° in easterly direction; F) 3.0 h, with a mean latitudinal moisture flow of 1.4° in northerly direction and mean longitudinal flow of 11.5° in easterly direction.

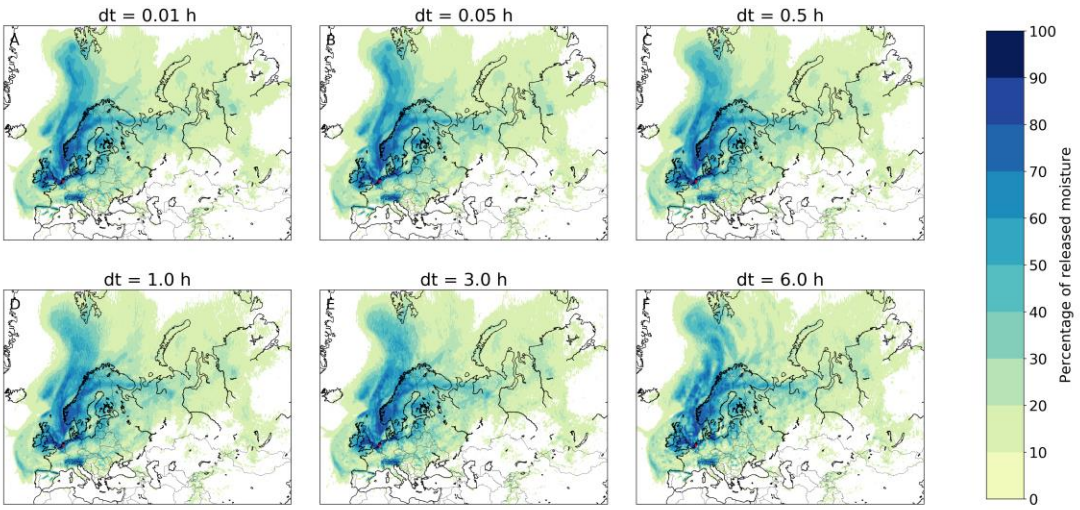

Figure ~~S37~~S43: Different footprints of moisture releases from Utrecht in July 2012 in a three-dimensional Lagrangian model with different time steps (dt): 0.01 hours, 0.05 hours, 0.5 hours, ~~and~~ 1.0 hours, 3.0 hours, and 6.0 hours. A) 0.01 h, with a mean latitudinal moisture flow of 6.2° in northerly direction and mean longitudinal flow of 15.3° in easterly direction; B) 0.05 h, with a mean latitudinal moisture flow of 6.1° in northerly direction and mean longitudinal flow of 15.3° in easterly direction; C) 0.5 h, with a mean latitudinal moisture flow of 5.9° in northerly direction and mean longitudinal flow of 15.3° in easterly direction; D) 1.0 h, with a mean latitudinal moisture flow of 5.9° in northerly direction and mean longitudinal flow of 15.2° in easterly direction~~.~~; E) 3.0 h, with a mean latitudinal moisture flow of 6.1° in northerly direction and mean longitudinal flow of 15.6° in easterly direction; F) 6.0 h, with a mean latitudinal moisture flow of 6.7° in northerly direction and mean longitudinal flow of 15.9° in easterly direction.

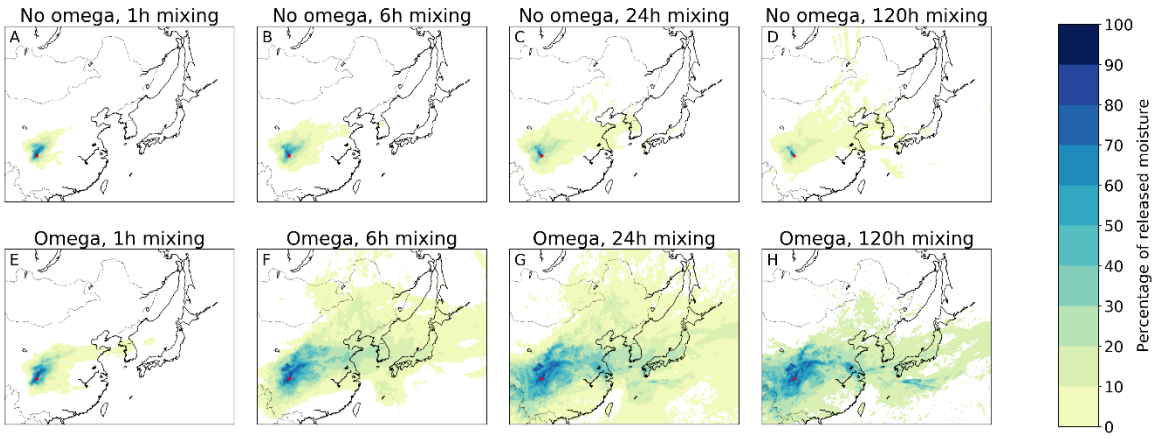

Figure ~~S38~~S44: Different footprints of moisture releases from Chendu in July 2012 in a three-dimensional Lagrangian model with different mixing assumptions: without and with accounting for the three-dimensional moisture flows in the ERA5 data (termed omega), and with different assumptions of additional vertical mixing speed (full mixing every 1 h, every 6 h, every 24 h, and every 120 h). A) Without omega, every 1 h mixing, with a mean latitudinal moisture flow of 1.6° in northerly direction and mean longitudinal flow of 1.3° in easterly direction; B) Without omega, every 6 h mixing, with a mean latitudinal moisture flow of 1.8° in northerly direction and mean longitudinal flow of 1.7° in easterly direction; C) Without omega, every 24 h mixing, with a mean latitudinal moisture flow of 2.0° in northerly direction and mean longitudinal flow of 1.8° in easterly direction; D) Without omega, every 120 h mixing, with a mean latitudinal moisture flow of 2.0° in northerly direction and mean longitudinal flow of 1.6° in easterly direction; E) With omega, every 1 h mixing, with a mean latitudinal moisture flow of 2.4° in northerly direction and mean longitudinal flow of 3.1° in easterly direction; F) With omega, every 6 h mixing, with a mean latitudinal moisture flow of 3.8° in northerly direction and mean longitudinal flow of 7.1° in easterly direction; G) With omega, every 24 h mixing, with a mean latitudinal moisture flow of 1.5° in northerly direction and mean longitudinal flow of 3.8° in easterly direction; H) With omega, every 120 h mixing, with a mean latitudinal moisture flow of 0.6° in southerly direction and mean longitudinal flow of 1.0° in easterly direction.

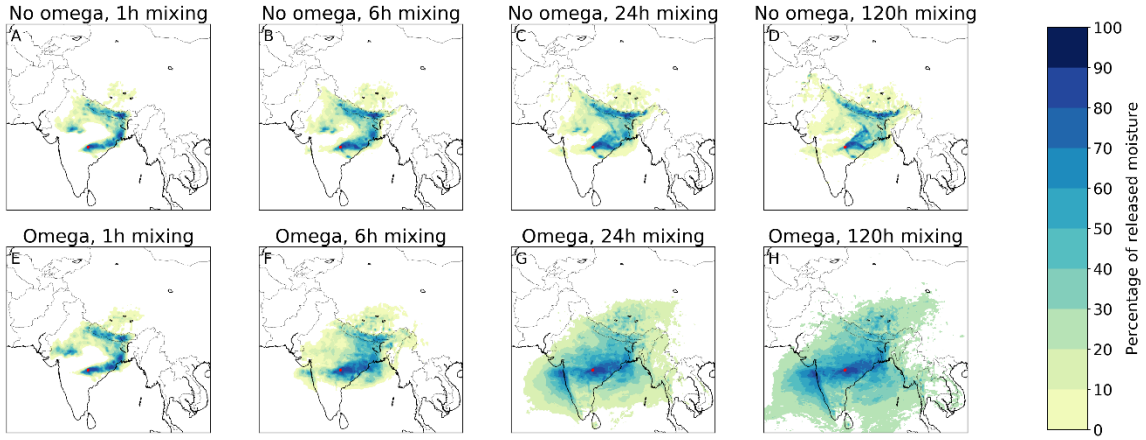

Figure ~~S39~~S45: Different footprints of moisture releases from Nagpur in July 2012 in a three-dimensional Lagrangian model with different mixing assumptions: without and with accounting for the three-dimensional moisture flows in the ERA5 data (termed omega), and with different assumptions of additional vertical mixing speed (full mixing every 1 h, every 6 h, every 24 h, and every 120 h). A) Without omega, every 1 h mixing, with a mean latitudinal moisture flow of 4.9° in northerly direction and mean longitudinal flow of 3.4° in easterly direction; B) Without omega, every 6 h mixing, with a mean latitudinal moisture flow of 4.7° in northerly direction and mean longitudinal flow of 3.6° in easterly direction; C) Without omega, every 24 h mixing, with a mean latitudinal moisture flow of 4.6° in northerly direction and mean longitudinal flow of 3.8° in easterly direction; D) Without omega, every 120 h mixing, with a mean latitudinal moisture flow of 4.5° in northerly direction and mean longitudinal flow of 3.9° in easterly direction; E) With omega, every 1 h mixing, with a mean latitudinal moisture flow of 4.6° in northerly direction and mean longitudinal flow of 3.4° in easterly direction; F) With omega, every 6 h mixing, with a mean latitudinal moisture flow of 2.7° in northerly direction and mean longitudinal flow of 3.9° in easterly direction; G) With omega, every 24 h mixing, with a mean latitudinal moisture flow of 1.1° in southerly direction and mean longitudinal flow of 1.1° in westerly direction; H) With omega, every 120 h mixing, with a mean latitudinal moisture flow of 3.7° in southerly direction and mean longitudinal flow of 0.5° in westerly direction.

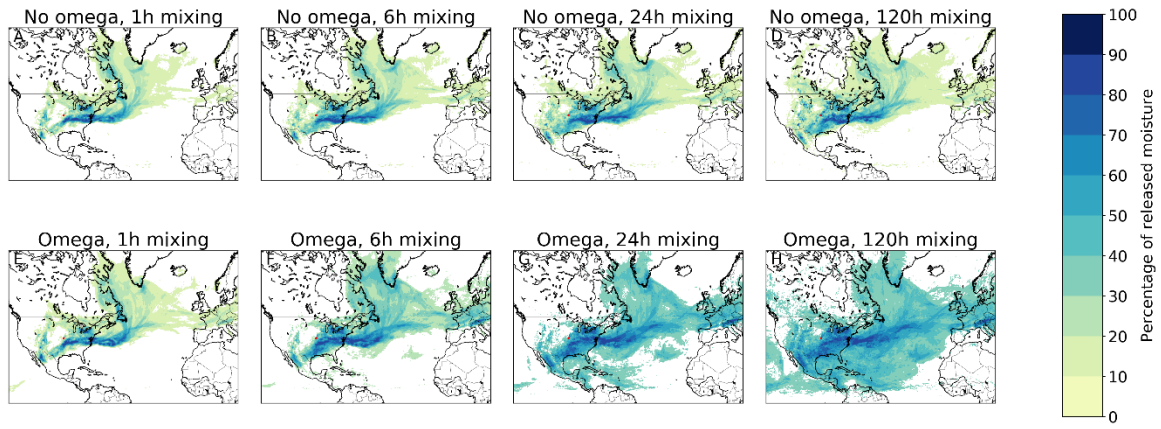

Figure ~~S40~~S46: Different footprints of moisture releases from Central Kansas in July 2012 in a three-dimensional Lagrangian model with different mixing assumptions: without and with accounting for the three-dimensional moisture flows in the ERA5 data (termed omega), and with different assumptions of additional vertical mixing speed (full mixing every 1 h, every 6 h, every 24 h, and every 120 h). A) Without omega, every 1 h mixing, with a mean latitudinal moisture flow of 4.3° in northerly direction and mean longitudinal flow of 16.4° in easterly direction; B) Without omega, every 6 h mixing, with a mean latitudinal moisture flow of 4.1° in northerly direction and mean longitudinal flow of 15.6° in easterly direction; C) Without omega, every 24 h mixing, with a mean latitudinal moisture flow of 3.7° in northerly direction and mean longitudinal flow of 14.6° in easterly direction; D) Without omega, every 120 h mixing, with a mean latitudinal moisture flow of 3.3° in northerly direction and mean longitudinal flow of 13.4° in easterly direction; E) With omega, every 1 h mixing, with a mean latitudinal moisture flow of 4.0° in northerly direction and mean longitudinal flow of 15.4° in easterly direction; F) With omega, every 6 h mixing, with a mean latitudinal moisture flow of 5.1° in northerly direction and mean longitudinal flow of 12.5° in easterly direction; G) With omega, every 24 h mixing, with a mean latitudinal moisture flow of 2.3° in northerly direction and mean longitudinal flow of 9.2° in easterly direction; H) With omega, every 120 h mixing, with a mean latitudinal moisture flow of 1.1° in southerly direction and mean longitudinal flow of 6.0° in easterly direction.

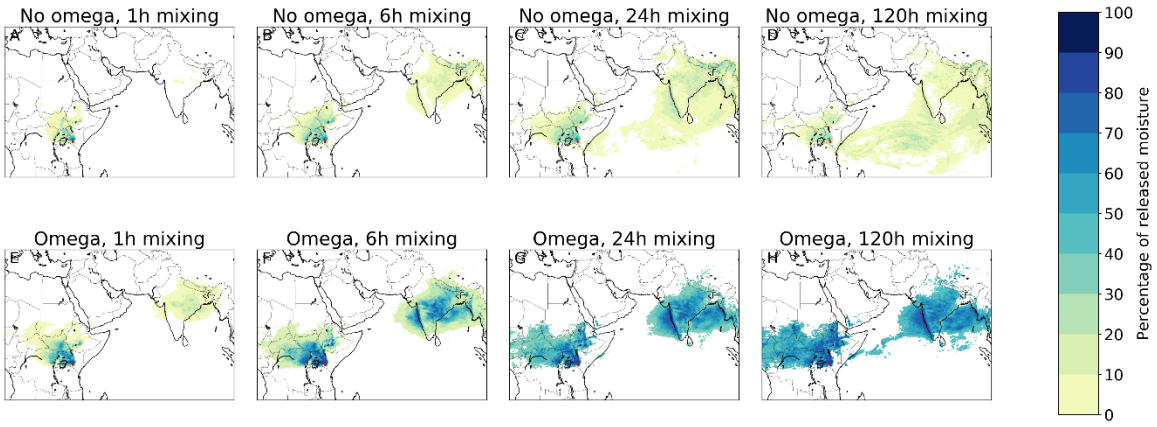

Figure ~~S41~~S47: Different footprints of moisture releases from Nairobi in July 2012 in a three-dimensional Lagrangian model with different mixing assumptions: without and with accounting for the three-dimensional moisture flows in the ERA5 data (termed omega), and with different assumptions of additional vertical mixing speed (full mixing every 1 h, every 6 h, every 24 h, and every 120 h). A) Without omega, every 1 h mixing, with a mean latitudinal moisture flow of 3.5° in northerly direction and mean longitudinal flow of 0.9° in westerly direction; B) Without omega, every 6 h mixing, with a mean latitudinal moisture flow of 6.5° in northerly direction and mean longitudinal flow of 2.8° in easterly direction; C) Without omega, every 24 h mixing, with a mean latitudinal moisture flow of 6.5° in northerly direction and mean longitudinal flow of 5.3° in easterly direction; D) Without omega, every 120 h mixing, with a mean latitudinal moisture flow of 3.6° in northerly direction and mean longitudinal flow of 5.4° in easterly direction; E) With omega, every 1 h mixing, with a mean latitudinal moisture flow of 6.9° in northerly direction and mean longitudinal flow of 0.1° in easterly direction; F) With omega, every 6 h mixing, with a mean latitudinal moisture flow of 12.9° in northerly direction and mean longitudinal flow of 9.5° in easterly direction; G) With omega, every 24 h mixing, with a mean latitudinal moisture flow of 12.5° in northerly direction and mean longitudinal flow of 10.2° in easterly direction; H) With omega, every 120 h mixing, with a mean latitudinal moisture flow of 11.0° in northerly direction and mean longitudinal flow of 8.8° in easterly direction.

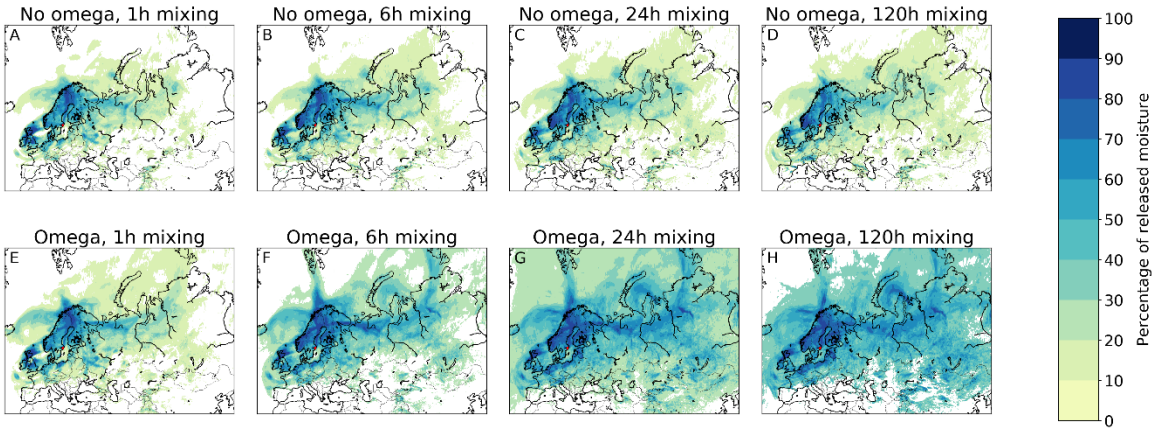

Figure ~~S42~~S48: Different footprints of moisture releases from Stockholm in July 2012 in a three-dimensional Lagrangian model with different mixing assumptions: without and with accounting for the three-dimensional moisture flows in the ERA5 data (termed omega), and with different assumptions of additional vertical mixing speed (full mixing every 1 h, every 6 h, every 24 h, and every 120 h). A) Without omega, every 1 h mixing, with a mean latitudinal moisture flow of 1.5° in northerly direction and mean longitudinal flow of 11.8° in easterly direction; B) Without omega, every 6 h mixing, with a mean latitudinal moisture flow of 1.5° in northerly direction and mean longitudinal flow of 11.0° in easterly direction; C) Without omega, every 24 h mixing, with a mean latitudinal moisture flow of 1.0° in northerly direction and mean longitudinal flow of 10.1° in easterly direction; D) Without omega, every 120 h mixing, with a mean latitudinal moisture flow of 0.4° in northerly direction and mean longitudinal flow of 8.3° in easterly direction; E) With omega, every 1 h mixing, with a mean latitudinal moisture flow of 1.3° in northerly direction and mean longitudinal flow of 12.6° in easterly direction; F) With omega, every 6 h mixing, with a mean latitudinal moisture flow of 1.2° in northerly direction and mean longitudinal flow of 13.6° in easterly direction; G) With omega, every 24 h mixing, with a mean latitudinal moisture flow of 0.0° in northerly/southerly direction and mean longitudinal flow of 14.2° in easterly direction; H) With omega, every 120 h mixing, with a mean latitudinal moisture flow of 0.8° in southerly direction and mean longitudinal flow of 14.2° in easterly direction.

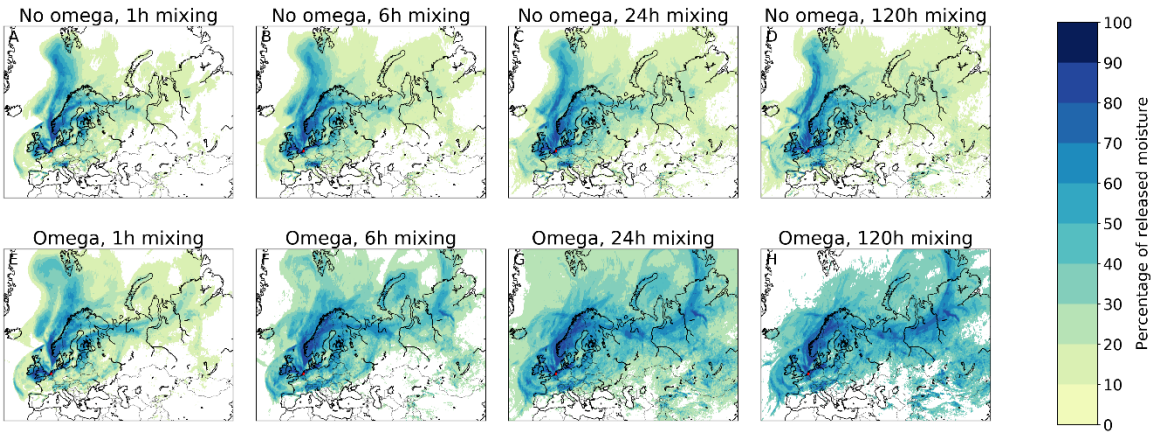

Figure ~~S43~~S49: Different footprints of moisture releases from Utrecht in July 2012 in a three-dimensional Lagrangian model with different mixing assumptions: without and with accounting for the three-dimensional moisture flows in the ERA5 data (termed omega), and with different assumptions of additional vertical mixing speed (full mixing every 1 h, every 6 h, every 24 h, and every 120 h). A) Without omega, every 1 h mixing, with a mean latitudinal moisture flow of 8.1° in northerly direction and mean longitudinal flow of 14.9° in easterly direction; B) Without omega, every 6 h mixing, with a mean latitudinal moisture flow of 6.3° in northerly direction and mean longitudinal flow of 15.4° in easterly direction; C) Without omega, every 24 h mixing, with a mean latitudinal moisture flow of 4.7° in northerly direction and mean longitudinal flow of 15.5° in easterly direction; D) Without omega, every 120 h mixing, with a mean latitudinal moisture flow of 3.6° in northerly direction and mean longitudinal flow of 15.6° in easterly direction; E) With omega, every 1 h mixing, with a mean latitudinal moisture flow of 8.8° in northerly direction and mean longitudinal flow of 17.5° in easterly direction; F) With omega, every 6 h mixing, with a mean latitudinal moisture flow of 6.2° in northerly direction and mean longitudinal flow of 17.9° in easterly direction; G) With omega, every 24 h mixing, with a mean latitudinal moisture flow of 4.4° in northerly direction and mean longitudinal flow of 18.1° in easterly direction; H) With omega, every 120 h mixing, with a mean latitudinal moisture flow of 3.9° in northerly direction and mean longitudinal flow of 18.4° in easterly direction.